# SELECTION OF APTAMERS TO CD20 AND THEIR APPLICATION AS INHIBITORS OF COMPLEMENT DEPENDENT CYTOTOXICITY

---

By

Nadia Al-Youssef

A Thesis Submitted to the Faculty of Graduate and Postdoctoral Studies in Partial Fulfillments of the Requirements for the M.Sc. Degree in Chemistry.

Department of Chemistry and Biomolecular Sciences
Faculty of Science
University of Ottawa

# DEDICATIONS

For Evah.

# ACKNOWLEDGMENTS

First, I would like to thank my supervisor Dr. Maxim Berezovski for his gracious support in pursing my work. It's been a privilege and I am grateful. I thank as well my fellow lab mates, who have all helped to teach me so much about critical assessments and objective thinking. In particular Shahrokh Ghodadloo and Darija Muharemagic for their scientific expertise, Pavil Milman for his resoundingly analytical leanings and experimental suggestions, Thao Nguyen and Ana Garguan for their kind encouragement.

I thank also Dr. Filion for his gentle guidance and novel insights. And, importantly, for teaching me flow cytometry- where the differences between something, anything and everything mean nothing except when seen in the light of proper controls.

Lastly and most fervently I thank my parents and my siblings whose devotion and diligence remain my greatest strength and inspiration; and my friends who accommodated late night plans way too often to be entirely normal.

# ABSTRACT

CD20 is an important oncological B-cell marker. Immunotherapy, using anti-CD20 antibodies, has revolutionized the treatment of B-cell cancers. Aptamers are highly specific DNA ligands, raised to identify virtually any target molecule through an iterative process known as SELEX (*s*ystemati*c* *e*volution of *l*igands by *ex*ponential amplification). Aptamers rival antibodies in both binding affinity and specificity. We developed a novel CD20 specific SELEX method, using a lentiviral system to transfect CD20 cDNA into HEK293 cells. Selection using CD20+HEK cells evolved pools of aptamers with stepwise increases in binding affinity for the transfected cell line. Sequenced aptamer clones exhibited an antagonistic effect with anti-CD20 antibody; and in a biological assay possessed a protective capacity, limiting the extent of antibody induced complement dependent cytotoxicity. Overall, genetic transfection is a novel targeted approach of ligand generation, producing aptamers endowed with both physical and biological capabilities.

# TABLE OF CONTENTS

**LIST OF FIGURES** ..... **VI**

**ABBREVIATIONS** ..... **IX**

**1 GENERAL INTRODUCTION** ..... **1**

1.1 TARGETED MOLECULES FOR DIAGNOSTICS AND THERAPY ..... 1
1.2 THERAPEUTIC MONOCLONALS ..... 2
*1.2.1 Structure and development* ..... *3*
*1.2.2 Effector Mechanisms of Monoclonals* ..... *5*
1.3 THE CD20 MOLECULE ..... 6
*1.3.1 Introduction and History of the CD20 Molecule* ..... *6*
*1.3.2 Anti-CD20 Antibodies* ..... *8*
1.4 APTAMER INTRODUCTION ..... 9
*1.4.1 Aptamers are created by SELEX* ..... *11*
*1.4.2 Cell-SELEX* ..... *12*
*1.4.3 Viral Transfection for Target Specific Cell SELEX* ..... *14*
*1.4.4 Target Positive Cell-SELEX using CD20 Transfected HEK Cells* ..... *16*
1.5 THESIS OVERVIEW ..... 19

**2 MATERIALS AND METHODS** ..... **20**

2.1 TRANSFECTION AND APTAMER POOL SELECTION OF CD20+HEK APTAMERS ..... 20
*2.1.1 Generation and Verification of CD20+HEK Cell line* ..... *20*
*2.1.2 Selection Protocol-Cell SELEX* ..... *23*
*2.1.3 Evaluating Aptamer Enrichment with CD20+HEK* ..... *25*
*2.1.4 Evaluating Aptamer Pools Across Cell Lines* ..... *25*
2.2 NGS ANALYSIS AND EVALUATION OF APTAMER CLONES ..... 26
*2.2.1 Sample Preparation* ..... *26*
*2.2.2 Aptamer Clone Assessment* ..... *26*
*2.2.3 Assessment of specificity* ..... *27*
*2.2.4 Co-stain experiments* ..... *27*
2.3 BIOLOGICAL ASSESSMENT ..... 28
*2.3.1 Initial CDC Assessment of CD20+HEK and CCL-86 Cells* ..... *28*
*2.3.2 Binding of Aptamer Clones to the CCL-86 cells* ..... *28*
*2.3.3 Aptamer Mediated Inhibition of CDC* ..... *29*
2.4 STATISTICAL ANALYSIS ..... 29

**3 TRANSFECTION AND APTAMER POOL SELECTION** ..... **30**

3.1 ABSTRACT ..... 30
3.2 BACKGROUND ..... 30
*3.2.1 Characteristic of Lentiviral System* ..... *30*
*3.2.2 Stringency Measures* ..... *37*
3.3 RESULTS ..... 39
*3.3.1 Evaluation of CD20 Transfection* ..... *39*

*3.3.2 SELEX generates pools of aptamer with progressively greater binding affinity to the CD20+HEK cells.* ... *45*
*3.3.3 Pool 10 CD20 positively labels the naturally CD20 expressing CCL-86 Cells but not the naturally CD20 negative Cell line TIB-152.* ... *47*
3.4 DISCUSSION ... 49
3.5 CONCLUSION ... 51

**4 NEXT GENERATION SEQUENCING AND THE EVALUATION OF APTAMER CLONES ... 52**

4.1 ABSTRACT ... 52
4.2 BACKGROUND ... 53
*4.2.1 Deconvolution of Aptamer Pools* ... *53*
*4.2.2 Aptamer Sequencing Past Methods: Introduction to Conventional Bacterial Cloning and Sanger Sequencing* ... *54*
*4.2.3 Introduction to Next-Generation-Sequencing (NGS) Technologies* ... *57*
4.3 RESULTS ... 62
*4.3.1 NGS Reveals that Pool 10 Exhibits Significant Sequence Convergence and Motif Emergence* ... *62*
*4.3.2 HCN are lead aptamer candidates.* ... *70*
*4.3.3 Aptamer Screening & $K_d$ Analysis: Sequenced Aptamers possess high affinity and selectivity.* ... *73*
4.4 DISCUSSION ... 79
4.5 CONCLUSION ... 81

**5 BIOLOGICAL EFFICACY OF APTAMERS IN COMPLEMENT DEPENDENT CYTOTOXICITY ... 82**

5.1 ABSTRACT ... 82
5.2 BACKGROUND ... 82
*5.2.1 Biological Action of Anti-CD20 Antibodies is Varied and Diverse* ... *82*
*5.2.2 Effector Action of anti-CD20 Antibodies* ... *83*
*5.2.3 Epitope Specificity* ... *88*
*5.2.4 Aptamer to Better Elucidate Target- Antibody Dynamics* ... *90*
5.3 RESULTS ... 90
*5.3.1 CDC is potently induced by anti-CD20 antibody in naturally CD20 expressing CCL-86 Cells but not in the transfected CD20+HEK cells.* ... *90*
*5.3.2 CD20+HEK aptamers can limit extent of CDC in CCL-86 Cells.* ... *93*
5.4 DISCUSSION ... 103
**5. CONCLUSION** ... 106

**6 GENERAL CONCLUSION ... 107**

**7 REFERENCES ... 110**

**8 APPENDIX ... 122**

# LIST OF FIGURES


| | | |
|---|---|---|
| Chapter 1 | Figure 1.1 General antibody structure | 4 |
| | Figure 1.2 Effector mechanisms of therapeutic monoclonal antibodies | 4 |
| | Figure 1.3 CD20 expression in B cell ontogeny | 7 |
| | Figure 1.4. The CD20 molecule | 7 |
| | Figure 1.5 Cell-SELEX | 13 |
| | Figure 1.6 Complete selection protocol for CD20 target positive cell-SELEX | 17 |
| Chapter 3 | Figure 3.1. The evolution of lentiviral vectors for the purpose of mammalian gene expression | 32 |
| | Figure 3.2 The tet system for conditional gene expression | 35 |
| | Figure 3.3 Generation of intact GOI-viruses by a packaging cell line | 35 |
| | Figure 3.4 Assessment of CD20 expression in transfected HEK293 cells | 40 |
| | Figure 3.5 Visual detection of CD20 expression in transfected HEK293 Cells | 42 |
| | Figure 3.6 CD20 expression in different cell lines | 44 |

| | | |
|---|---|---|
| | Figure60 3.7 Binding affinity of aptamer pools with CD20+HEK cells | 46 |
| | Figure 3.8 Binding affinity of aptamer pools 1 and 10 with cell lines of varying CD20 expression | 48 |
| Chapter 4 | Figure 4.1 Bacterial cloning | 56 |
| | Figure 4.2 Illumina overview | 60 |
| | Figure 4.3 Pool 10 exhibits significant sequence convergence | 64 |
| | Figure 4.4 Sequence comparison of HCNs and their closest related sequence | 67 |
| | Figure 4.5 DREME motif analysis for Pool 10 | 69 |
| | Figure 4.6 Nucleotide sequence of lead aptamer candidates | 71 |
| | Figure 4.7 Purported secondary structure of lead candidate aptamers | 72 |
| | Figure 4.8 $K_d$ analysis of NLA aptamers | 74 |
| | Figure 4.9 Evaluation of aptamer specificity | 76 |
| | Figure 4.10 NLA aptamers inhibit the binding of anti-CD20 antibody | 78 |
| Chapter 5 | Figure 5.1 Anti-CD20 effector actions. | 84 |
| | Figure 5.2 Clinical status of anti-CD20 antibodies | 89 |

Figure 5.3 Comparison of CDC induction in naturally CD20 expressing CCL-86 and transfected CD20+HEK cell lines 92

Figure 5.4 NLA aptamer show specific affinity with the CD20 positive CCL-86 and not the CD20 negative TIB-152 94

Figure 5.5 Complement dependent cytotoxicity in CCL-86: controls samples 97

Figure 5.6 NLA aptamers limit the extent of complement dependent cytotoxicity in CCL-86 cells 98

Figure 5.7 NLA protected CCL-86 cells exhibit greater viability and have decreased staining of the pro-apoptotic marker annexin-V 102

# ABBREVIATIONS

| | |
|---|---|
| 7-AAD | 7-Aminoactinomycin D |
| ADCC | Antibody dependant cell-mediated cytotoxicity |
| ADCP | Antibody dependent cellular phagocytosis |
| BLAST | Basic local alignment search tool |
| CCL-86 | Small non-cleaved cell lymphoma (Burkitt's) |
| CD20 | Cluster of differentiation -20 |
| CDC | Complement dependent cytotoxicity |
| cDNA | Complementary deoxyribonucleic triphosphate |
| CLL | Chronic lymphocytic leukemia |
| CRT | Cyclic reversible termination |
| CTL | Cytotoxic T lymphocytes |
| CTLA-4 | Cytotoxic T lymphocyte-associated protein 4 |
| DAPI | 4',6'-diamidino-2-phenylindole |
| ddNTP | Dideoxynucleotide triphosphates |
| DREME | Discriminative regular expression motif elicitation |
| EGFR | Epidermal growth factor receptor |
| Fab | Fragment of antigen binding |
| Fc | Fragment crystallisable |
| FcδR | Fragment crystallisable gamma receptor |
| FITC | Fluorescein isothiocyanate |
| GOI | Gene of interest |

| | |
|---|---|
| HCN | High copy number sequence |
| HEK293 | Human embryonic kidney 293 |
| HiHS | Heat inactivated human serum |
| HS | Human serum |
| HTA | High throughput analysis |
| IgG | Immunoglobulin G |
| $K_d$ | Dissociation constant |
| mAB | Monoclonal antibody |
| MAC | Membrane attack complex |
| MFI | Median fluorescence intensity |
| MS4A1 | Membrane spanning 4 domains subfamily A member 1 |
| NGS | Next generation sequencing |
| NTP | Nucleoside triphosphate |
| PD-1 | Programmed cell death 1 |
| PBS | Phosphate buffered saline |
| tTA | tetracycline trans-activator |
| rtTA | reverse tetracycline controlled trans-activator |
| SELEX | Systematic evolution of ligands by exponential amplification |
| shRNA | Short hairpin ribonucleotide triphosphate |
| ssDNA | Single stranded deoxyribonucleotide triphosphate |
| TIB-152 | Acute T cell leukemia |
| VSV-G | Vesicular stomatitis virus envelope glycoprotein |

# 1 GENERAL INTRODUCTION

## 1.1 TARGETED MOLECULES FOR DIAGNOSTICS AND THERAPY

The cornerstone of all biochemical interactions is molecular recognition. It is the foundation on which gene expression, catalytic enzymes, and all manners of cellular signaling cascades rely upon (1). Targeted molecules are agents that can specifically detect and augment critical biomarkers (2-4). Modern medicine has benefitted enormously from the advent of targeted ligands, both as diagnostics as well as therapeutics. Targeted diagnostics can reliably evaluate disease emergence and progression (5); while targeted therapies directed to virulence specific proteins or biochemical pathways (6-8) aid in pathogenic clearance. Together they have not only contributed significantly to the better understanding of disease but, as drugs they are generally more efficacious, associated with fewer side effects and can significantly limit the extent of damage to surrounding cells and tissues (2, 9).

Targeted therapeutics include agents as diverse as antibiotics, anti-virals, small molecule inhibitors, shRNA and monoclonal antibodies (mABs). Antibodies are among the most prolific of targeted molecules and currently dominate both in diagnostics, best exemplified by ELISA kits (5, 10, 11), but also as highly successful therapies (2, 12, 13). Aptamers, which are targeted DNA molecules, rival antibodies in several key characteristics. They possess comparable specificity, in the nano to picomolar range (14-16), as well as a target specific mode of generation (17-19). Unlike proteinacious antibodies, aptamers are significantly more stable at ambient conditions, making them more amenable to diagnostic uses (20). They are non-immunogenic and can be selected

against virtually any target: protein, small molecules, and even whole cells (15, 16, 21-23). Aptamers have great potential and are becoming a rapidly growing consideration in the field of targeted molecular development.

The last 20 years have seen remarkable improvements in cancer treatments heralded by advancements in targeted therapies (13). Contributing significantly to this new age in oncology are therapeutic monoclonal antibodies (24-26). CD20 is a B-cell specific biomarker with vital anti-cancer considerations (27-29). To its credit, there are 12 anti-CD20 antibodies which treat a variety of immunological malignancies. We endeavoured to use a biologically conscious selection method to generate CD20 specific aptamers and to evaluate and compare their role and functionality against native anti-CD20 antibodies.

## 1.2 THERAPEUTIC MONOCLONALS

Monoclonal antibodies (mAbs) are an ideal marriage of target specificity and potent effector mechanisms, making them highly discriminative and biologically active drugs. Their prominence in oncology is significant. Targeted therapeutics make up 56% of all drugs used in cancer treatments (30). Of these 86% of all sales can be ascribed to just 5 drugs which—with the sole exception of Imatinib a small molecule inhibitor— are monoclonal antibodies (30). Unabated the global sales of anti-cancer medications are projected to reach $100 billion as early as 2016 (31). There is then great incentive to pursue targeted ligand development.

### 1.2.1 Structure and development

Therapeutic antibodies became technical possibilities after the advent of hybridoma technology, developed by Kohler and Milstein in 1975 (32). Hybridomas are the fusion product of antigen challenged and antibody producing B-cells with a highly proliferative myeloma, a B-cell cancer. The end product is a long-lived immortalized cell line which produces consistently large amounts of a single antibody (33).

With antigen inoculation performed in-vivo and the requisite cellular assays in-vitro the actual production of antibodies is both time consuming and laborious, in discovery as well as in commercial practise. In the research stages, every hybridoma and the antibody it secretes must be evaluated for specificity, function and potency (34). Commercial antibodies require clarification, purification, ultrafiltration and concentration as well as a quality control validation procedure performed on a batch by batch basis, as variability is common (33, 35). Even then, as proteins, their shelf life is inherently limited. These constraints make antibodies among the most expensive of drugs. Leukemia treatment using alemtuzumab, an anti-CD52 antibody, is $54,000 yearly (36); which pales to the $500,000 price-tag of eculizumab (37) a monoclonal developed for paroxysmal nocturnal hemoglobinuria—a disease with orphan status.

The antibodies themselves are heterodimeric proteins, composed of two light chains (one $V_L$ and one $C_L$ unit) and two heavy chains (one $V_H$ and 3 $C_H$ units) linked by disulfide bonds, see Figure 1.1. Pepsin digestion cleaves antibodies into two functional fragments, the Fab or *f*ragment of *a*ntigen *b*inding, which determines target specificity, and the *c*rystallisable constant domain or the Fc fragment, which controls the effector functions.

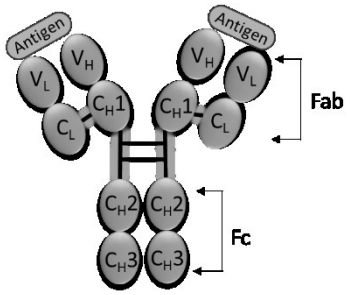


**Figure 1.1. General antibody structure.** Antibodies are composed of 2 functional domains linked together by disulfide bonds. The Fab fragment determines antigen specificity while the Fc portion mediates immune effector actions.

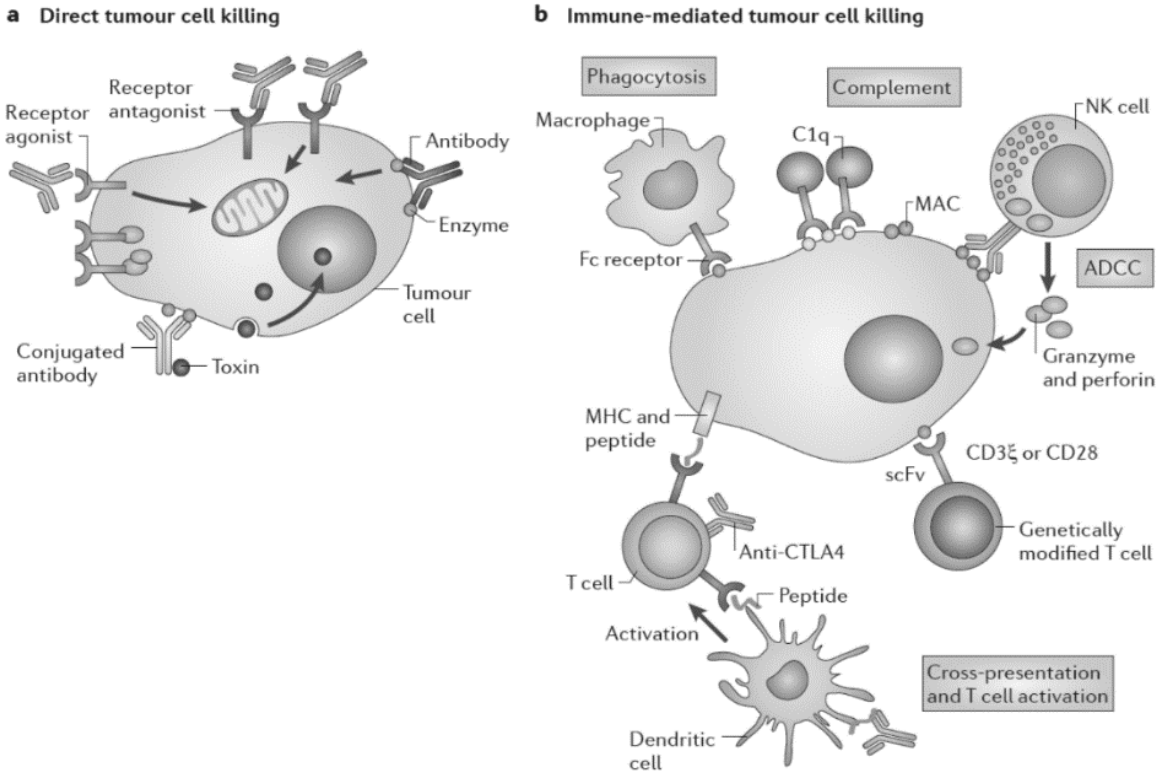


**Figure 1.2. Effector mechanisms of therapeutic monoclonal antibodies.** The cytolytic mechanisms of oncolytic monoclonal antibodies include both direct **(a)** and indirect strategies **(b)**. Direct methods are the result of antibody binding the target molecule stimulating pro-apoptotic cascades. Indirect methods are induced by the Fc portion and require the additional input of immune components in the form of serum proteins for CDC, or cells for ADCC, ADCP and cross presentation. Reproduced with permission: Scott, A.M. *et al*. Antibody therapy of cancer. *Nature Reviews Cancer*. **12**, 278-287 (2012).

### 1.2.2 Effector Mechanisms of Monoclonals

Antibodies are effective drugs due to their biological actions (13). Cytotoxicity can be induced directly, the result of Fab binding, or indirectly using the Fc region. See Figure 1.2. Direct cytotoxicity occurs when the antibody binds its target; the agonistic or antagonistic effect depends directly on the nature of the receptor. For example, many cancers cells are associated with the up-regulation of growth factors like EGFR (38). Anti-EGFR antibodies exert an antagonistic influence, hindering signal transduction, leading to cell death (39). This is the same mechanism by which other clinically efficacious antibodies including anti-CTLA4 (40) and anti-PD1 operate (41).

Indirect actions are mediated through the Fc domain and require additional immune components in the form of proteins (for CDC or complement dependent cytotoxicity) or cells (for ADCC: antibody dependent cell mediated cytotoxicity, ADCP: antibody dependent cellular phagocytosis, and cross presentation) (13). There are 4 indirect effector mechanisms noted in Figure 1.2. CDC is the result of an Fc specific interaction with serum complement factors resulting in the formation of a cytolytic membrane attack complex (MAC), which by disrupting osmotic homeostasis leads to cell lysis. In ADCC, antibodies recruit leukocytes to destroy opsonized targets via the controlled release of granulocytic enzymes. In ADCP the Fc fragment acts as phagocytic signal resulting in cellular digestion. In cross presentation the antibodies prime dendritic cells to activate cytotoxic T-cells against cancer specific markers. Antibody mediated cellular clearance is multifactorial and an immunologically complicated event.

The FDA approved the first antibody for cancer treatment in 1997. That antibody- rituximab- targets the CD20 molecule and has become the single most important

treatment of B-cell malignancies discovered within the last 20 years (12). This is in spite of the fact that the role and function of CD20 is not clear and that its natural ligand is also unknown. These factors aside it has not hindered drug development; CD20 is the target of 4 therapeutic mAbs currently approved and another 8 still in clinical development (42).

## 1.3 THE CD20 MOLECULE

### 1.3.1 Introduction and History of the CD20 Molecule

CD20 was the first B-cell differentiation antigen identified (43) and is a characteristic B-cell marker from the pre-B cell stage until plasma cell differentiation (44), see the Figure 1.3 below. It is a member of the MS4A1 gene family which encodes a 30-37kDa transmembrane phosphoprotein, depicted in Figure 1.4. CD20 spans the cellular membrane 4 times with 2 extracellular loops and both amino and carboxy termini located within the cytoplasm (45, 46).

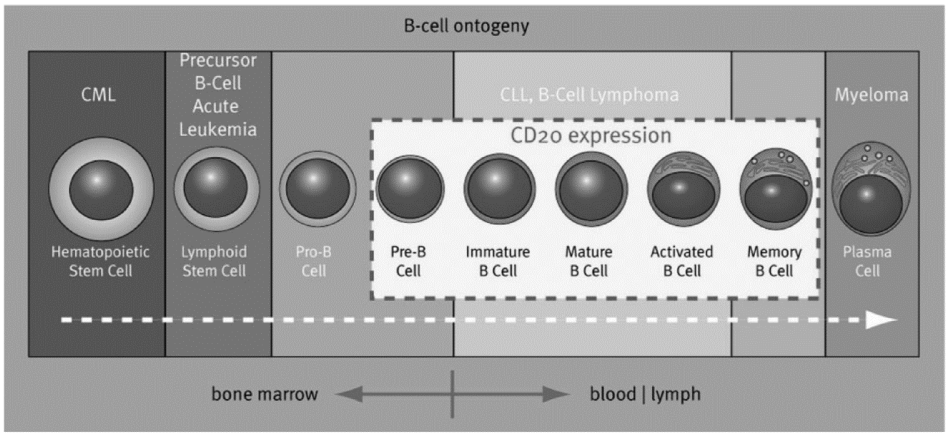


**Figure 1.3. CD20 expression in B cell ontogeny.** CD20 is a marker of B-cell development and maturation from the pre-B cell to memory B-cell stages. Therapeutic anti-CD20 antibodies are restricted to CLL (chronic lymphocytic leukemia) and B-cell lymphomas, cancers that exhibit positive CD20 expression. Reproduced with permission: Ruuls, S.R. *et al*. Novel human antibody therapeutics: the age of Umabs. *Biotechnology Journal*. **3**, 1157-71 (2008).

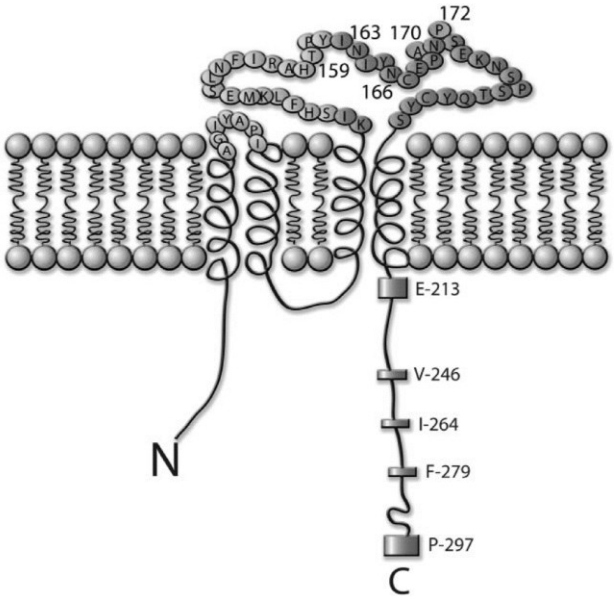


**Figure 1.4. The CD20 molecule.** CD20 is 30-37kDa transmembrane phosphoprotein with 2 extracellular domains. It spans the cellular membrane 4 times with both N and C termini located within the cellular interior. Mapping epitope studies have revealed that the binding site for rituximab lies along the larger amino acid loop and exhibits an absolute requirement for the ANP residues of 170-172. The binding of ofatumumab is disparate and localized to the smaller 7 amino acid loop. Reproduced with permission: Ruuls, S.R. *et al*. Novel human antibody therapeutics: the age of Umabs. *Biotechnology Journal*. **3**, 1157-71 (2008).

Structurally, CD20 exhibits significant similarity to ion channels proteins and studies have suggested that it may be involved in the regulation of calcium transport (47). The transfection of CD20 into lymphoid and non-lymphoid cells resulted in significantly elevated transmembrane calcium conductance, the use of anti-CD20 antibodies not only further increased conductance but also resulted in alterations in cell cycle progression (47). Golay et al showed that CD20 ligation in tonsillar B-lymphocytes could induce *c-myc* and *b-myb* gene expression, required for B-cell proliferation (48). Interestingly CD20 knock-out mice retain normal B-cell number, development, and responses; but the B-cells they produce exhibit 20-30% reduced IgM expression as well as lowered calcium responses when compared to the wildtype (49). In 2009 the case of a human patient with cryptic splicing in her MS4A1 gene was investigated. Though B-cell counts were normal, the patient exhibited a complete lack of CD20 expression, persistently low IgG levels, a decreased frequency of somatic hyper-mutations and a strongly reduced ability to mount T-cell independent immune responses (43). CD20 and its influence on immunity is still very much a matter of ongoing research.

### 1.3.2 Anti-CD20 Antibodies

Though the function of CD20 remains elusive, a consistent feature is that binding of anti-CD20 antibodies induce rampant and relatively widespread cellular depletion. Their use against CD20+ B-cell malignancies has been incredibly successful. There are currently 4 (Canada and US) approved anti-CD20 antibodies: rituximab, ofatumumab and the radio-conjugates bexxar and zevalin. Rituximab was originally licenced to treat aggressive and indolent Non-Hodgkin's lymphoma (50), it is now widely used against many CD20+ B-cell cancers and even rheumatoid arthritis (51, 52). Bexxar and zevalin

are the radio-conjugates, bound respectively, to radioactive yttrium-90 and iodine-131. Ofatumumab was the most recently approved, in 2009, to treat alemtuzumab and fludarabine resistant CLL (chronic lymphocytic leukemia) (53, 54). Epitope mapping studies have shown that ofatumumab recognizes a distinctly different site on the CD20 molecule than rituximab. Ofatumab specifically binds the smaller loop proximal to the cell membrane, while rituximab's binding is restricted to the larger extracellular domain (29, 55). When compared to rituximab in in-vitro trials, ofatumumab is also a consistently more potent inducer of CDC (55, 56).

While the relationship between epitope specificity and effector mechanisms remain to be entirely elucidated; the growing interest in the development of anti-CD20 antibodies highlights the increased demand for targeted ligands. Especially to a molecule whose effects, if not well that well understood, are profound. Aptamers with targeted specificity to CD20 would serve as enhanced diagnostic and therapeutic vehicles with broader utility than antibodies. With a longer shelf life and structure invariability, they are more economical and a more widely applicable tool for diagnostic assays. As therapies, they can be formulated as functional agents or carrier molecules delivering cytotoxic drugs in a target specific manner. Aptamers could greatly contribute to and would greatly further the current understanding of this molecule. With this in mind, we endeavoured to generate a CD20 specific aptamer selection protocol.

## 1.4 APTAMER INTRODUCTION

Aptamers are short DNA or RNA molecules, typically 60-120 nucleotides long, raised to specifically recognize a target of interest in a process known as selection (18, 57). They fold into stabilized 3D forms and have the capacity to label, detect and augment the

biological interactions of their target with a high degree of avidity and affinity (23, 58, 59). These characteristics have seen them commonly referred to as a "chemist's antibody" (60).

Despite this moniker, aptamers possess significant advantages to antibodies. Aptamers are artificially generated and do not require the labour intensive and considerably expensive methods of in-vivo selection (59). Being wholly synthetic endows them with a capacity to withstand long-term storage conditions. DNA is significantly more stable across a variety of temperatures and can be denatured and re-natured without degradation (61). Antibodies, however, must be maintained in a temperature controlled environment to preserve structure and function, and even with preservative agents still possess an inherently limited shelf life. Moreover antibodies can vary batch by batch, and require routine performance validation (62) while aptamers are synthesized consistently and with great accuracy every time. Nucleotide modifications can greatly broaden an aptamers utility. The use of unnatural nucleotides or functionalized moieties can be used to protect aptamers from nucleases and increase their stability and in-vivo retention (63, 64). Unlike antibodies which can only be generated to antigens with immuno-stimulatory capacities (65, 66), aptamers can be raised to virtually any target-including ions, small molecules, proteins, and agents which would not otherwise elicit a potent immune response. Aptamers have successfully been selected for zinc ions (21), anthrax spores (67), influenza virus (68), a multitude of proteins including alpha-thrombin and tenascin-C (15, 23), and even whole cells (16, 69-71).

Like antibodies, aptamers have the potential to be therapeutically efficacious. Macugen is an aptamer raised to VEGF (vascular endothelial growth factor) and is clinically

approved for wet age-related macular degeneration (72). There are another 10 aptamers, for various therapeutic indications, in clinical trials (73).

### 1.4.1 Aptamers are created by SELEX

Aptamers are generated from an initial randomized library through an iterative selection process known as SELEX or the *S*ystematic *E*volution of *L*igands through *EX*ponential amplification. Discovered independently in 1990 by two groups of researchers, Golds (57) and Szostak (18), SELEX begins with a library composed of $1x10^{15-20}$ different DNA or RNA sequences. Each round of selection isolates and retains increasingly higher affinity ligands while weak and non-binding sequences are discarded. This sequential enrichment process culminates with a pool containing high affinity aptamers.

Selection methods can vary extensively and include solid support strategies that immobile the target of interest onto beads (14, 74, 75), membranes affinity columns (21), and nitrocellulose filters (76, 77). There are also gel and liquid based selection techniques like electrophoretic (78) and microfluidic SELEX (79), in-vitro cell based strategies (19, 80) and relatively recently in-vivo selection (81). Solid support systems like beads or membranes represent the most controlled environment, with parameters like concentration and abundance determined at the users' discretion. A major caveat is the lack of physiological context (80, 82). As target-specific as solid support systems are there is no guarantee that aptamers selected in this manner—to artificially immobilized purified protein extracts—will retain their specificity in an in-vitro setting. Their capacity to function in-vivo is equally uncertain. Thus, to better account for the in-vitro

environment and the dynamic complexity of living samples cell-SELEX was developed (19, 60).

### 1.4.2 Cell-SELEX

Cell-SELEX can generate aptamers whose specificity is to whole cells, (Figure 1.5). Weak and non-binding aptamers are removed by washing or by using negative (counter) selection with a competing background cell group. By coupling positive and negative selection it enhances the discriminative capacity of a pool. In one of the first recorded instance of its use, Wang's incorporation of what he called "subtractive" SELEX was able to generate aptamers specific only to nerve growth factor (NGF) differentiated PC12 cells, an embryonic cell line, and not their original parental form (71). Cell-SELEX has also successfully identified aptamers that discriminatively label lung adenocarcinomas (16), liver cancer cells (70), and gastric carcinoma (83, 84), among others.

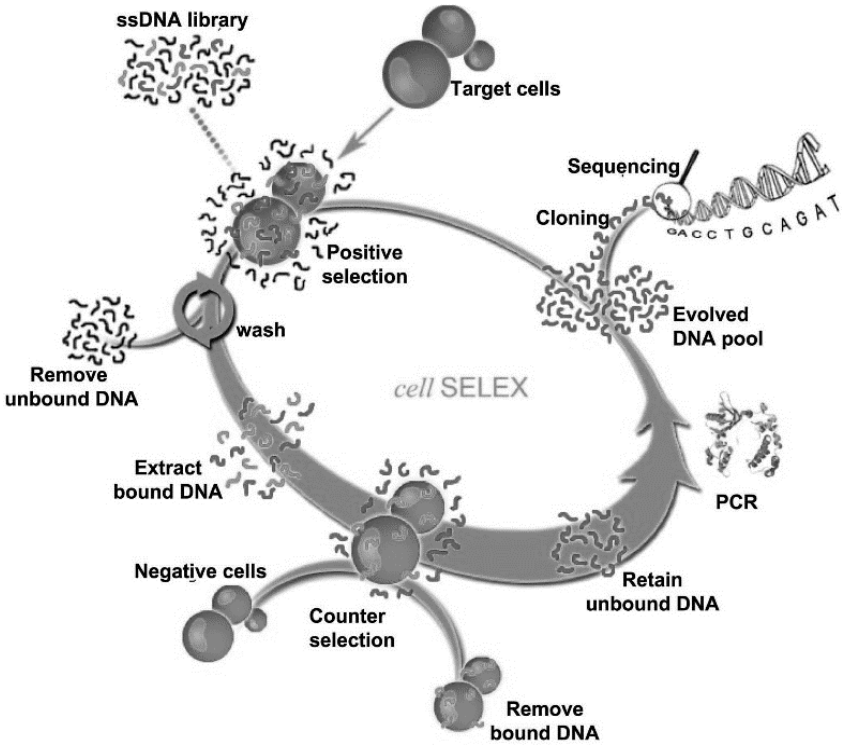


**Figure 1.5. Cell-SELEX.** Generalized selection scheme of cell-SELEX using positive and negative cells. The use of duelling cell lines enhances the discriminative capacity of the aptamers generated. Aptamers that bind positive cells are retained, while aptamer that associate with negative cells are discarded. Reproduced with permission: Sefah, K. *et al*. Development of DNA aptamers using cell-SELEX. *Nature Protocols*. **5**, 1169-1185 (2010).

The major advantage of cell-SELEX is biomarker discovery (85). Aptamers that label and specifically detect cancer cells can be used to better inform on cancer specific characteristics including different phenotypes, the over or under expression of target proteins or mutations on the genetic level. However, cell-SELEX is hampered by the lack of target identity. Elucidating the target of a high affinity aptamer generated through conventional cell-SELEX is daunting work, given the plethora of possible binding sites on cells. These may include embedded and peripheral proteins, any of their distinct epitopes, branched glycosylated groups as well as the heterogenetic membrane lipids themselves. Thus, with cell-SELEX what is gained by the biological context is tempered by the lack of target identity.

To counter this, some SELEX strategies incorporate more than one selection method (86). Cross-SELEX uses target-specific solid selection initially and follows up with cell-SELEX for biological context. And while it has proven effective (15, 87, 88), it is inefficient and does not guarantee the truest high affinity binders but rather the one that best accommodates both techniques. Genetic transfection of cells, which couples target specificity with a cellular environment, is a solution to this dilemma.

### 1.4.3 Viral Transfection for Target Specific Cell SELEX

Transfection broadly refers to the transfer of genetic material into a cell for the purposes of modulating its expression profile. Current techniques are divided into transient transfection where expression is limited, or stable transfection—significantly the viral mediated strategies—where expression is more permanent (89).

Stable transfection is a technique that emerged after the discovery of DNA-integrating and transforming viruses (90, 91). Originally it was observed that Rous sarcoma virus,

papovaviruses, and adenoviruses could, in the course of infection, convert an otherwise normal cell into its cancerous neoplastic version. Studies later showed that this is achieved via the insertion of proto-oncogenes directly into host DNA, thereby deregulating vital functions leading to malignancies. The chromosomal integration of these genes is heritable and passed down from mother to daughter cells (91). Modern day viral mediated gene transfer was founded on these principals, and by exploiting viral machinery can achieve the same goals, culminating in the site-specific insertion and expression of a gene of interest (GOI).

In contrast, in non-viral methods the GOI is carried on a plasmid and then subjected to microinjection, electroporation and/or calcium phosphate transfection into the host cell. However, without a strategy to ensure their genetic incorporation, the information encoded in the plasmid is most often lost during the next subsequent cell division. Non-viral transfection is inherently time-sensitive resulting in transient, not stable, gene expression (92).

For stable transfection, retroviruses and lentiviruses make for compact and effective gene delivery vectors. They come packaged with all the necessary components to mediate cellular entry, localization signals for nuclear trafficking, integration factors to insert into the host genome, and mechanisms that even allow for modular GOI expression. We used a lentiviral based gene transfer system to generate a CD20 specific cell-SELEX protocol. In this method of cell-SELEX, target positive cells expressed CD20; target negative untransfected cells did not. This strategy fuses the target specificity of immobilized SELEX methods but in the contextually relevant confines of a live cellular system.

### 1.4.4 Target Positive Cell-SELEX using CD20 Transfected HEK Cells

The selection protocol for generating CD20 specific aptamers is depicted in its entirety in Figure 1.6 below. The initial DNA library consisted of approximately $1x10^{15}$ random single stranded sequences, 100 bases in length. As indicated in Figure 1.6A every DNA molecule possesses two 20 nucleotide long primer regions found at the 5' and 3' termini, which facilitate PCR amplification, and an internal randomized 60 nucleotide segment. Figure 1.6B pictorially represents the target positive CD20 transfected cells (CD20+HEK) and the untransfected target negative (HEK) cells with CD20 expression indicated by the red star. 10 rounds of selection were performed using both positive and negative cells. Positive selection denotes the incubation and retention of the DNA ligands that associate with the CD20+HEK transfected cells whereas negative selection exerts a purifying influence by eliminating DNA ligands that associate with the native and untransfected HEK cells. In this way aptamers are evolved with heightened specificity to the key difference between the two cell lines—CD20 expression.

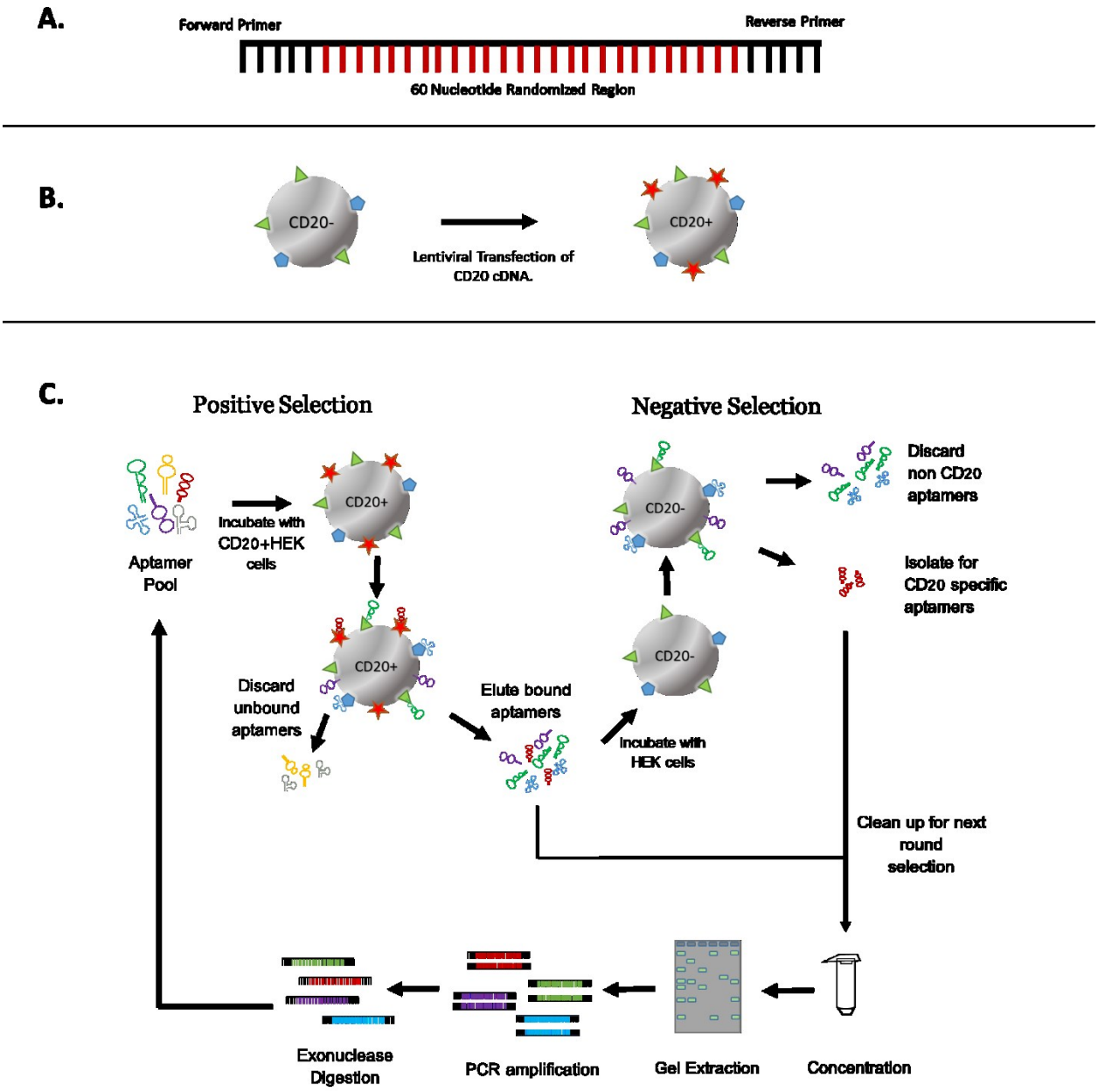


**Figure 1.6. Complete selection protocol for CD20 target positive cell-SELEX.** **A)** A schematic of a single DNA aptamer including the 20 nucleotide long forward and reverse primer regions and the internalized 60 nucleotide variable region. **B)** A depiction of CD20+HEK cells, with CD20 pictorially represented as a red star, and untransfected HEK control cells. **C)** Generalized selection protocol cells for generating CD20 specific aptamers. In total 10 rounds of selection using CD20+HEK as positive and untnransfected HEK control cells were performed. The preparatory clean-up protocol used to purify and amplify DNA pools in between subsequent rounds of selection is also included.

The selection regime begins with heat denaturation and rapid snap cooling of the DNA to ensure that the sequences assume their unique energetically stabilized secondary structure, prior to incubation with the target CD20+HEK cells. Unbound or weakly bound sequences are washed away and CD20+ specific aptamer are eluted. For the first few rounds of selection, it is important to enrich the pool in sequences specific to the positive cell line and so negative selection is not performed. When negative selection becomes applicable, the eluted DNA pool is denatured and subsequently incubated with the untransfected HEK cells. In negative selection only the aptamers which do not bind HEK cells are desired; for that reason the supernatant is retained while both the negative cells and the sequences bound to them are discarded.

In order to purify, amplify and prepare each pool for the next subsequent round of selection, an appropriate work up was necessary. Eluted DNA pools are typically collected in a volume of 1 mL and may contain extraneous materials (proteins, lipids, and other cellular debris) acquired during selection. These contaminants complicate PCR amplification and will generally degrade a pool over time. To remedy this the pool is concentrated, with the use of a molecular weight cut-off filter, to a workable volume. Secondly the aptamer DNA is purified using agarose gel extraction and then PCR amplified for the next round of selection using PCR. The last step is the digestion of the 5'- 3' strand of the amplified DNA using a T4 exonuclease. Single stranded DNA is more amenable to SELEX as it can assume the secondary structures required to bind the target of interest.

In total, 10 rounds of aptamer selection were performed. Pools were evaluated with the transfected cells for total binding capacity; and for specificity, were evaluated with

independent cells lines of varying CD20 expression. Next generation sequencing of the best binding pool was used to characteristically analyze and isolate for the most representative aptamers. These were also evaluated for affinity, specificity and their impact on the biologically motivated and anti-CD20 antibody induced complement dependent cytotoxicity.

## 1.5 THESIS OVERVIEW

The thesis has been separated into 4 chapters. Chapter 2 is a cumulative list summary of the materials and methods used for the proceeding sections. Chapter 3 details the genetic transfection, the establishment of CD20+HEK cells and the aptamer pool selection. Chapter 4 covers the next generation sequencing results and the binding and target specificity of the aptamer clones. Chapter 5 provides the biological results, specifically CDC induction and the protective effect of the aptamers. A general conclusion is also included which summarizes the major findings.

# 2 MATERIALS AND METHODS

## 2.1 TRANSFECTION AND APTAMER POOL SELECTION OF CD20+HEK APTAMERS

### 2.1.1 Generation and Verification of CD20+HEK Cell line

#### *2.1.1.1 Construction of CD20 containing pLVX-TRE3G Vector*

Wildtype CD20 cDNA was a kind gift from Genmab. The circularized pLVX-TRE3G vector was linearized using MiuI and EcoRI restriction endonucleases, with incubation performed at 37°C for 3 hours. To purify the vector DNA, the linearized DNA product was run through a 1% agarose gel with a molecular weight ladder and excised using the GeneJET gel extraction kit. To subclone, the cDNA was first amplified using Clontech Laboratories CloneAmp HiFi PCR premix using 15 base pair extended primers with homologous ends to the linearized pLVX-TRE3G vector. Ligation of the amplified PCR product with the linearized vector was performed using Clontech's Fusion HD cloning kit; using 50ng of the purified CD20 cDNA, 100ng of the linearized vector, 2µL of 5x In-fusion HD enzyme premix and 7µL of deionized water. The insertion of CD20 cDNA in the vector was verified using PCR and gel electrophoresis.

To generate sufficient quantities of the vector for transfection, 2.5 ng of the cloned pLVX-TRE3G were mixed on ice with one reaction vessel (50µL) of Clonetech's Stellar Chemically Competent Cells. The mixture was heat shocked for 45 seconds at 42°C, and then cooled on ice for 2 minutes. Super optimal broth with catabolite repression (SOC) media was added to a final volume of 500 µL and the cellular suspension plated on 100 µg/ml ampicillin fortified agar media overnight at 37°C. Individual bacterial cells were

picked from the plate, and grown in ampicillin fortified LB media (100 mg/mL) for 12 hours. Plasmids were extracted using the GeneJET plasmid miniprep kit according to the manufactures instruction. Purified plasmids were sequenced at The Centre for Applied Genomics (TCAG) to validate CD20 insertion.

#### *2.1.1.2 Lentiviral Production and Transfection*

The CD20 containing pLVX-TRE3G plasmids were transfected into the Lenti-293 packaging cell line using Clontech's Lenti-X HTX Packaging System, part of the Lenti-X Tet-on 3G Inducible Expression System, according to the manufactures instructions. Virus particles were harvested 48 hours after initial transfection, with viral concentration exceeded 50,000 IFU/mL as measured using the Lenti-X Go-STIX. Freshly harvested lentivirus was used to transfect wildtype HEK293 cells, according to the manufactures instructions. Briefly, viral stocks were diluted in polybrene (final concentration: 4 μg/mL) in 10% FBS fortified Dulbecco's modified eagle media (DMEM) and added dropwise to the plated cells. To increase transfection efficiency the plated cells were centrifuged at 1,200 RCF at 32°C for 60 minutes, before being placed into the incubator at 37°C for 48 hours. To select for and isolate successfully transfected cells the media was fortified with G418 (1 mg/mL). Cells were re-cultured every 3-4 days as needed for 2 weeks. The pLVX-TRE-3G vector incorporates the inducible tet-on operon upstream of the multiple cloning site, once cell growth after selection had stabilized, the induction of CD20 was initiated using doxycycline (500ng/mL).

#### *2.1.1.3 Cellular Maintenance*

All cells were maintained in a humidified incubator at 37°C and 5% $CO_2$ an in 100 $mm^2$ plates. Both untransfected and CD20+HEK cells were maintained in DMEM containing

10% fetal bovine serum. CD20+HEK cellular media was fortified with doxycycline (500 ng/mL) to ensure constant expression. TIB-152 and CCL-86 were purchased from American Type Culture Collection (ATCC) and grown in Roswell Park Memorial Institute media (RPMI-1640) supplemented with 10% FBS.

#### *2.1.1.4 Flow Cytometry Detection of CD20*

To evaluate CD20 expression cells adherent CD20+HEK and HEK control cells were liberated into single celled suspension using non-enzymatic cell stripper. Cellular quality is assessed using the Muse count and viability reagent, according to the manufacture's instruction, only cells with greater than 90% viability were used. 500,000 cells were aliquoted into micro-centrifuge tube and incubated with 10 ng/µL FITC labelled anti-CD20 antibody for 30 minutes on ice. Cells were washed twice with PBS, re-suspended in the buffer and evaluated using a Beckman Coulter FC500 flow cytometer where 40,000 events were counted. Fluorescence data was analysed using GraphPad Prism Software version 5.0.

#### *2.1.1.5 Immunofluorescence Detection of CD20+HEK*

CD20+HEK and the untransfected HEK control cells were grown in imaging chambers until 80% confluent in doxycycline fortified DMEM media. For imaging, the spent media is aspirated and the monolayer washed with PBS. Cells were fixed using 4% PFA for 20 minutes. For analysis, the fixed cells were blocked using a solution of 10% FBS in PBS for 2 hours and then incubated with primary FITC labelled anti-CD20 antibody (50ng/µL) for 1 hour in the dark. After washing the cells were counterstained with DAPI (4',6'-diamidino-2-phenylindole), mounted on glass slides and imaged using a conventional fluorescence microscope.

#### *2.1.1.6 Contextual anti-CD20 Expression*

To contextualize CD20 expression the lymphocytic CCL-86 cells and TIB-152 cells were used alongside the CD20+HEK transfected cells. CCL-86 cells are a B-cell line that naturally express CD20 while TIB-152 T-cells do not. 500,000 cells were aliquoted into micro-centrifuge tubes, washed twice in PBS, and then re-suspended in FITC labelled primary anti-CD20 antibody diluted at the following concentrations for 30 minutes on ice: 100 ng/µL, 50 ng/µL, 10 ng/µL, 5 ng/µL, 2.5 ng/µL and 1 ng/µL. After washing, cells were evaluated using a FC500 flow cytometer where 40,000 events were counted. Fluorescence data was analyzed using GraphPad Prism Software version 5.0.

### 2.1.2 Selection Protocol-Cell SELEX

#### *2.1.2.1 DNA Preparation and Aptamer Pool Selection*

The initial library was purchased from IDT (Integrated DNA Technologies) and contains $10^{15}$ random sequences. It is 100 base lengths in size consisting of a 60 base length randomized internal region flanked on either side by constant primer regions as such: 5' CTCCTCTGACTGTAACCACG-N60-GCATAGGTAGTCCAGAAGCC 3'. The initial lyphophilzed stock was re-suspended in 1X-TE buffer at a final concentration of 100µM as per the manufacturer's instructions. Prior to each round of selection the DNA sample is diluted to the requisite concentration (see Chapter 3 Table 1), denatured at 95°C for 10 minutes and snap cooled on ice for a minimum of 5 minutes before use.

Positive selection denotes selection performed using transfected cells CD20+HEK and is always performed before negative selection using un-transfected HEK cells. Each round of selection consumes 1 100mm$^2$ polystyrene plate with cells grown to 90% confluency. For selection, the spent media is aspirated and the monolayer of cells washed with PBS

twice. The DNA solution denatured, snap cooled and diluted to a final volume of 1000 µL is applied drop-wise to the CD20+HEK monolayer. The sample is incubated at 37°C on a heated shaker. For rounds 1 through 4 no negative selection was used, therefore after incubation the cells are collected into a 15mL Falcon tube and washed twice with PBS. To elute the aptamers the cellular pellet is heated to 95°C with gently vortexing for 10 minutes, centrifuged at 1000RCF for 5 minutes and the supernatant collected.

For selection rounds that incorporate negative selection, rounds 4-10 inclusive, after the eluted aptamers are collected they are applied to a 100mm² plate containing washed un-transfected HEK cells. The aptamers are applied drop-wise to the cellular monolayer, and are incubated for the allotted time indicated in Chapter 3 table 1. The supernatant, containing unbound aptamers, is then carefully collected. This comprises the cell-based component of selection.

#### *2.1.2.2 Selection Protocol-Work Up*

To prepare each pool for the next subsequent of selection the samples is concentrated using Amicon 5000kDa molecular weight cut-off filters. This device is bipartite; first the DNA pool is first applied to the upper filter and spun using a table top centrifuge at 2800 RCF for 2 hours, the filtrate containing low molecular weight debris is discarded. In the second step the internal compartment is reversed and spun down again at 2800 RCF for 5 minutes. 1 mL of solution was concentrated to a typical final volume of 50µL. The concentrated DNA pool is then purified using agarose gel extraction. The DNA pools are run alongside a MW ladder on a 3% agarose gel for 30-45 min at 200V. The 100bp band is excised and purified with the GeneJET extraction kit. The collected and extracted DNA pool is PCR amplified with Thermoscientific Phire Hot Start DNA

Polymerase kit according to the manufactures instructions. In each 50 µL of the reaction mixture is 1x phire reaction buffer, 2%DMSO, 200 µM of dNTPs, 0.02U/µL of the Phire Hot Start II DNA Polymerase and 0.5 µM of both primers the 5'-Cy5-labeled forward primer and the 5´-phosphorylated reverse primer. 30 cycles of PCR were performed according to the following: denaturation at 95 °C for 30s, annealing at 56°C for 15s, and extension at 72°C for 10s. DNA amplification is verified on a 3% agarose gel. To generate a single stranded product Lambda exonuclease (New England Biolabs), was used according to the manufactures instruction, for 2 hours at 37°C.

### 2.1.3 Evaluating Aptamer Enrichment with CD20+HEK

Adherent CD20+HEK cells were removed from the plate using non-enzymatic cell stripper. Cells were washed twice in PBS, and counted using Muse cell count and viability reagent. 250,000 cells were aliquoted into each micro-centrifuge tube and incubated with relevant DNA pools derived from the unselected library and pools 1,5 and 10 of selection at a concentration of 200nM. Cells were incubated at 37°C for 30 minutes, washed twice with PBS, re-suspended in buffer and evaluated by a Beckman Coulter FC500 flow cytometer where 40,000 events were read. The MFI values of each curve were measured using Free Flowing Software and tabulated using GraphPad Prism Software version 5.0.

### 2.1.4 Evaluating Aptamer Pools Across Cell Lines

In addition to CD20+HEK and the untransfected HEK control cells the lymphocytic cells lines, CCL-86 and TIB-152, were used. Adherent cells were treated as above, while lymphocytic cells were harvested from suspension. 500,000 cells were aliquoted into micro-centrifuge tubes and incubated for 30 minutes with aptamer pools 1 and 10 at

37°C for 30 minutes. Cells were washed with PBS, re-suspended in buffer and evaluated using a Beckman Coulter FC500 flow cytometer where 40,000 events were read. The MFI values of each curve were measured using Free Flowing Software and tabulated using GraphPad Prism Software version 5.0.

## 2.2 NGS Analysis and Evaluation of Aptamer Clones

### 2.2.1 Sample Preparation

Aptamer pool 10 was amplified using Illumina specific bar codes (5' ACACTGTC). The DNA was run on a 3% ultrapure agarose gel and purified using the GeneJET extraction kit. The final amount of 200ng was combined with other samples and sequenced in a single lane of Illumina Mi-Seq by the Eurofins Genomics Company. Data was received as a compiled fastaq file and subsequently uploaded, converted to fasta format and analyzed using the online Galaxy module (93-95). Data was clipped for length and collapsed to amalgamate sequences. To analyze sequence dependent relationships and build the phylogenetic trees the sequences were uploaded and analyzed using Clustal Omega (96). Their website is found at http://www.ebi.ac.uk/Tools/msa/clustalo/. Motif analysis was performed online using the DREME motif analyzer (97) part of the MEME NCBR database at http://meme.nbcr.net/meme/doc/dreme.html. The shape of the candidate sequences was analyzed using the RNAstructure platform (98), found online at http://rna.urmc.rochester.edu/RNAstructureWeb/.

### 2.2.2 Aptamer Clone Assessment

Aptamers NLA-1 to NLA-4 were ordered as Cy-5 labelled clones from IDT (Integrated DNA Technologies). For $K_d$ assessment the aptamers were diluted to the required

concentrations, denatured at 95°C for 10 minutes and snap cooled prior to use. CD20+HEK cells were prepared as above by sloughing from plate, washing in PBS, and then re-suspending the cells in the diluted aptamer clones for 30 minutes at 37°C. Cells were washed with PBS, re-suspended in buffer and analyzed using a FC500 flow cytometer where 40,000 events were read. For $K_d$ analysis the tabulated MFI were input into GraphPad Prism Software version 5.0 and the data fitted using a non-linear regression. $K_d$ value was measured per the formula $Y = B_{max}X/( K_d + X)$, where Bmax represents the maximal binding limit, $X$ is for the concentration of ligand and the $Y$ is the bound fraction.

### 2.2.3 Assessment of specificity

NLA aptamers were diluted to 300nM, heat denatured at 95°C for 10 minutes and then snap cooled on ice. The aptamer were incubated with prepared CD20+HEK and the untransfected HEK cells for 30 minutes at 37°C. The samples were washed, re-suspended in buffer and analyzed using an FC500 flow cytometer. The MFI values of each curve were measured using free flowing software and tabulated using GraphPad Prism Software version 5.0.

### 2.2.4 Co-stain experiments

CD20+HEK cells were prepared as above. Cellular aliquots consisting of 500,000 cells were incubated with separately with initial DNA library, or a pool containing an equimolar combination of the NLA aptamers and incubated for 30 minutes at 37°C. For the co-stain samples, FITC anti-CD20 antibody was added at a concentration of 10ng/µL and incubated for an additional 30 minutes. The cells were washed and evaluated by a Beckman Coulter Gallios flow cytometer. The MFI readings in the FL1

channel, for FITC detection, were measured using Kaluza software and tabulated using GraphPad Prism Software version 5.0.

## 2.3 BIOLOGICAL ASSESSMENT

### 2.3.1 Initial CDC Assessment of CD20+HEK and CCL-86 Cells

Adherent transfected CD20+HEK cells were collected as above while CCL-86 cells were collected from cellular suspension. Cells were washed in PBS and re-equilibrated by incubating in un-supplemented media for 1 hour prior to use. Initial viability was assessed using the Muse count and viability reagent per manufacture's instruction. 150,000 cells were aliquoted into micro-centrifuge tubes and incubated with 10ng/μL of anti-CD20 antibody or 15 minutes before the addition of either PBS, PBS with 50% fresh frozen human serum or PBS with 50% heat inactivated human serum. The latter is generated by heating frozen human serum for 1 hours at 57°C as is referenced in Moore et al (99) and Lida et al (100). Cellular viability was assessed after 4 hours at 37°C, when CDC was considered complete.

### 2.3.2 Binding of Aptamer Clones to the CCL-86 cells

To evaluate the binding of the aptamers with CCL-86 cells, the cells were first collected from suspension and washed in PBS. 200,000 cells were aliquoted into micro-centrifuge tubes and incubated with 2μM of either the DNA library or a pooled collection of the Cy5 labelled NLA aptamers for 30 minutes at 37°C. After which the cells were washed, re-suspended in buffer and evaluated using a Beckman-Coulter Gallios Flow Cytometer and analyzed using Kaluza Software. Tabulated data was generated using GraphPad Prism Software version 5.0.

### 2.3.3 Aptamer Mediated Inhibition of CDC

CCL-86 cells were collected from suspension, washed twice with PBS and equilibrated by incubating in un-supplemented RPMI-1640 media for 1 hour prior to use. Cellular quality was assessed using the Muse count and viability reagent, only cells with greater than 90% viability were used. Cell solutions containing 300,000 cells were aliquoted, spun down and re-suspended in 2μM aliquots of PBS diluted NLA aptamers or DNA library for 30 minutes at 37°C. CDC was induced using 10μg/mL of anti-CD20 antibody in a solution of PBS with either 50% fresh frozen human serum or, as a control, 50% heat inactivated human serum, at 37°C for 4 hours. To assess viability in more depth we used the BD Pharmingen PE-Annexin V Apoptosis Detection Kit, according to manufactures instruction. Samples from the cellular aliquots were added to 1X Annexin-V buffer and incubated with 7-AAD and PE labelled anti-annexin-V antibody for 15 minutes in the dark. Cells were evaluated using a Beckman Coulter Gallios flow cytometer where 50,000 cells were measured. The data was analyzed using Kaluza software and the MFIs for FL2 (PE-annexin-V) and FL4 (7-AAD) were tabulated using GraphPad Prism Software version 5.0.

## 2.4 Statistical Analysis

Statistical analysis was performed using GraphPad Prism Software version 5.0 for Windows, with values represented as means with standard error of the mean (SEM). Statistical significance was calculated using the student *t*-test and evaluated where $p<0.05$.

# 3 TRANSFECTION AND APTAMER POOL SELECTION

## 3.1 ABSTRACT

CD20 is a clinically important receptor and the target of several anti-cancer immunotherapeutics. HEK293 cells, an ordinarily CD20 negative cell line, were stably transfected using a lentiviral system for the constitutive expression of this marker. Target positive (CD20+HEK) and target negative (CD20-HEK) were the basis for a CD20 specific cell-SELEX protocol. CD20 expression was verified using flow cytometry and fluorescence microscopy. 10 rounds of cell-SELEX with the CD20+HEK cells evolved a pool of high affinity and discriminative aptamers with increased binding associations to the transfected CD20+HEK cell line, and not with the untransfected HEK cells. Pool 10, which contained the highest affinity binders, also showed heightened affinity to a naturally CD20 positive B-cell line, CCL-86, but not the naturally CD20 negative T-cell line, TIB-152. Therefore, SELEX using target positive transfected cells is an effective strategy for evolving high affinity and discriminative aptamers.

## 3.2 BACKGROUND

### 3.2.1 Characteristic of Lentiviral System

We employed a lentiviral based gene transfection system in order to generate CD20 target positive cells for aptamer selection. Lentiviral transfection methods are based on the prototypic lentivirus—HIV (101). But in the 20 plus years of their development, and in their current fifth generation, they have undergone significant genetic engineering

designed to increase safety, remove pathogenicity, broaden tropism, and even regulate GOI (gene of interest) expression (91).

#### *3.2.1.1 Gene Expression is controlled by Modular Cassettes*

Figure 3.1 summarizes some of the most significant modifications of lentiviral vectors within the last 20 years (91). Lentiviruses for gene expression must still operate as DNA transformation viruses, but with strict safety restrictions that help to eliminate the risk of creating replication competent lentiviruses (RCLs). Doing so necessitated the modification and eventual segregation of the required genes onto modular cassettes. Cis-acting elements encode the genes required for RNA synthesis, packaging, reverse transcription and integration. These are wholly separated from the trans-encoding elements, which encode the structural and enzymatic proteins (91). The success of modern lentiviral vectors can be attribute to various critical innovations, some of which are briefly covered below.

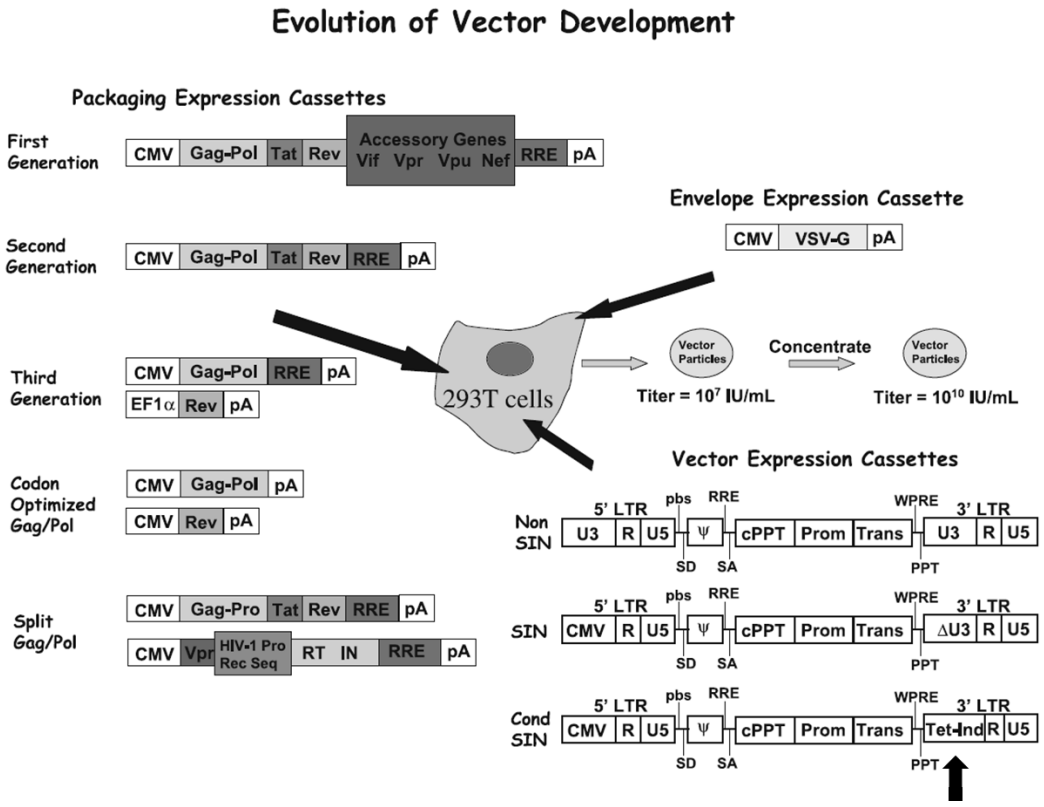


**Figure 3.1. The evolution of lentiviral vectors for the purposes of mammalian gene expression**. Lentiviral transfection requires 3 key genetic components, here divided into cassettes. The envelope expression cassette determines cellular tropism through the VSV-G capsid protein. The packaging and expression cassette carries the trans-elements and encodes the structural and enzymatic proteins. The vector expression cassette encodes the GOI and carries the cis-acting elements, which regulate its activity. Here, all 3 cassettes are shown transfecting HEK293T cells a *h*uman *e*mbryonic *k*idney cell line known for being highly susceptible and amenable to genetic engineering. Reproduced with permission: Cockrell, A.S. *et al*. Gene delivery by lentiviral vector. *Molecular Biotechnology*. **26**,184-204 (2007).

One of the first and most important developments was the substitution of the original HIV envelope genes to the *VSV-G* glycoprotein; see the envelope expression cassette in Figure 3.1. This was associated with notable improvements most importantly it broadened tropism, directed endocytic entry, and stabilized the vector during centrifugation (102).

The packaging/expression cassettes have undergone the most extensive modifications, and are currently in their 5$^{th}$ generation. They encode the trans-elements most critically the gag and pol genes which aid in the synthesis of the structural and enzymatic proteins required for functional vector particles. An early significant breakthrough, and one that helped to eliminate pathogenicity, was the removal of viral accessory genes *vif, vpr,vpu* and *nef*. This increased efficiency but, more importantly, without these proteins the viral vectors are rendered non-pathogenic (103).

The vector expression cassette encodes the cis-acting elements and, most importantly, the GOI; in Figure 3.1 it is indicated as the trans (transgene) cassette downstream of a prom (promoter) element. The vector expression cassettes have also been modified to increase safety. SIN vectors, where SIN=*s*elf-*in*activating, were generated by deleting the promoter and enhancer elements inherent to the 3'LTR. Because the 5'LTR is copied from the 3'LTR during reverse transcription, this deletion ensured that the integrated provirus remains replication incompetent (101). Another key modification, and a variation on SIN vectors is cond-SIN, this involved the incorporation of the tetracycline-inducible element Tet-Ind (see black arrow in Figure 3.1) to permit modular gene expression.

#### *3.2.1.2 Conditional Gene Expression using Tet-System*

Lentiviruses that incorporate the tetracycline inducible system permit the regulated control of GOI expression (104). The Tet system was derived originally from the tetracycline resistance operon in *Escherichia coli* (105). For the purposes of regulating gene expression, the original Tet-operon was reformulated and genetically engineered into two distinct systems. There is the original Tet-off using the *tTA* gene (tetracycline trans-activator) (105) or the Tet-on using the *rtTA* gene (reverse tetracycline controlled trans-activator) (106), they exert similar but entirely opposite actions. These are depicted in Figure 3.2. In Tet-off, transcription of *tTA* gene generates a TetR protein called tTA which will only bind the Tet-op promoter and transcribe the gene of interest in the absence of tetracyclines. The presence of tetracyclines, to which tTA affinity is very high, will turn expression of the GOI off. In the Tet-on or the rtTA system however, the opposite is true. Here transcription from the *rtTA* gene generates an rtTA protein which will only bind the Tet-op promoter and allow the expression of the GOI in the presence of tetracyclines.

By embedding TetO in close proximity to the GOI it enables modular gene expression. In either system, Tet-off or Tet-on, by titrating the amount of tetracycline, one can directly influence the degree to which the GOI protein is expressed (105, 106). As eponymous as it may be, expression of either system is most effective using doxycycline, and not tetracycline. Doxycycline's significant binding association ($K_a=10^{10}$) can activate tet-system elements at concentrations 100-fold lower than tetracycline (107).

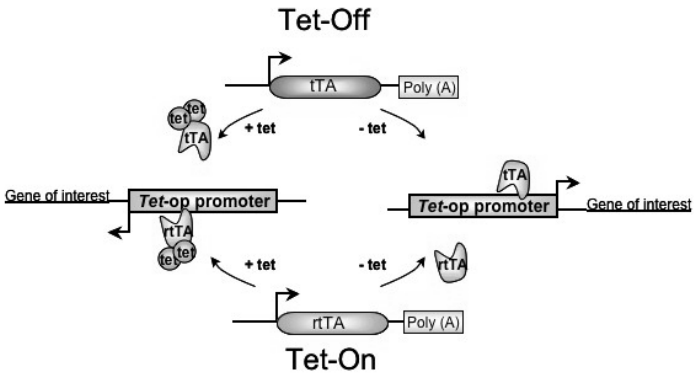


**Figure 3.2. The Tet system for conditional gene expression.** The tetracycline inducible system permits modular gene expression. In tet-off transcription of *tTA* generates a tTA protein which enhances the transcription of the GOI from the *Tet-op* site. In tet-off tetracyclines abrogate transcription. In tet-on, transcription of *rtTA* generates an rtTA protein fused with a reverse transactivator element. In tet-on, rtTA can only bind and promote transcription of the GOI when tetracyclines are provided. Reproduced with permission: copyright GenOway.

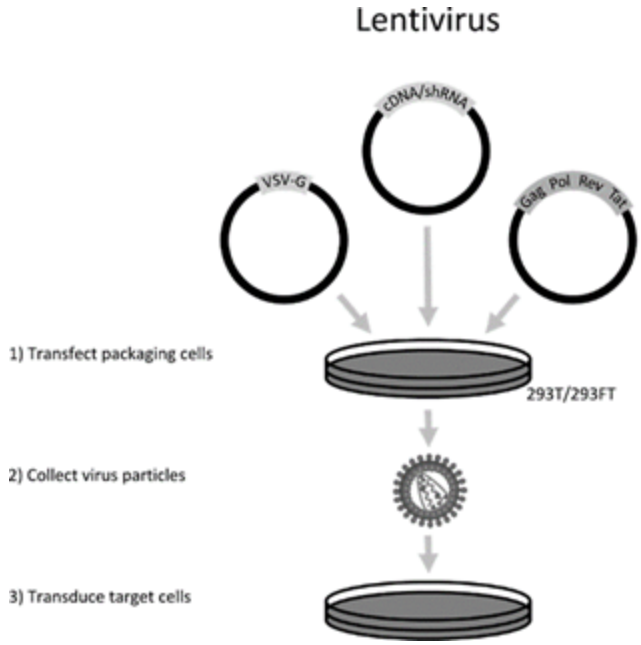


**Figure 3.3. Generation of intact-GOI-viruses by a packaging cell line.** Packaging cell lines produce infectious GOI- carrying virions. Here the packaging cell is shown as being transfected with all necessary gene-encoding cassettes for transcribing, producing and packaging live and infectious virions. These are harvested from the cellular supernatant for downstream application. Reproduced with permission: copyright AddGene.

#### *3.2.1.3 Packaging Cells Produce the GOI-containing Lentivirus for Transfection*

While the cassettes carry the vital genes, the generation of the actual virus must occur within a packaging cell (91). As Figure 3.3 illustrates, the packaging cell is where the archetypal viral gag and pol proteins precipitate the steps required for the recognition, transcription and packaging of competent and viable virus particles. Infectious GOI-carrying viruses are harvested from the cellular media to transfect the choice target cells (101). Viral integration is one time event, once transfected target cells serve only to express—constitutively and stably— the GOI. To validate transfection, the transgene cassette often contains a selectable marker commonly for antibiotic resistance. Transfected target cells are grown in antibiotic fortified media in order to selectively isolate for cells that have been successfully transfected. Antibiotic selection is carried out for 1-4 weeks and is dependent on cellular turnover. Once cell growth has stabilized, conditional expression, using doxycycline, can be initiated.

Not all target cells are equally amenable to transfection. Characteristics including cellular type (adherent or suspension), growth rate, the composition of the cellular membrane, as well as internal regulatory pathways may all impact with what facultative ease or difficulty the target cell may be successfully transfected. HEK293 cells are *h*uman *e*mbryonic *k*idney cells and are one of the best established and most easily transfectable cell lines available (108).

Here, a lentiviral system was used to transfect CD20 cDNA into a HEK293 cells, a cell line normally lacking this marker. Cells were positively selected using ampicillin, and CD20 expression induced using doxycycline. This resulted in the generation of CD20+HEK cells used for positive selection, and the untransfected HEK293 cells for

negative selection. The use of stable transfection of a known marker for the purposes of cell-SELEX has been suggested in critical literature, however, to the best of our knowledge, this is the first time it has been employed in a discrete fashion.

### 3.2.2 Stringency Measures

SELEX is only as effective as its conditions are stringent. The selection parameters exert a direct influence on the quantity, quality, and specificity of the evolved ligands (109). The more stringent the conditions the greater the binding affinity and discriminative capacity of the final pool. During our selection regime stringency was increased incrementally every 2-3 rounds until an appreciable increase in the binding affinity of the pool was achieved, see Table 3. Stringency measures included increases in the number of washes, decreased incubation time with the positive cells, increased incubation time with negative cells, and incrementally decreasing the incubatory concentration of the DNA pools.

| Round Number | DNA Concentration (nM) | Negative Selection (N=no and Y=yes) | # Washes | Incubation Time with Positive Cells (min) | Incubation Time with Negative Cells (min) |
|---|---|---|---|---|---|
| 1 | 500 | N | 1 | 45 | 0 |
| 2-3 | 500 | N | 2 | 45 | 0 |
| 3-4 | 250 | N | 2 | 45 | 0 |
| 4-6 | 250 | Y | 2 | 30 | 30 |
| 6-8 | 250 | Y | 3 | 30 | 30 |
| 8-10 | 100 | Y | 3 | 20 | 40 |

**Table 3. Selection regime.** Increases in the stringency of selection aid in evolving high affinity aptamer pools. Here stringency is increased incrementally over 10 rounds of selection. Positive and negative cell line denote, respectively, the CD20 transfected HEK cell line (CD20+HEK) and the untransfected HEK cell line. For round 1 the initial DNA pool is the unselected DNA library. Stringency measures included limiting concentration, increasing washes and varying the duration of incubations.

## 3.3 RESULTS

### 3.3.1 Evaluation of CD20 Transfection

A lentiviral gene expression system was used to stably transfect HEK293 with CD20 cDNA. After selection using puromycin and induction of GOI using doxycycline the cells were evaluated for CD20 expression.

#### *3.3.1.1 Flow Cytometry*

Figure 3.5 panel A depicts the dot plots of untransfected control HEK and the transfected CD20+HEK cells before and after staining with fluorescently labelled anti-CD20 antibody. The X and Y axis represent respectively CD20 expression and internal complexity (SS). The cells exhibited consistent internal characteristics indicated by their occupying a relatively uniform distribution. Staining CD20+HEK with anti-CD20 antibody causes a shift in the cells population along the X-axis- this denotes greater antibody binding. A similar staining of the HEK control cells however did not induce a shift. Therefore anti-CD20 antibody positively label the CD20+HEK but not the untransfected control. This information is also represented with the histogram in Figure 3.5 panel B which depicts an overlay composite comparing the antibody signal of both samples. There is a significant shift in the in fluorescence signal between the HEK control (grey filled) and CD20+HEK cells (white filled) which confirms that CD20+HEK cells exhibit elevated amounts of anti-CD20 binding compared to the HEK control cells. Therefore, the lentiviral transfection of cells is successful with a CD20+HEK cell line established.

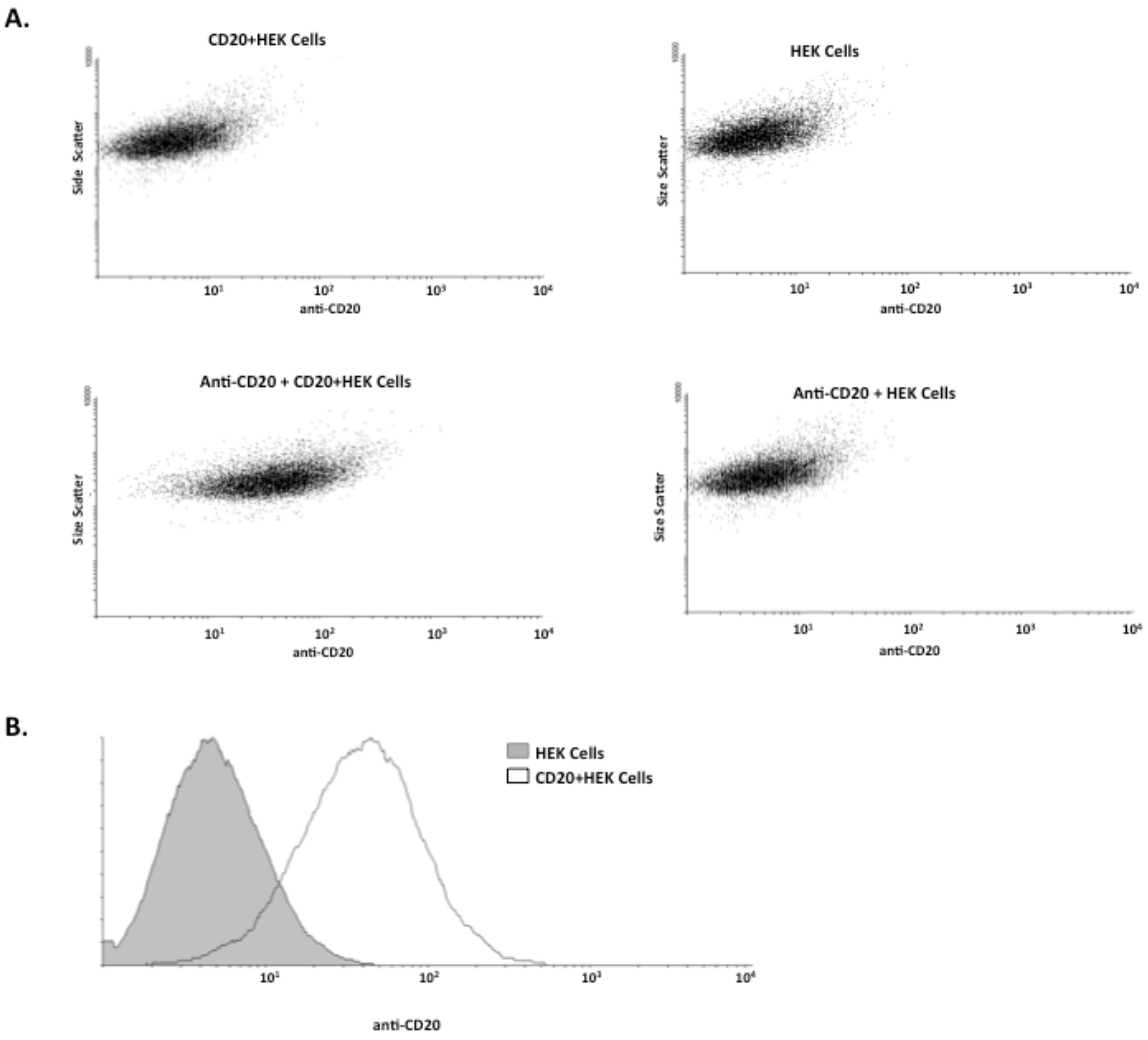


**Figure 3.4. Assessment of CD20 expression in transfected HEK293 Cells.** To evaluate and compare CD20 expression between untransfected and CD20+HEK transfected samples, live cells were incubated with 10ng/µL of FITC labelled anti-CD20 antibody for 30 minutes on ice. The cells were washed, re-suspended in buffer and fluorescence measured using a Beckman FC500 flow cytometer where 20,000 events were counted. **A)** Representative dot plots of cells before and after antibody incubation. **B)** Relevant histograms of the antibody labelled cells. Only the transfected CD20+HEK cells are positively labelled by the anti-CD20 antibody.

#### *3.3.1.2 Fluorescence Microscopy*

To further verify transfection we visualized antibody labelled cells using fluorescence microscopy. We stained cells with FITC-labelled anti-CD20 antibody (excitation 495nm; emission 519nm) and with DAPI (4',6'-diamidino-2-phenylindole) a DNA intercalating dye (excitation 358nm; emission 461nm). In live or fixed cells, DAPI fluoresces with strict localization to the nucleus. The results of microscopy are presented in Figure 3.6. Only CD20+HEK cells show the distinct anti-CD20 labelling, the HEK control does not. CD20 is a transmembrane protein. In the overlay figure, only CD20+HEK cells exhibit anti-CD20 staining along the cellular membrane, clearly delineated from the DAPI stained nucleus. Together this confirms the successful expression of the CD20 molecule in the CD20+HEK cell line.

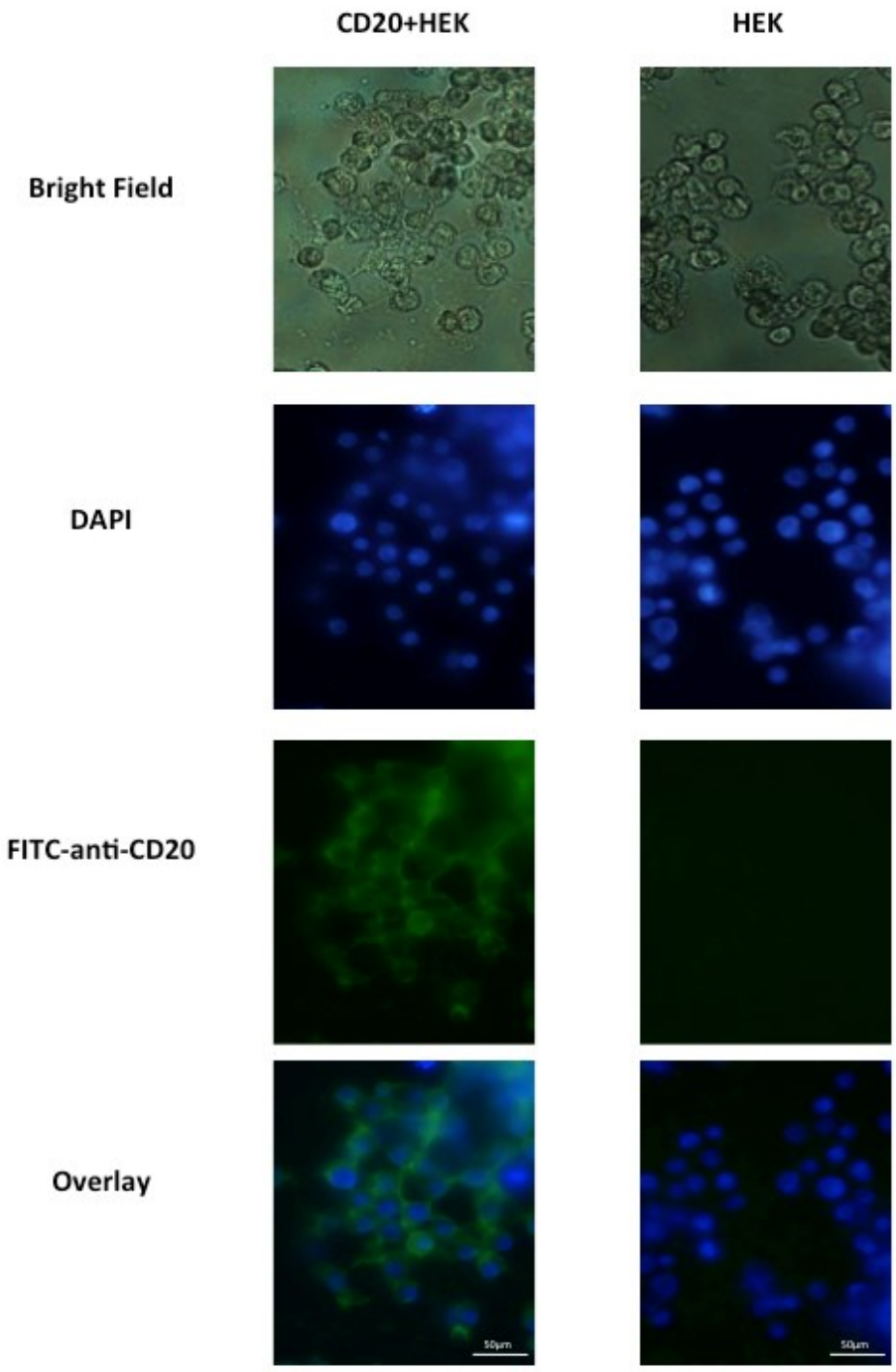


**Figure 3.5. Visual detection of CD20 expression in transfected HEK293 Cells.** Fluorescence microscopy for the visual detection of CD20 was performed 2 weeks after induction using doxycycline. Cells were fixed with 4% PFA and stained with FITC anti-CD20 antibody at 50 ng/µL for 4 hours. Cells were co-stained with DAPI for nuclear elucidation. Only CD20+HEK cells were positively labelled with the anti-CD20 antibody.

#### *3.3.1.3 Contextual Anti-CD20 Expression*

For context, we titrated the anti-CD20 antibody with CD20+HEK cells and compared it the level expressed with CCL-86, a naturally CD20 expressing cell line, and TIB-152, a naturally CD20 negative cell line. The results are depicted in Figure 3.7. Signal intensity is quantified by the median fluorescence intensity or MFI; the higher the MFI value the greater the signal strength. Note the consistently low MFI values with the TIB-152 cells. This demonstrates that the antibody fails to bind to TIB-152 cells to any appreciable degree regardless of the concentration. TIB-152 cells therefore do not express CD20. This is starkly opposed by the CCL-86 cell line which shows substantially higher MFI levels. And while the CD20+HEK cell line exhibits significant CD20 staining it is saturated at levels lower than that observed with the CCL-86 cells. This suggest that while the transfected cells do possess the CD20 molecule it is not as abundantly expressed as on the CCL-86 cells.

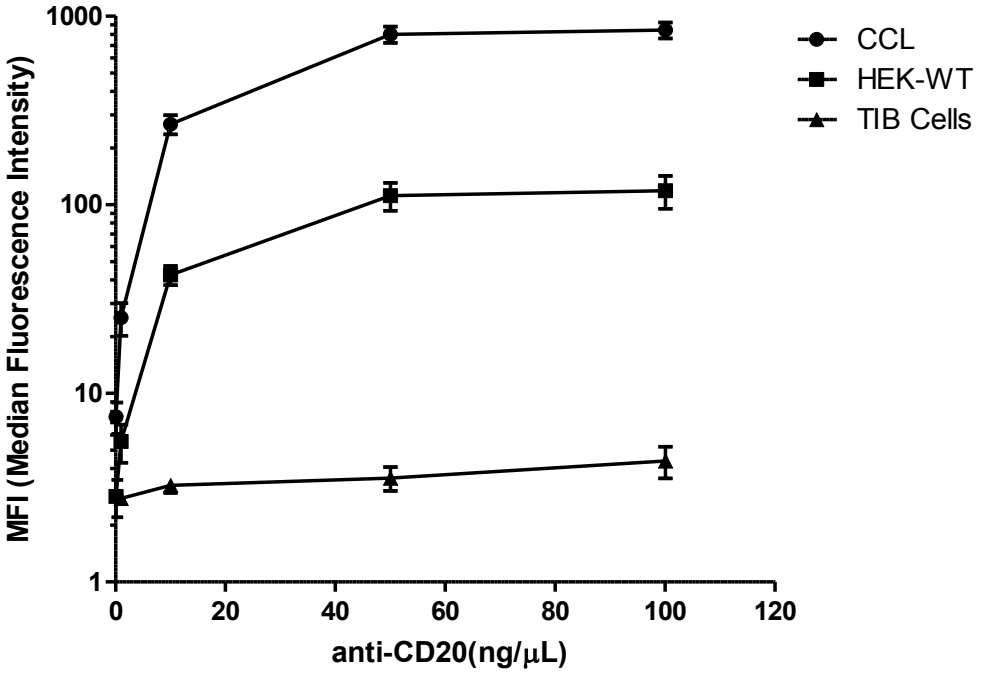


**Figure 3.6. CD20 expression in different cell lines.** To contextualize and compare CD20 expression the anti-CD20 antibody was titrated with various cell lines including the CD20+HEK transfected cell line, CCL-86 a naturally CD20 expressing cell line, and TIB-152 a naturally CD20 negative cell line. The staining was performed in triplicate. The antibody signal for CD20+HEK cells is saturated at much lower MFI intensities than with the naturally CCL-86 cells. This suggests that CD20 is less abundantly expressed on CD20+HEK cells than it is on CCL-86 cells.

### 3.3.2 SELEX generates pools of aptamer with progressively greater binding affinity to the CD20+HEK cells.

10 rounds of selection using CD20+HEK cells were performed. To evaluate selection the CD20+HEK cells were incubated with fluorescently labelled aptamer pools derived from rounds 1, 5 and 10 which represent respectively the start, middle and end points of selection. As a control the cells were also stained with the unselected DNA library. The individual binding results are indicated in Figure 3.8A. Unstained cells are depicted by the grey filled histogram. Note that cells incubated with the library (grey curve) exhibit a shift in fluorescence; this represents the basal binding capacity of the library. Each subsequent round of selection, round 1 in red, round 5 in green and round 10 in purple, exhibit increasing rightward shifts, with pool 10 possessing the greatest movement. Therefore the selection regime is successful in generating pools of aptamers with cycle dependent increases in affinity with CD20+HEK cells. For clarity, Figure 3.8B is an overlay histogram of all the samples and the MFI values of each curve are tabulated in Figure 3.8C. Unstained cells have a basal MFI value of 2, the library possess an MFI of 22, pool 1 at 26, pool 5 at 32 and Pool 10 with the strongest MFI value at 46. The signal intensity of pool 10 was found to be statistically significant when assessed by the student *t*-test. This progressive increase in MFI, as a consequence of the selection round performed, shows that the SELEX protocol successfully evolved stronger binding pools of aptamers with affinity to the CD20+HEK transfected cell line.

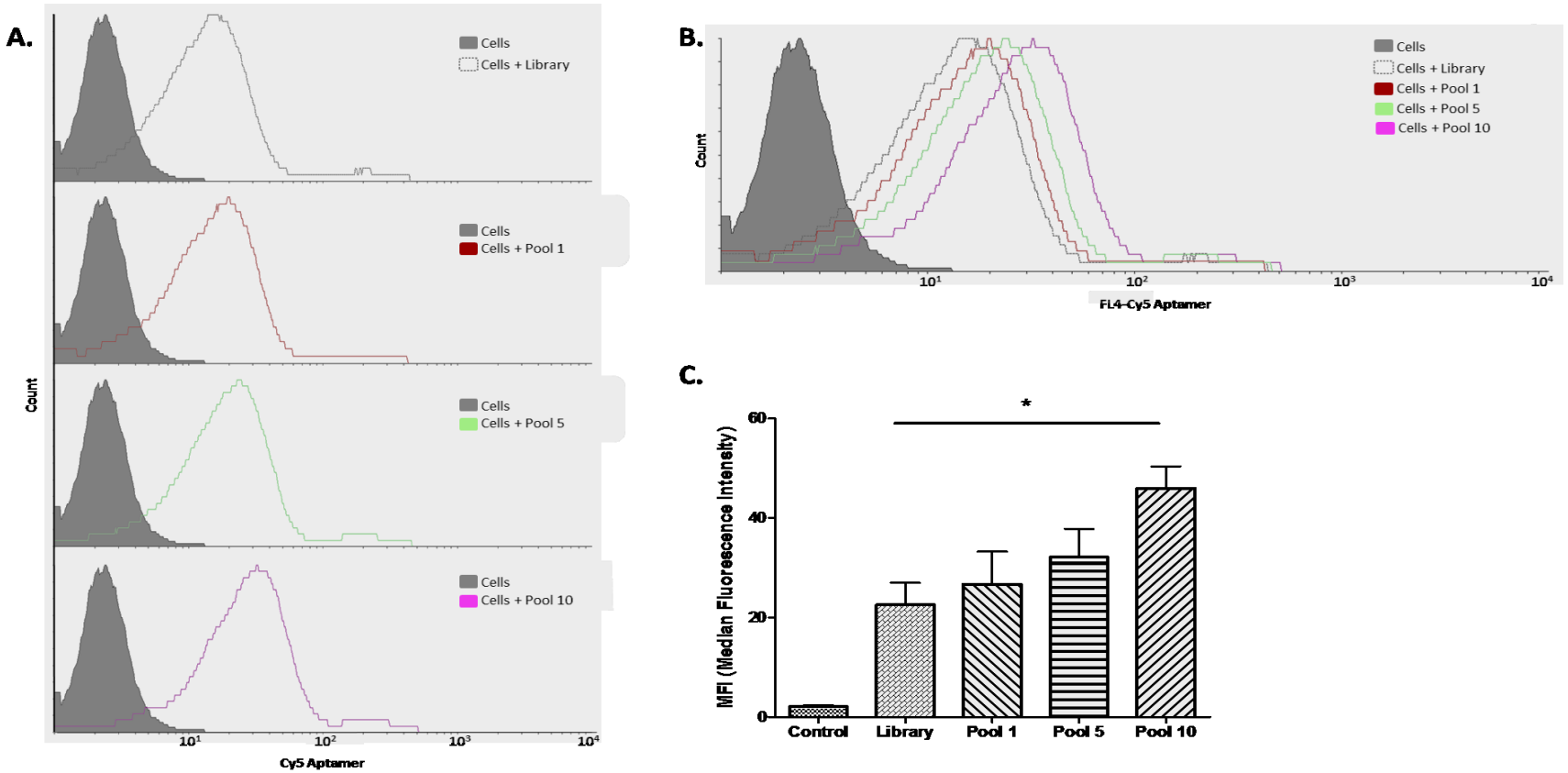


**Figure 3.7. Binding affinity of aptamer pools with CD20+HEK cells.** To evaluate the SELEX process CD20+HEK cells were incubated with 200nM aliquots of Cy5 labelled DNA library, aptamer pools 1, pool 5 and pool 10, in triplicate**. A)** Unstained control cells are represented by grey filled curve. The stained samples include CD20+HEK cells incubated, respectively, with the library (unfilled grey), aptamer pool 1 (red), aptamer pool 5 (green) and aptamer pool 10 (purple). **B)** Overlay composite of all samples**. C)** The tabulated MFI values of each curve. Selection using CD20+HEK cells resulted in aptamer pools that exhibited cycle dependent increases in affinity with the transfected cells. After 10 rounds of selection aptamer pools 10 binds CD20+HEK cells with significantly more affinity than the unselected DNA library, $p<0.05$.

### 3.3.3 Pool 10 CD20 positively labels the naturally CD20 expressing CCL-86 Cells but not the naturally CD20 negative Cell line TIB-152.

To better evaluate the CD20 specificity of the aptamers we incubated pools 1 and 10 with untransfected HEK cells and also independent cell lines of varying CD20 expression. TIB-152 is a T-cell line and naturally CD20 negative; CCL-86 cells are B-cells (Burkett's lymphoma) and are naturally CD20 positive. As can be seen from tabulated MFI data in Figure 3.9, pool 1 is a low affinity binder of all 4 cell lines with relatively consistent MFI values in all. Pool 10 is not only an effective binder of CD20+HEK but it is also discriminative, possessing low level associations with the untransfected HEK.

In the independent cell lines, neither Pool 1 nor pool 10 possessed any significant binding with the CD20 negative cell line TIB-152. Therefore the aptamers selected are not for markers prevalent on TIB-152 cells. When evaluated with the naturally CD20 expressing CCL-86 cells only Pool 10, and not Pool 1, positively associated with CCL-86 cells. Pool 10's MFI with CCl-86 is 38, and was a statistically significant association when evaluated with the student *t*-test.

Pool 1s low affinity with all the cell lines shows that selection has not yet cultivated sufficient target sensitivity. By round 10 the aptamer pool show a heighted affinity for CD20+HEK and not their target negative HEK counterparts. When compared to the independent CD20 positive cell line CCL-86, only pool 10 and not pool 1 possessed significant association. Together this data demonstrates that pool 10 appears to harbour aptamer sequences with specific binding affinity to the CD20 molecule. Therefore, cell-SELEX using transfected target positive CD20+HEK cells is an effective method for generating high affinity and discriminative pools of aptamers.

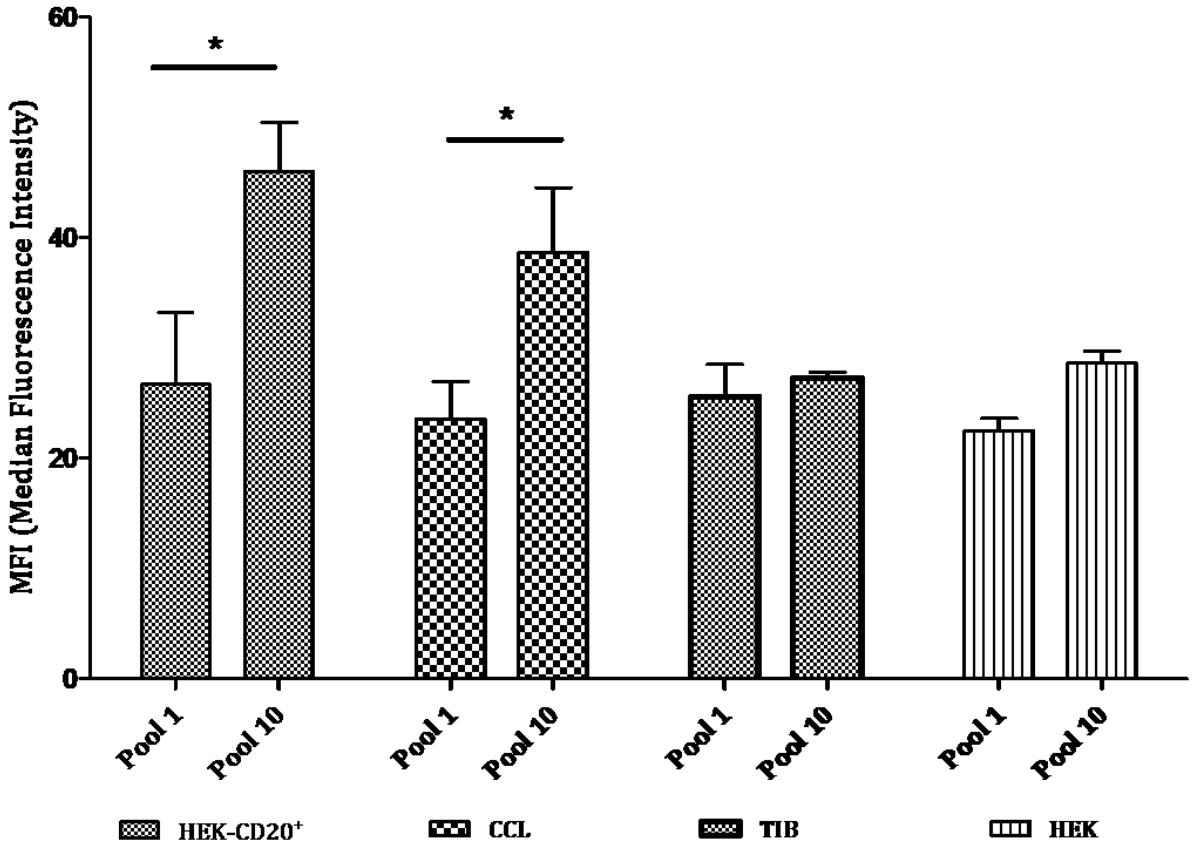


**Figure 3.8. Binding affinity of aptamer pools 1 and 10 with cell lines of varying CD20 expression**. To evaluate the specificity of the aptamers and investigate their selectivity for CD20, the binding affinity of pools 1 and 10 (200nM) were compared amongst the CD20+HEK, the untransfected HEK cells, and two independent cell lines: the naturally CD20 expressing cell line CCL and the naturally CD20 negative TIB. The cells were stained in triplicates. Only aptamer pool 10, and not aptamer pool 1, exhibits significantly increased binding affinity with both CD20 positive cell lines CD20+HEK and CCL-86, *$p<0.05$. Neither pool 1 nor pool 10 possessed significant binding with either TIB or the untransfected HEK cells. Therefore aptamer pool 10, derived by targeted selection with CD20+HEK can positively identify and validate CD20 expression in independent cell lines.

## 3.4 DISCUSSION

SELEX is a well-established method of generating high affinity DNA ligands. Solid-state selection where the target of interest is conjugated onto a membrane or bead may allow for the target specific generation of aptamers however it fails to replicate the complexity of a cellular setting. Cell-SELEX is a more physiological conscious method. Aptamers are selected in a more natural environment and are better adapted for future in-vitro and in-vivo analyses. A significant caveat of most cell SELEX is that while aptamers can be generated with high specificity and affinity for a particular cell type-the actual identity of the intended molecule to which the aptamer binds is not known. This represents a significant hurdle as without specific target identity, the functional role of an aptamer is limited.

Lentiviral transfection of genes represents one of greatest advancement in modern biological engineering. We generated live and infectious CD20 carrying lentiviruses. These were subsequently used to introduce the CD20 gene into HEK293 cells— a cell line that does not express it. The result was the formation of 2 cell lines, the negative control consisting of the untransfected HEK and the positively transfected CD20+HEK. These inherently identical cell lines, but for the expression of CD20, represent a novel cell-SELEX strategy that couple target specificity and a physiologically relevant environment.

The transfection of HEK cells was evaluated using both flow cytometry and fluorescence microscopy. After the requisite negative screening with puromycin and gene induction using doxycycline we evaluated CD20+HEK cells for CD20 expression. In Figure 3.5 flow cytometry using anti-CD20 antibodies verified the expression of CD20 only on

CD20+HEK and not the HEK control. Fluorescence microscopy, in Figure 3.6, further validates the expression of CD20 on the cell membrane of CD20+HEK. Together these verify CD20 transfection and the production of a CD20+HEK cell line. By titrating anti-CD20 antibody in Figure 3.7 we were better able to contextualize CD20 expression. We found that CD20 expression in the transfected cell line is less abundant than CD20 expression with CCL-86 cells. This is plausible as CCL-86 are a lymphocytic B-cell line, and CD20 a characteristic B-cell marker. This also explains its significant absence in TIB-152 cells, a T-cell line.

Using both positive and negative cell lines we performed 10 rounds of alternating cell-SELEX, selecting for aptamers that associate with the CD20+HEK cells and eliminating those whose specificity was for markers on HEK cells. The hallmark of SELEX is the iterative enrichment and the stepwise generation of target specific pools. As shown in Figure 3.8, pools 1, 5 and 10 show gradual increases in affinity for the CD20+HEK cell lines. This demonstrates that the stringency measures were effective. By increasing stringency and therefore the selection pressure it encouraged the retention of progressively higher affinity ligands. In Figure 3.9 we show that pool 10 was not only the highest affinity pool, with significantly greater binding to the CD20+HEK than the initial library, but it is also a discriminative binder associating with the untransfected HEK to a negligible degree. Pool 10's binding with the control HEK cells was slightly elevated when compared to pool 1, $MFI_1$=25, $MFI_{10}$=30. Though this is not statistically significant it does suggest that some of the aptamers in pool 10 could be general binders of HEK cells and not the CD20 molecule. That these aptamer were able to persist regardless of stringency suggests the existence of a basal threshold limit.

To show target, and not merely cellular, specificity we evaluated the binding of pools 1 and 10 with independent cells of varying CD20 expression. We showed that only sequences in aptamer pool 10 and not pool 1, exhibited enhanced binding to the naturally CD20 expressing CCL-86 cells. Neither pool 1 nor pool 10 appear to associate with the TIB-152 cells to any appreciable degree. Pool 10's specificity to cells with positive CD20 expression appears to corroborate that target positive cell-SELEX can raise aptamers specific only to the transfected marker.

## 3.5 CONCLUSION

A lentiviral based and CD20-specific cell-SELEX strategy was used to evolve aptamer pools with heightened affinity and specificity for the transfected marker. Cell-SELEX using this method evolved aptamers pools that showed incremental increases in binding affinity with the CD20+HEK cell line, and not with the untransfected control. Pool 10, the most significant binder of CD20+HEK, and not Pool 1, also exhibited increased affinity with CCL-86, a naturally CD20 positive cell line and not with TIB-152, a naturally CD20 negative cell line. This suggests that selection using transfected CD20+HEK cells was successful in evolving an aptamer pool with targeted specificity to the CD20 marker.

# 4 NEXT GENERATION SEQUENCING AND THE EVALUATION OF APTAMER CLONES

## 4.1 ABSTRACT

Pool 10 was sent for next generation sequencing (NGS) to elucidate and evaluate individual aptamers. The DNA was analysed using the web based bioinformatic platform Galaxy; with sequence similarity assessed with Clustal Omega, common motif evaluation performed using DREME, and secondary structure derived using RNAstructure. Pool 10 exhibited significant sequence convergence with 70% of all sequences grouped into 5 clusters. Enrichment was demonstrated by the presence of exceptionally high copy number sequences (HCN) in each cluster. DREME detected 3 common consensus motifs, the most pervasive of which was identified in 84% of all sequences. Together, these results demonstrate that selection was successful in cultivating a consolidated pool of aptamers.

For cellular evaluation all HCNs aptamers, NLA-1 through NLA-4, exhibited high binding affinity, with $K_d$ values less than 100nM. Clones NLA-3, and NLA-4 had $K_d$s less than 60nM, and possessed the most specific binding to CD20+HEK cells. Co-staining cells with both NLA aptamers and anti-CD20 antibody resulted in the decrease of antibody signal intensity, suggesting that the aptamers and antibody compete for binding at mutual sites. Cumulatively, this data confirms that selection using CD20+HEK transfected cells and the analysis of the resultant data using NGS, was successful in identifying discrete aptamers sequences that possessed heightened affinity and specificity with the CD20+HEK cell line.

## 4.2 BACKGROUND

### 4.2.1 Deconvolution of Aptamer Pools

Aptamer pools are by definition heterogeneous (110). The goal of selection is to condense a massive combinatorial library into a highly specific aptamer pool containing sequences with heightened affinity to the target of interest. The goal of sequencing is to transform that pool into discrete and individual aptamers to critically evaluate their attributes including structure, shape, interaction dynamics, and importantly any biological considerations. Once the initial sequence is known, its characteristics can be enhanced with modifications. Macugen- a clinically licenced aptamer for the treatment of wet age-related macular degeneration (72, 111), Pegnivacogin- an anti-coagulative aptamer developed for acute coronary syndrome (112), and Spinach a fluorescence activating RNA aptamer for live cellular tracking (113) are all aptamers whose optimization required extensive post-selection modifications. These included nucleotide substitution to resist nucleases, truncation to fold into more stable secondary structures and PEGylating to increase retention (114, 115) . Selection may yield a high affinity pool but it is the modifications of individual sequences that truly refine an aptamer potency and efficacy.

Identifying high quality aptamers is hampered significantly by the inherent sequence complexity that persists even in an evolved pool (116). Though selection may remove the majority of non-sequences in the library, the final pool itself could still contain thousands of different species. Together the sequencing of aptamer pools and the requisite screening assays to evaluate functionality have represented, until very recently, the two largest hindrances in efficient aptamer development (86).

Next Generation Sequencing (NGS) coupled with bioinformatics is a very powerful high throughput method of analysis; and has dramatically changed how large-scale genomic studies are performed (117-119). It's also proven equally illuminating with respect to aptamer sequencing; where NGS can identify, count, and categorize each discrete DNA molecule. This information can then be used to evaluate each individual aptamers contained in the pool, to assess the convergence of popular motifs, and chart the evolution of high affinity sequences (110). NGS has also been used to better understand the factors, both inherent and obscure, that operate on SELEX, the effect that negative selection can have (79, 120), how stringency affects enrichment (116), and how PCR amplification may exert undue influence on ligand development (23, 121). Its speed, output and applicative potential have seen it become the preeminent strategy for aptamer sequencing.

### 4.2.2 Aptamer Sequencing Past Methods: Introduction to Conventional Bacterial Cloning and Sanger Sequencing

SELEX was developed in the 1990s and most aptamers of that time sequenced using bacterial cloning and Sanger sequencing (59, 111, 122). Both are labour intensive, low-throughput, and are considered, by today's standards, wanting.

Transformation is the acquisition and stable replication of exogenous pieces of DNA. A common phenomenon in bacteria, it was the pioneering work of Stanley Cohen et al in 1972 (123) which brought it to the forefront of molecular cloning. In bacterial transformation the DNA of interest is subcloned into circularized vectors, which are introduced into viable and competent bacterial cells either by a chemical method like calcium chloride exposure or a physical method like electroporation. See Figure 4.1 for

details. Transformed bacterial cells are plated on antibiotic fortified agar at a concentration low enough to ensure that single colonies emerge as a result of only one progenitor. The multiple cloning site (MCS) usually lies within a reporter gene, like LacZ, which makes it easy to phenotypically evaluate between bacterial colonies carrying a recombinant vector positive for the target DNA, and bacterial cells carrying an empty vector which does not (124). Functional LacZ encodes a protein that activates β-galactosidase which then cleaves the molecule X-gal generating a blue pigment (124). The successful incorporation of insert DNA at the MCS however, will not yield active β-galactosidase, as a result X-gal remains uncleaved, and the bacterial colony is white.

Bacterial cloning and amplification remain a mainstay of modern molecular biology, even well after the advent of PCR. Bacterial logarithmic growth coupled with a high copy number plasmid can, in the space of less than 12 hours, massively amplify plasmid DNA from the initial nanogram amount used for transformation to microgram quantities after purification. What differentiates this from PCR, is that genes amplified within a bacterial system have the benefit of proof-reading and repair exonucleases. PCRs taq polymerase is notoriously error prone with an error rate among the highest of all polymerases at $2x10^{-4}$ errors per nucleotide synthesized (125, 126); it also lacks repair mechanisms to correct mis-incorporated nucleotides (127). As a result, whenever there is a requirement for high fidelity gene synthesis bacterial cloning is still widely employed.

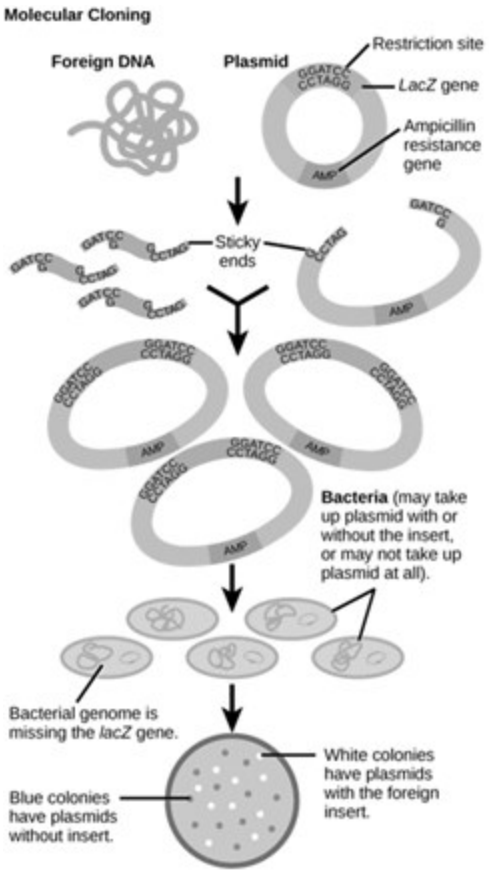


**Figure 4.1. Bacterial cloning.** In bacterial cloning the DNA of interest is first introduced into a circularized vector, typically within the MCS of a reporter gene like LacZ. Restriction endonucleases cleave the double stranded DNA of both the vector and the insert at palindromic sequences. Reciprical end ligation and annealing generate a recombinant vector which is used to transform bacterial cells. Bacterial cells will uptake, maintain and replicate the vector. After plating on antibiotic fortified agar, bacterial colonies carrying the recombinant vector can be easily distinguished by their white colour. Reproduced under the terms of the Creative Commons Attribution Licence. Openstax College, Cloning and Genetic Engineering. Openstax, CNX, 2013.

Bacterial cloning and Sanger sequencing are complementary techniques that evolved together; and up until the early 1990s the latter was a mainstay of all sequencing technologies. In Sanger sequencing, DNA is amplified with a mastermix spiked with chain terminating dideoxynucleotide triphosphates (ddNTPs). Unlike natural deoxynucleotide triphosphates (dNTPs), the incorporation of the 3'OH lacking ddNTPs abrogate any further extension of the complementary strand (128). Due to the stochastic incorporation of ddNTPs the result is the amplification of DNA strands prematurely terminated at every possible nucleotide position. Using gel or capillary electrophoresis the DNA strands are sorted according to their molecular weight (118), and differential labelling of each ddNTPs permits the ordered reading of the DNA sequence in a nucleotide specific manner.

High fidelity bacterial cloning and Sanger sequencing are highly precise techniques, genes and genome sequenced in this manner have a significantly reduced error rate achieving 99.999% fidelity (128). For this reason the Sanger method was the gold standard for nucleic acid sequencing for more than two and half decades (119) but its limited approach, restricted automation, and prohibitive costs have seen it replaced with the cheaper, faster and massively parallel techniques collectively identified as "next generation sequencing" or NGS.

### 4.2.3 Introduction to Next-Generation-Sequencing (NGS) Technologies

NGSs are high throughput approaches, simultaneous sequencing millions of DNA fragments (119) at a fraction of the costs and time of conventional Sanger sequencing. Although only commercially available since 2004 (129) the high throughput nature of these techniques, their amenability to automation, and their capacity to uncover and

identify genes, regulatory elements and even expression trends have made them critical and important tools for all aspects of genome analysis (130). All of which has prompted their use in the exploration of aptamer pools as well. Of the 4 major platforms for high throughput analysis (HTA), the Illumina/Solexa Genome Analyzer is the most economical and accessible to researchers.

#### *4.2.3.1 Illumina Overview and Use of Bioinformatics to Extract Meaningful Information*

A typical Illumina procedure incorporates 3 elements, template preparation, sequencing coupled imaging and data analysis (117). See Figure 4.2. First, template DNA is amplified using specific 5' and 3' adapter primers generating an Ilumina specific adapter library. Solid synthesis immobilizes identical adapter oligomers on the surface of a glass flow cell (117), see panel 4.2A.The adapter-amplified template library is denatured and distributed at a low concentration over the immobilized adapter sequences to which it will hybridize (118). Unlabelled nucleotides and DNA polymerase are added to build the complementary strand via bridge amplification. This ensures the clonal amplification of the target DNA sequence, and culminates with the formation of dense clusters containing several thousand to a million copies of one original template strand. This amplification is required to ensure adequate signal detection in subsequent steps.

For sequencing and imaging, see Figure 4.2B, Illumina uses cyclic reversible termination (CRT), an approach similar to Sanger's chain terminating ddNTPs (117). In lieu of irreversibly removing the nucleotides 3'OH, in CRT the 3'OH group is simply blocked. This ensures that the complementary strand can only be synthesized one fluorescently labelled nucleotide at a time. By coupling DNA synthesis with DNA

sequencing, this technique is more commonly referred to as “sequencing by synthesis”. Initially all four nucleotides are bathed onto the surface of the flow cell, where only the complementary nucleotide to the template will bind. The laser light is shone and the identity of the uniquely fluorescently labelled bound nucleotide detected. Because the 3’OH is blocked no further extension of the strand is possible. To initiate a new cycle, remnant nucleotides and enzymes are washed away, the 3’OH chemically unblocked, new labelled nucleotides added, annealed, and the identity of the next newly incorporated base detected. This cycle is repeated until the strand is fully sequenced (117).

Modern NGS strategies outperform the older Sanger sequencing methods by factors of 100-1000 (118). The rapid acquisition of sequences—millions of nucleotides in length—is possible within weeks. In order to extract meaningful information highly processive bioinformatic tools are required. To align sequences against reference genomes there is BLAST and its many permutations including blastn for genomes, blastp for proteins, blastx for cDNA which are publically licenced, freely available over the internet, and updated by researchers (131, 132). Multiple alignment software, like ClustalW and Clustal-Omega, are pairwise sequence alignment tools and can inform on the homology of related sequences, protein or DNA (133). Motif analysis tools for consensus sequence discovery include MEME (97) and Gibbs Motif Sampler (134). DNA and RNA folding software like mfold (135) and RNAstructure (98) are also available to predict shape, structure and stability of sequences. Softwares and tools like these are important and pivotal for research; both their current applications and future endeavours will continue to be advanced by next generation sequencing.

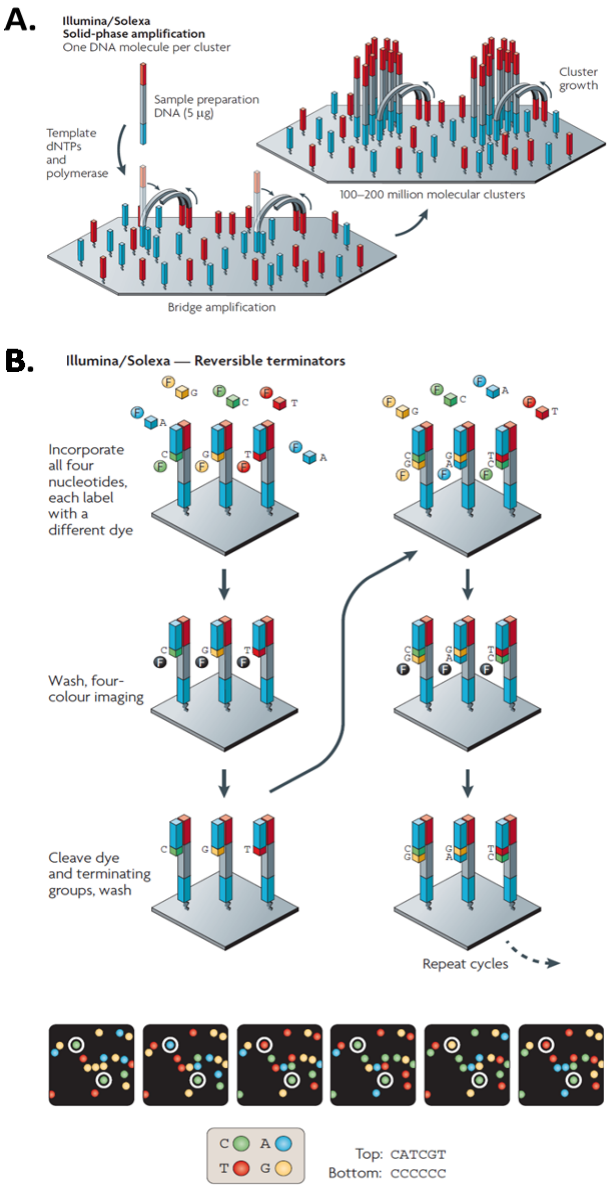


**Figure 4.2. Illumina/Solexa Overview. A) Clonal amplification of sample.** Target DNA is amplified using Illumina specific adapter primers and bathed onto a flow cell which also contains identically immobilized oligomers. Bridge amplification ensures the clonal amplification of strands resulting in high density template DNA clusters. **B) Sequencing by synthesis.** For sequencing blocked dNTPs are provided and hybridized by DNA polymerase to the template strand. The identity of the incorporated nucleotide is possible due to their unique fluorescently labelled tags. The incorporation of each nucleotide is an isolated event requiring chemically unlinking for the addition of new nucleotides. In this way, the complementary DNA strand is sequenced as it is being synthesized—one base pair at a time. Reproduced and adapted with permission: Metzker, Michael L. Sequencing technologies- the next generation. *Nature Reviews Genetics*. **11**, 31-46 (2010).

#### *4.2.3.2 NGS as applied to Aptamers*

Until relatively recently (2010-onwards) most aptamers were derived only after bacterial cloning and Sanger sequencing. As slow and expensive as Sanger sequencing is, it was not the biggest hurdle to overcome. Practically speaking, bacterial cloning is inherently limited. In a pool of, conservatively estimating, hundreds of different species, the requirement to grow thousands of bacterial clones to ensure ample coverage and sequence each one individually is prohibitive. In fact most publications estimate an average of 50 clones are sequenced (17). Therefore there is no guarantee that the sequences acquired with bacterial cloning are true representative of the pool as a whole nor that they'll be target specific and efficacious. The risk of sequencing artifacts, aptamers inadvertently raised against a procedural reagent or those that persisted in the pool because they exhibit a PCR advantage, is a considerably more significant concern when the total breadth of analysis is limited to only 50 clones.

These limitations have made the advent of NGS a significant improvement for the purposes of aptamer sequencing. NGS can thoroughly report on all the sequences contained in a pool. Bioinformatics can refine the data by describing their abundance, length, copy number and even motifs. By evaluating all the sequences based on objective criteria it greatly simplifies aptamer analysis and help to rationally derive optimal aptamer candidates. NGS also has probative considerations. It can critically evaluate selection parameters and their influence on cultivating a high affinity pool. Sequencing an aptamer pool by NGS makes for a more comprehensive study of the trends and patterns evolved during selection, and can independently evaluate aptamer sequences in a quantitative and quantitative manner.

## 4.3 RESULTS

### 4.3.1 NGS Reveals that Pool 10 Exhibits Significant Sequence Convergence and Motif Emergence

#### *4.3.1.1 Phylogenetic Assessment of Sequences Identifies 5 Distinct Clusters*

Pool 10, the greatest binder of the CD20+HEK cells was sent for NGS analysis. Illumina read a total of 17,613,460 discrete sequences; of these 627,826 were clipped to the barcode specific to CD20 Pool 10. These sequences were clipped by length, isolating for aptamers 100 nucleotides in size- the original length of the library. After clipping, a total 541,258 total reads were retained. This corresponds to 86% of total sequences, therefore 14% or 86,268 sequences were discarded based on length alone. To evaluate the copy number or the total frequency of specific sequences, the data was collapsed. This removes redundancies by merging identical sequence together. Collapsing the data reduced the total number from 541,258 individual sequences to 62,737 collapsed reads. The greater the copy number the more abundant the aptamer sequence was in pool 10.

Figure 4.3 is a phylogenetic representation of the top 29 collapsed sequences. This was performed using Clustal-Omega, a pairwise alignment software. Every sequence is represented numerically with both an identification number as well a copy number indicating its frequency. For example the first sequence in the analysis below is #31-438; where 31 is the identification number and 438 is its copy number. Therefore, in pool 10 sequence 31 is present 438 times. Clustal-Omega can comparative analyze gene and protein sequences, by constructing a phylogenetic tree evolutionary and mutational trends can be charted and measured. In much the same way here, Clustal-Omega was used to analyze the similarity and differences between aptamer sequences. Clustered

groups indicate closely related sequences with outliers representing isolated and therefore unrelated sequences.

The top 29 sequences of pool 10 range in copy number from 84 at the scarcest to 11,019 at their most plentiful. Cumulatively, the total copy number of all 29 sequences is 43,700 which reflects about 70% of all sequences. The remaining sequences were excluded from analysis due to their low copy number. As can be seen from Figure 4.3, pool 10s aptamers can be broadly divided into 5 distinct groups A through E. A hypothetical ancestral root sequence, common to each cluster, is indicated by a black arrow. With the exception of group E, each of the remaining clusters possesses a significantly high copy number sequence (HCN) indicated by the grey stars. SELEX relies on an iterative selection process therefore, the greater the copy number of a sequence, the more persistent or enriched it was in selection, and so presumably the more specific it is to the target CD20+HEK cells.

Groups A and C possess only a single sequence dominant HCN sequence, groups B and D both possess 2 HCNs. In group A the HCN sequence is #7 with a copy number 2826, in group C it is sequence is #6 with the highest of all copy numbers 11,019. Group B possess 2 HCNs, as indicated they are sequences 12-5810 and 13-7036. Group D's HCNs are sequence #23-2958, and sequence #5 with copy number 4983. There does not appear to be any relationship between the number of HCNs and the size of each cluster.

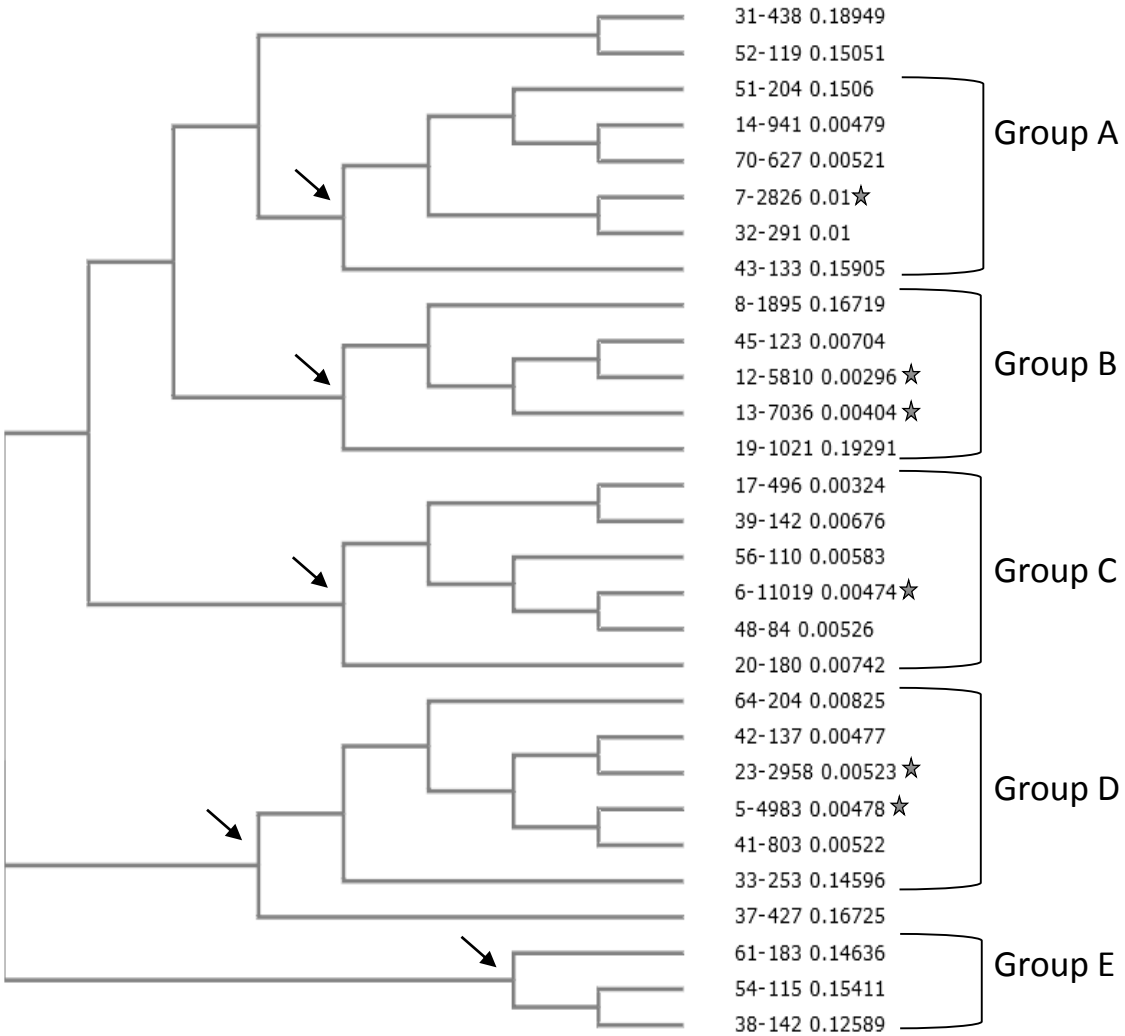


**Figure 4.3. Pool 10 exhibits significant sequence convergence.** Indicated above is the phylogenetic assessment of the top 29 clipped, merged and collapsed sequences in Pool 10, performed using Clustal-Omega. In each instance the identification number precedes the copy number, for example in 31-438, 31 is the arbitrary identification number of the sequence and 438 is its copy number. Sequences were resolved into 5 distinct clusters, groups A through E. Black arrows denote ahypothetical common ancestral sequence, the root of each cluster. Each group contains one or more significantly high copy number sequence HCNs (grey stars). As the most over-represented species of each cluster, HCNs best reflect the inherent characteristics of pool 10.

#### *4.3.1.2 HCN Sequences are Significantly Preferred to their Closest Relation*

Although sequences are grouped into different clusters the extent of variation is not great. And yet in spite of the sequence similarity all HCN sequences exhibit significantly higher frequencies when compared to their closest relation. A list of all the HCN derived from groups A-D and their closest related sequence are shown in Figure 4.4. The first panel for Group A depicts its HCN #7-2826 and its closest relation #32-291. For simplicity both the forward and the reverse primers have been omitted, only the randomized N60 portion is represented. Because they are clustered within the same family the two sequences are virtually identical. The differences, in bold, are that sequence #7-2826 possess an A at position 3 and G at position 9, while sequence #32-291 bears at the same sites a C and T respectively. When comparing copy numbers, sequence #7 is favoured at a ratio of 9:1 to sequence number #32. Therefore, though the sequences are highly similar, there is a marked preference for sequence #7. This trend is typical of all of the HCN sequences, most impressively by sequence #6 in group C where the copy number ratio between it and its closest relative, sequence # 48, is more than 131:1; here a G residue is favoured to a T.

This trend persists even with Groups B and D which both possess 2 HCN per cluster. Selection will still favour the HCNs when compared to their closest relation; but intra-HCN comparison do not exhibit a significant copy number bias. For example, group B's dominant HCN sequences are #12 and #13, the sole nucleotide difference being a C to T transition. Like all HCNs, sequence #12 is favoured significantly, by a ratio of 47:1, to sequence #45. However, an intra-HCN comparison between sequences #13 and #12 does not exhibit a significant bias, as the frequency difference between these two HCNs is a paltry 1.2:1. Group D also possesses 2 HCN—sequences #5 and #23. Sequence #5 is

preferred at a ratio of 6:1 to sequence #41- the lowest difference for any HCN encountered. While sequence #23 is favoured at a ratio of 21:1 to sequence #42. Like group B, an intra-HCN comparison between #5 and #23 is marginal. The intra-HCN variation between sequences #5 and #23 —an A-C modification at position 3 and a G-T modification at position 8— lead to a difference in frequency of 1.6:1.

Phylogenetic assessment grouped the top 70% of all pool 10s sequences into 5 distinct groups. The consolidation of aptamers into distinct groups that exhibited only minimal nucleotide variation, is proof that selection was effective. Each cluster possessed one or more dominant HCN sequence, which were markedly preferred even when compared to highly similar sequences. This demonstrates the selection strategy for aptamer pool 10 resulted in the enrichment of highly specific sequences.

| | |
|---|---|
| Group A | 7-2826<br>GC**A**CGTAC**G**AAACGCATGAGTGCGGACATCCACGCGGCGCGCTCACATGGCTATGTGTAC |
| | 32-291<br>GC**C**CGTAC**T**AAACGCATGAGTGCGGACATCCACGCGGCGCGCTCACATGGCTATGTGTAC |

| | |
|---|---|
| Group C | 6-11019<br>CCGTATGTCCGAAATACGGAGAACAGCACTCATATGCAAGCCATACGCGGA**G**GTGCACGC |
| | 48-84<br>CCGTATGTCCGAAATACGGAGAACAGCACTCATATGCAAGCCATACGCGGA**T**GTGCACGC |

| | |
|---|---|
| Group B | 12-5810<br>CTGCCCACTCCA**C**AGGCCTGCGCCGTCAATCACTTCATGCACGCTCGCGTTTACCCGTAT |
| | 45-123<br>CTGCCCACTCCA**T**AGGCCTGCGCCGTCAATCACTTCATGCACGCTCGCGTTTACCCGTAT |

| | |
|---|---|
| Group B | 13-7036<br>CTGCCCACTCCA**C**ATGCCTGCGCCGTCAATCACTTCATGCACGCTCGCGTTTACCCGTAT |

| | |
|---|---|
| Group D | 5-4983<br>AC**A**CACGGAGGGCATGTGCACGAAGATACATGGGCGTAACATGCTTGCCGCATCGCGCGT |
| | 41-803<br>AC**C**CACGGAGGGCATGTGCACGAAGATACATGGGCGTAACATGCTTGCCGCATCGCGCGT |

| | |
|---|---|
| Group D | 23-2958<br>AC**C**CACGTAGGGCATGTGCACGAAGATACATGGGCGTAACATGCTTGCCGCATCGCGCGT |
| | 42-137<br>AC**A**CACGTAGGGCATGTGCACGAAGATACATGGGCGTAACATGCTTGCCGCATCGCGCGT |

**Figure 4.4. Sequence comparison of HCNs and closest related sequence.** Depicted above are the 60-nucleotide internal sequences of each HCN(s) and its closest related sequence. Groups A and C possess only 1 HCN (sequence #7 and #6 respectively). Both group B and D possess each 2 HCN sequence (group B sequence #12 and #13; group D sequence #5 and #23). Nucleotide differences are shown in bold if they are between the HCN and its closet related sequence, and underlined when they represent intra-HCN nucleotide differences.

#### *4.3.1.3 DREME identifies 3 Distinct Motifs*

To further refine analysis the top 77 collapsed sequences, reflecting greater than 95% of all aptamers in pool 10, were subjected to motif analysis using DREME. DREME is the *d*iscriminative *r*egular *e*xpression *m*otif *e*licitation and can be used to discover short, ungapped motifs within DNA. This information is consolidated into a graphic that depicts the frequency of each nucleotide by size. DREME motif renderings for aptamer pool 10 are presented in Figure 4.5. The most common motif is GGRCA where R is any purine residues, found in 66 out of 77 total sequences. Of both variations, the GGACA variant was present in 36 of the collapsed sequences, while the GGGCA was found in 29. The second most common motif, but the longest in size, was CAMTCA where M represents either cytosine or adenine. This sequence was less common, found in 40 of 77 sequences. The CACTCA variant is more than twice as common as the CAATCA. The third most common motif and the shortest is GWAA, where W can represent either thymine or adenine. This motif was found in 52 of 77 of all sequences, with the GTAA variant being more favoured. The retention and abundance of common motifs is another indication that selection was successful in producing a highly specific and enriched pool of aptamers.

| | Motif | Sequence | Variant | Positive (/77) |
|---|---|---|---|---|
| 1 |  | GGRCA | GGACA | 36 |
| | | | GGGCA | 29 |
| 2 |  | CAMTCA | CACTCA | 28 |
| | | | CAATCA | 12 |
| 3 |  | GWAA | GTAA | 32 |
| | | | GAAA | 20 |

**Figure 4.5. DREME motif analysis for Pool 10.** DREME motif analysis identified 3 common motifs. GGRCA was found in 65 of 77 collapsed sequences or 84% of all sequences read by NGS. CAMTCA was the second most common motif in 52% of all sequences; the CACTCA was twofold more common than the CAATCA motif. The shortest motif was GWAA. The presence and prevalence of common motifs shows that selection was stringent enough to favour the discrete evolution of specific sequences.

### 4.3.2 HCN are lead aptamer candidates.

The nucleotide sequence of the top HCN sequences from each of the 4 dominant clusters is represented in Figure 4.6. The presence of the DREME motifs is indicated in the coloured stretch of nucleotides. Motif 1 GGRCA, is illustrated in red, motif 2 CAMTCA in yellow, and motif 3 GWAA in blue. All dominant HCN possessed at least one of these motifs. Some such as #6-11019 and #5-4983 possessed two. The presence and abundance of DREME motifs in the HCNs is yet another indicator of sequence consolidation. With both phylogenetic data and DREME analysis in their favour the HCN sequences depicted below can be considered the best representatives of selection. These sequences, referred to as NLA-1 through NLA-4, were synthesized as pure clones for affinity and binding analysis. Their putative secondary structure, derived from the RNAstructure software, is illustrated in Figure 4.7.

| | | |
|---|---|---|
| Group A | 7-2826<br>GCACGTACGAAACGCATGAGTGCGGACATCCACGCGGCGCGCTCACATGGCTATGTGTAC | NLA-1 |
| Group B | 13-7036<br>CTGCCCACTCCACATGCCTGCGCCGTCAATCACTTCATGCACGCTCGCGTTTACCCGTAT | NLA-2 |
| Group C | 6-11019<br>CCGTATGTCCGAAATACGGAGAACAGCACTCATATGCAAGCCATACGCGGAGGTGCACGC | NLA-3 |
| Group D | 5-4983<br>ACACACGGAGGGCATGTGCACGAAGATACATGGGCGTAACATGCTTGCCGCATCGCGCGT | NLA-4 |

**Figure 4.6. Nucleotide sequence of lead aptamer candidates.** The internal 60 nucleotide region for the top HCN sequences derived from each phylogenetic group is depicted above. For simplicity the forward and reverse primer sequences are omitted. Lead aptamer candidate were renamed NLA-1 through NLA-4. DREME motifs are represented by colour with motif 1 GGRCA in red, CAMTCA in yellow and GWAA in blue. As the top HCN sequences of each cluster, and in possession of one or more DREME motifs, these NLA aptamers best represent the intrinsic characteristics of pool 10.

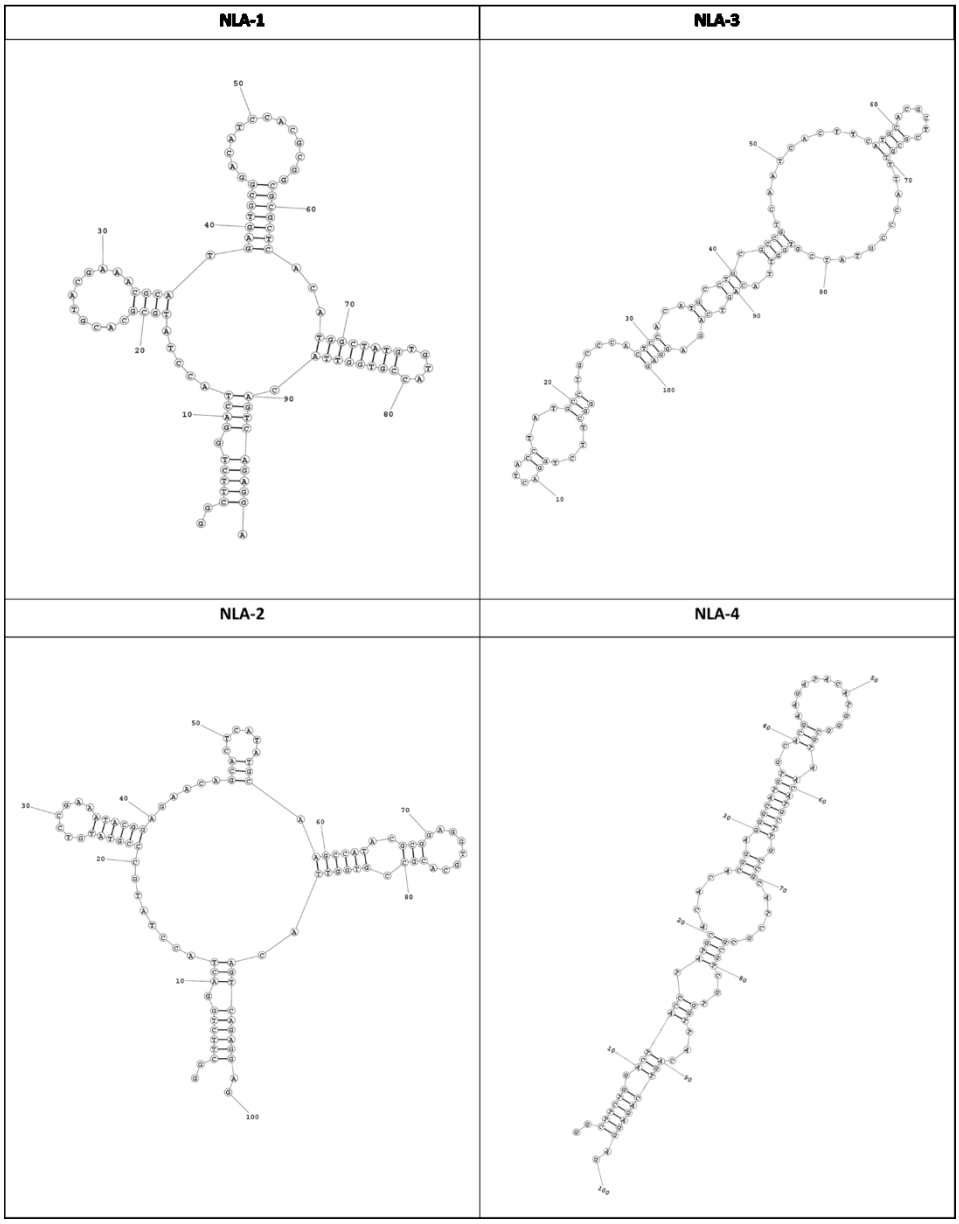


**Figure 4.7. Purported secondary structure of lead candidate aptamers**. RNAstructure is an online predictive module that can estimate, based on free energy calculations, the secondary structure of DNA or RNA strands. Lead NLA aptamer candidates were evaluated using this software and, represented above, are the lowest minimum free energy depictions of each.

### 4.3.3 Aptamer Screening & $K_d$ Analysis: Sequenced Aptamers possess high affinity and selectivity.

#### *4.3.3.1 NLA-3 and NLA-4 as the most specific and potent binders of CD20+HEK cells.*

To determine affinity and calculate $K_d$ the fluorescently labelled aptamers were titrated and incubated with the transfected CD20+HEK cells. The resultant fluorescence was measured using flow cytometry. The signal intensity is charted as the MFI (median fluorescence intensity) and graphically represented in Figure 4.8. The data was fitted using a non-linear regression to measure $K_d$. $K_d$ is the equilibrium disassociation constant, and represents the affinity between two molecules. Graphically, it is the concentration of aptamers necessary to bind half the target sites on CD20+HEK cells. $K_d$ was calculated according to the following formula using the software GraphPad. Bmax refers to the saturation limit, X and Y are calculated values from the graph.

$$Formula\ (1)\ \ y = \frac{Bmax \times X}{Kd + X}$$

All of the candidate aptamer show signal saturation at concentration exceeding 200nM. This corresponds with the final rounds of selection which were performed with DNA pools at 100nM. The calculation of the disassociation constant $K_d$ revealed that all the aptamers exhibited appreciable affinity with $K_d$s significantly less than 75nM. In particular, aptamers NLA-3 and NLA-4 possess the smallest $K_d$ values at 58.4nM and 49.3nM respectively. It is notable that NLA-3 and NLA-4 which both possess 2 DREME motifs also possessed lower $K_d$ values than aptamers NLA-1 and NLA-2 which contained 1 DREME motif each. This suggests that possession of consensus motifs could be used to better predict aptamer affinity.

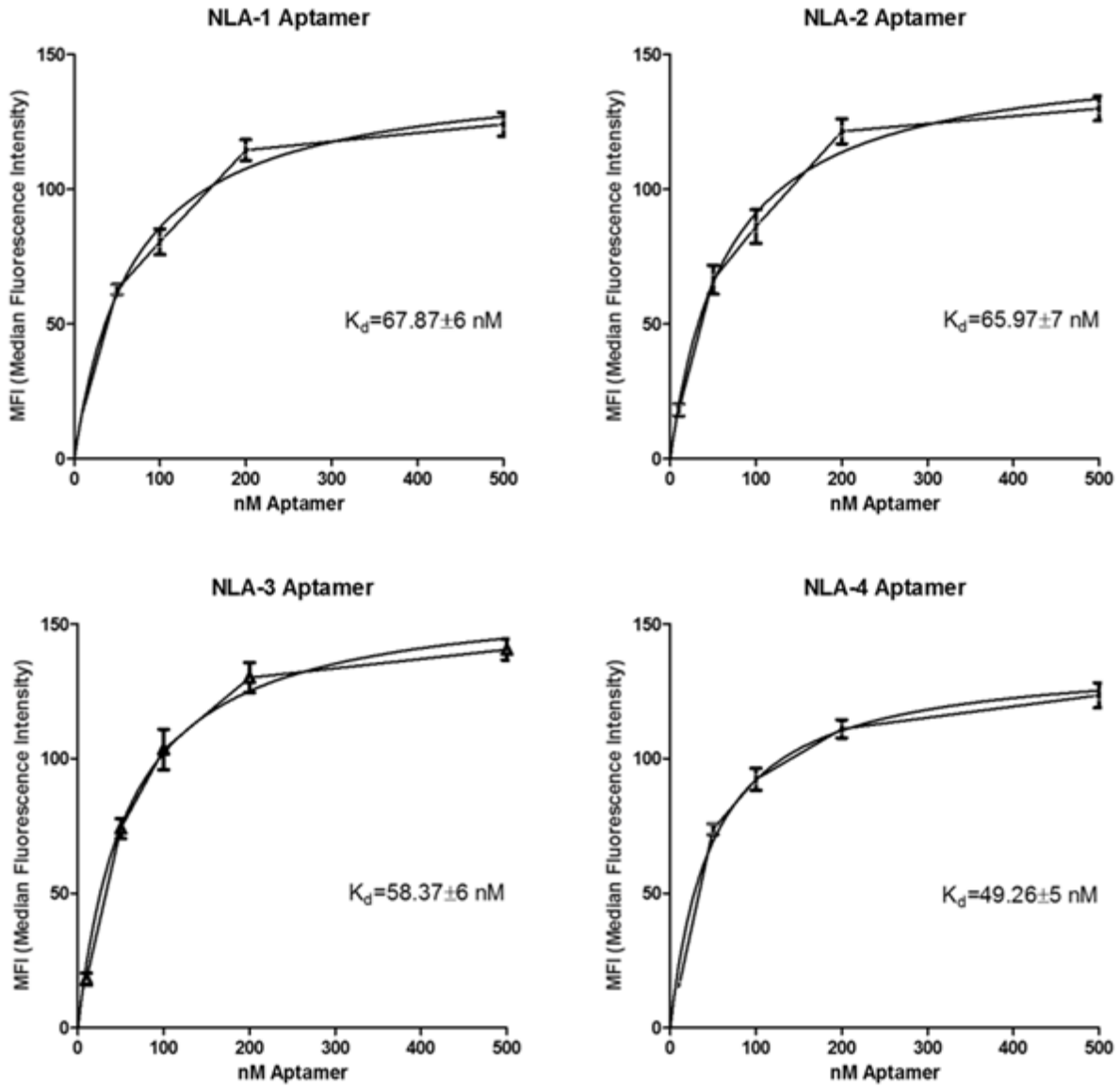


**Figure 4.8.** $K_d$ **analysis of NLA aptamers.** CD20+HEK cells were titrated in triplicate with fluorescently tagged aptamer at indicated concentration (10nM, 50nM, 100nM, 200nM and 500nM) and binding measured as the MFI signal intensity. The data was fitted using a non-linear regression and $K_d$ calculated from the graph using GraphPad software. All aptamers exhibited relatively appreciable binding, with $K_d$s less than 100nM. Aptamers NLA-3 and NLA-4, in particular, were the best binder of CD20+HEK cells possessing the smallest $K_d$ at 58.4nM and 49.3nM respectively.

#### *4.3.3.2 Aptamer show selective binding to CD20+ HEK cells*

To evaluate specificity, saturating concentrations of NLA aptamers were incubated with both CD20+HEK cells and, separately, the untransfected HEK cells. After washing the cells were re-suspended in buffer and the resultant fluorescence measured. The MFI values are depicted in Figure 4.9. In all cases, the aptamers exhibited elevated MFI values when incubated with the transfected CD20+HEK cells, relative to the original and untransfected HEK cells. This difference in binding was found to be statistically significant when assessed using the student *t*-test. The most discriminative aptamers were NLA-3 and NLA-4 which exhibited the greatest difference in MFI signals between the two cell lines. In particular, NLA-3 bound the CD20+HEK cells three times more avidly than the untransfected cells. That the sequenced aptamer clones possess increased binding association with the transfected CD20+HEK cells and not with the untransfected HEK cells shows that selection was successful in cultivating a pool of aptamer whose specificity is to the transfected marker, CD20. That all of the candidate aptamers possess this characteristic illustrates the utility of using NGS to characteristically evaluate sequences.

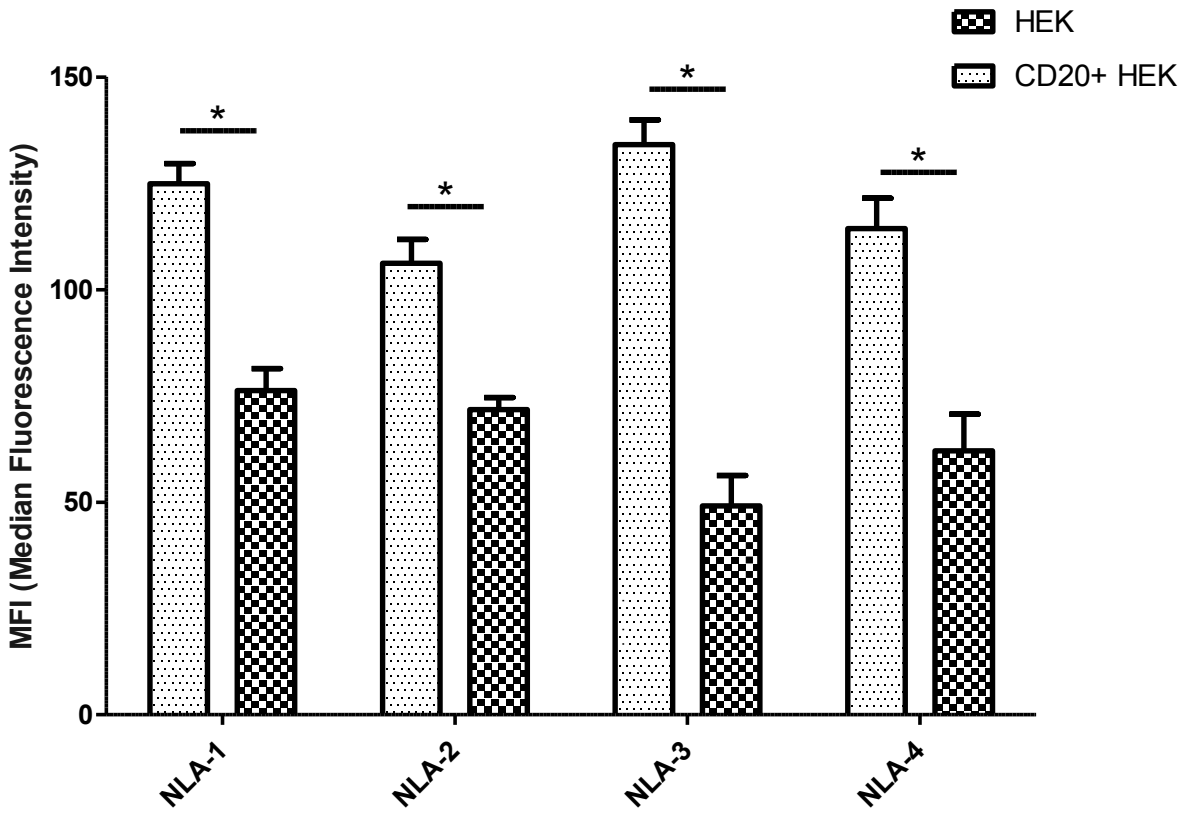


**Figure 4.9. Evaluation of aptamer specificity.** To appraise the original selection regime, the binding intensity of the lead aptamer candidates were compared between the CD20+HEK and the untransfected HEK control cells. Cells were stained in triplicate. In all cases the NLA aptamers (300nM) had statistically greater MFI values when incubated with the CD20+HEK cells and not the original HEK cells, *$p<0.05$. NLA-3 and NLA-4 were the most specific binders of the transfected cell line. Therefore, the NGS analysis of pool 10 successfully identified sequences that possessed heightened affinity to the CD20+HEK cells.

#### *4.3.3.3 Pooled NLA Aptamers Exhibit Competitive Binding with anti-CD20 Antibody*

To evaluate aptamer specificity, a co-staining experiment using NLA aptamer and anti-C20 antibody was performed. Transfected cells were initially incubated with either the unselected DNA library or the pooled NLA aptamers, and then counter stained using anti-CD20 antibody. The amount of antibody labelling in co-stained cells was compared to singly stained controls. The results are depicted in Figure 4.10. The solid black bar represents the antibody signal intensity of CD20+HEK cells singly stained with the anti-CD20 antibody, MFI=50.3. Alongside it are the MFI values in the same antibody specific channel for library or NLA aptamer co-stained samples. Note that incubating CD20+HEK cells with the pooled NLA aptamers substantially and significantly decreases the antibody signal. Incubating CD20+HEK cells with the DNA library however, does not result in any significant changes. The antagonism of antibody binding with the NLA aptamers appears to be concentration dependent. Cells incubated with 2μM of the pooled aptamers exhibit a much more significant reduction in the antibody signal, down to MFI=14, than cells incubated pooled NLA aptamers at 1 μM, a decrease to MFI=23. There was no detectable difference between incubating with pooled NLA mixtures or equimolar amounts of a single sequence.

The co-staining experiments show that the NLA aptamers do not behave as random species, like the DNA library. Unspecific aptamers not subject to targeted selection, prove incapable of altering significantly the amount of anti-CD20 binding. This data appears to suggest that the NLA aptamers specifically compete with the antibody for binding and may recognize and bind to identical epitopes on the CD20 molecule as the antibody itself.

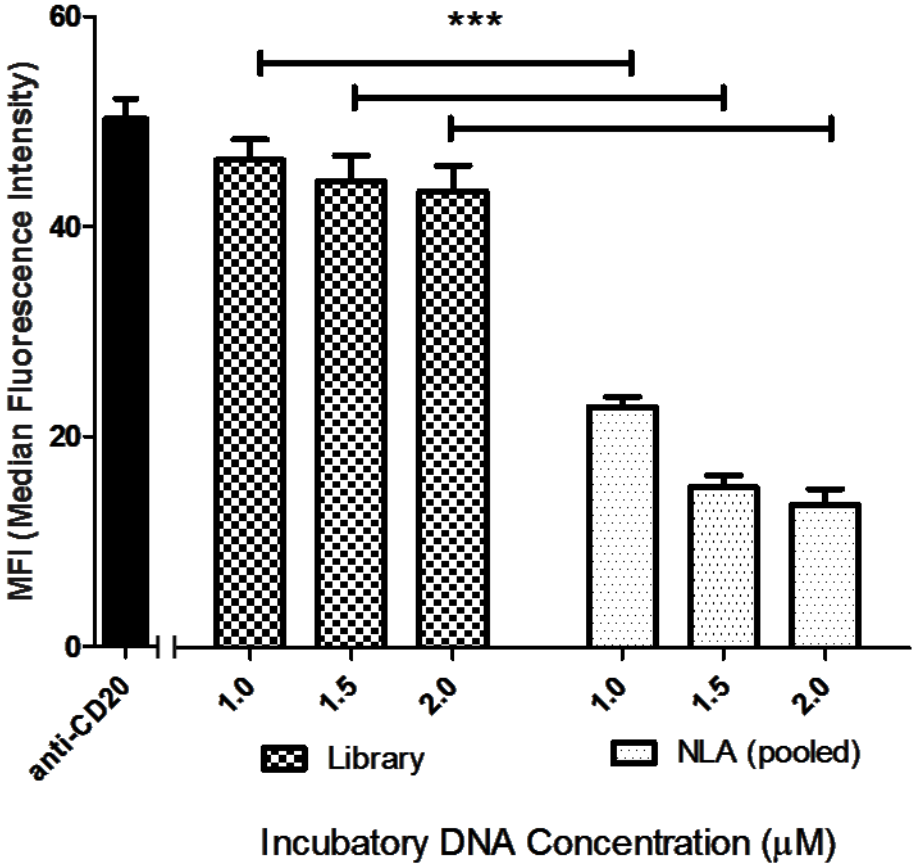


**Figure 4.10. NLA aptamers inhibit the binding of anti-CD20 antibody.** CD20+HEK cells were co-stained using anti-CD20 antibody (10ng/µL) and DNA derived from either the unselected DNA library, or a pooled mixture of all the candidate aptamers NLA-1 to NLA-4. Samples were assessed in triplicate. Co-stained samples are compared to the singly stained anti-CD20 control (solid black bar). Incubating the cells with the aptamers dose dependently decreased the binding of anti-CD20 antibody. This reduction was significantly greater than when cells were incubated with the unselected DNA library, *$p<0.05$. The antagonism of antibody binding suggests that NLA aptamers and the antibody compete for binding at mutual sites on the CD20 molecule.

## 4.4 DISCUSSION

Next generation sequencing is a powerful method of evaluating millions of discrete DNA species efficiently and robustly. Aptamer Pool 10 was the strongest and most specific binder of CD20+HEK cells. As such, it was important to elucidate the key aptamer sequences responsible for this association and to evaluate their characteristics. NGS analysis confirmed that pool 10 exhibited significant sequence convergence- a hallmark of a successful selection. After collapsing the data the total number of sequences was reduced from 541,258 to 62,737, an 8-fold reduction. The top 29 sequences accounted for nearly 70% of all sequences and as the phylogenetic assessment showed exhibited significant sequence similarity. In total there were 5 dominant clusters each of which possessed 1 or more significantly high copy number (HCN) sequence. These HCNs reflect the most over-represented sequences in pool 10 and in turn became the lead aptamer candidates NLA-1 to NLA-4. Their retention and over-expression indicates that they are the sequences that best reflect the intrinsic characteristics of CD20+HEK based SELEX. DREME analysis refined the pools characteristics. It identified 3 consensus motifs, the most prevalent of which GGRCA, was found in 84% of all sequences. All NLA aptamers were in possession of one or more of these motifs.

It is notable that HCN sequences were preferred even to closely related and virtually identical sequences. And that where variation existed the biased nucleotides were G or C. For example between sequences #6 and #38, copy number bias favours sequence #6 by 131:1. Sequence #6 and #48 differ by only one nucleotide, the #6's G to sequence #48's T. This was also observed between sequence #12 and #45 which were the second most heavily skewed. Here the ratio favoured sequence #12's C to sequence #45's T by a

factor of 47:1. It is known that Taq polymerase is biased against GC rich DNA (136, 137). That lead aptamer candidates would persist with a high copy number in spite of this polymerase bias is further evidence that selection was specifically isolating distinct and specific sequences. Relevantly, sequence # 6, the sequence with the greatest copy number and the most significant bias, would become NLA-3 among the most potent and specific of all the aptamer candidates.

Cumulatively, NGS analysis was able to describe, quantify and evaluate aptamer candidates with a high degree of resolution. To its testament, all of the lead aptamer candidates bound CD20+HEK cells with $K_d$s less than 100nM. And when compared to the untransfected cell line all of the aptamers possessed heightened specificity for the CD20+HEK cells than to the untransfected HEK control. Therefore the NGS analysis helped to elucidate key sequences responsible for the heightened affinity and specificity observed with aptamer pool 10.

To further evaluate specificity we performed a co-staining experiment to gauge what mutual interaction, if any, the aptamers and the anti-CD20 antibody had. We compared DNA library or aptamer co-stained cells to a singly stained antibody controls. The incubation of CD20+HEK cells with pooled NLA aptamers resulted in a much more significant reduction in antibody binding than when cells were incubated with the unselected DNA library. The aptamers ability to limit the binding of anti-CD20 antibody was concentration dependent, the greater the concentration of the pooled NLA aptamers the more significant the reduction in the antibody signal. That this was appreciable only with the NLA sequences and not the DNA library shows that it is an intrinsic characteristic of the NLA aptamers themselves and not the arbitrary influence of DNA.

This antagonistic action suggests that both aptamers and antibody recognize mutual epitopes on the CD20 molecule.

Cumulatively these results confirm that an in-vitro CD20 target positive selection strategy is an effective way to generate highly specific CD20 aptamers. And that NGS analysis is a robust method of sequence evaluation, critically identifying highly potent and highly specific aptamers.

## 4.5 CONCLUSION

NGS analysis represents an extremely effective method of sequence discovery and organization. We showed that pool 10 exhibits significant sequence convergence by phylogenetic determination, possessed high copy number sequences, which all contained one or more highly common consensus motifs. Lead HCN aptamers exhibited high frequency ratios even when compared to highly similar sequences, and were preferred in spite of a PCR bias. All NLA aptamers exhibited potent binding, with $K_d$s less than 100nM, and possessed specific binding to the CD20+HEK cells. Incubating CD20+HEK cells with NLA aptamers, and not the DNA library, significantly reduced the binding of the anti-CD20 antibody. This co-staining experiment suggest that NLA aptamers and antibodies recognize mutual sites. Aptamer NLA-3 is a testament to the resolving capacity of NGS, it was the most abundant aptamer in pool 10, with the highest overall copy number of 11,019 and the possessor of 2 common motifs, it was one of the strongest affinity aptamers ($K_d$=58.4 nM) and the most discriminative binder of CD20+HEK. In summary, NGS analysis of pool 10 helped to identify highly potent and specific aptamers with appreciable and detectable CD20 sensitivity.

# 5 BIOLOGICAL EFFICACY OF APTAMERS IN COMPLEMENT DEPENDENT CYTOTOXICITY

## 5.1 ABSTRACT

One effector mechanism of anti-CD20 antibodies is complement dependent cytotoxicity (CDC). Here, we evaluated CDC induction in transfected CD20+HEK and the naturally CD20 expressing cell line CCL-86. We found that CDC could only be induced in the CCL-86 cells; CD20+HEK cells were refractive to stimulation. Interestingly NLA aptamers, selected to CD20+HEK, exerted a protective effect against CDC induction with the CCL-86 cells— limiting the total amount of cell death by 10%, and significantly decreasing the intensity of pro-apoptotic markers 7-AAD and annexin-V. The unselected DNA library exerted no protective influence. These findings show that CDC induction relies on factors which the expression of CD20 alone on HEK293 cells cannot facilitate. Aptamers selected against transfected CD20, however, will exhibit an antagonistic action, limiting the extent of CDC induced cell death in naturally CD20 expressing cells. This finding further corroborates the specificity of the aptamers and helps to define their mechanism of action.

## 5.2 BACKGROUND

### 5.2.1 Biological Action of Anti-CD20 Antibodies is Varied and Diverse

Therapeutic antibodies have revolutionized the treatment of disease; by combining target specificity with effective clearance mechanisms they represent a highly specific and extremely potent class of drugs for ailments as diverse as inflammation,

autoimmune conditions and cancer (130). Though efficacy is apparent the immunological mechanism by which it is achieved can be elusive. In oncology, few targets are as avidly pursued as CD20. Indeed the first FDA approved therapeutic antibody, rituximab, was raised against the CD20 molecule. Its wide success prompted the clinical approval of an additional three anti-CD20 antibodies, with eight more still in clinical development. One interesting implication of this longevity has been a more thorough investigation of both anti-CD20 epitopes and their effector mechanisms.

### 5.2.2 Effector Action of anti-CD20 Antibodies

The therapeutic action of all monoclonals is currently limited to 4 mechanisms. They are, as depicted in Figure 5.1, PCD or programmed cell death, ADCC or antibody dependent cell mediated cytotoxicity, ADCP antibody dependent phagocytosis and CDC complement dependent cytotoxicity. To a significant extent, research into the effector action of anti-CD20 antibodies has been primarily focused on ADCC and CDC.

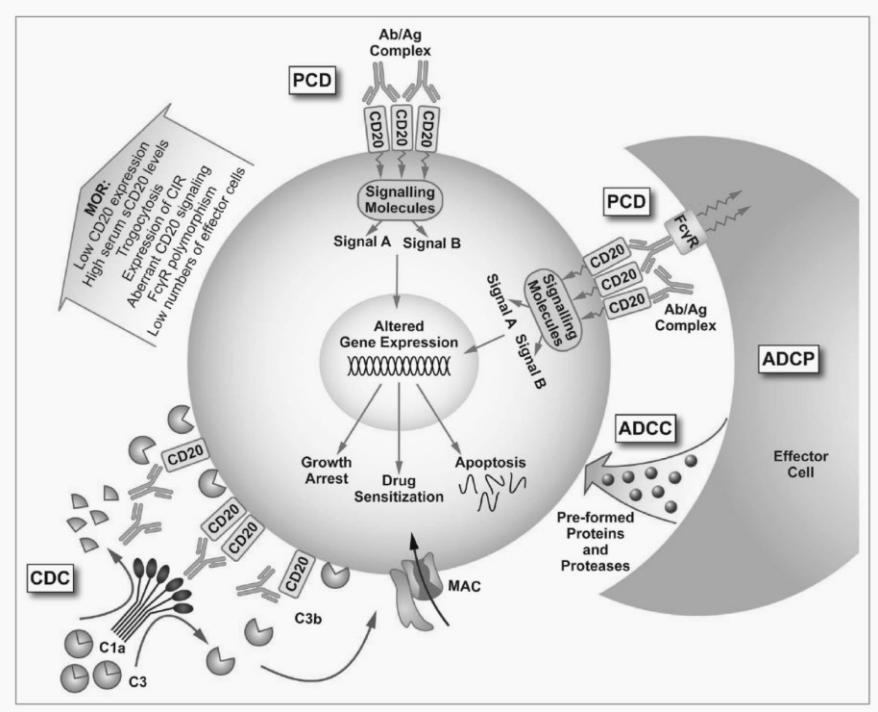


**Figure 5.1. Anti-CD20 effector actions.** CD20 ligation induces rapid and potent cellular depletion elicited by the following effector mechanisms: PCD, ADCC, ADCP and CDC. PCD or programmed cell death, is facilitated by antibody binding and the subsequent activation of pro-apoptotic signaling cascades. Both ADCC, antibody dependent cell mediated cytotoxicity and ADCP-antibody dependent cellular phagocytosis, rely on effector leukocytes and require Fc to Fc$\delta$R interactions. In ADCC, activation results in the subsequent release of granulocytic enzymes from the effector cell. In ADCP, it results in the engulfment and digestion of the antibody bound cell. CDC or complement dependent cytotoxicity is initiated by the Fc mediated cleavage of serum complement proteins. These bring about cell lysis by self-assembling into cytolytic transmembrane pores known as the membrane attack complex (MAC). Reproduced with permission: Oflazoglu, E., Audoly L.P. Evolution of anti-CD20 monoclonal antibody therapeutics in oncology. *Mabs*. **2** (1): 14-19 (2010).

#### *5.2.2.1 PCD: Programmed Cell Death*

PCD refers to programmed cell death, when the binding of an antibody turns on or off signalling pathways resulting in the induction of apoptosis. Rituximab is a potent PCD agent in-vitro when crosslinked using a secondary antibody. Although how this could operate in-vivo is not well defined (42). It is interesting that the clinical side effect of all anti-CD20 antibodies is the rapid and conserved depletion of CD20 positive cells from the blood. So while the clinical mechanism of PCD may not be entirely clear its manifestation is obvious.

#### *5.2.2.2 ADCC: Antibody Dependent Cell mediated Cytotoxicity*

ADCC is mediated through the Fc domain of bound antibodies. Exposed IgG Fc domains are recognized by cognate Fcδ receptors (FcδR), which are expressed on a variety of effector leukocytes including natural killer cells, monocytes, macrophages and neutrophils (32, 42). There are different isoforms of FcδR with varying affinities and activities. The successful union between Fc and active FcδR stimulates the release of cytotoxic granules containing enzymes like perforin, granulysin and granzymes from the effector cells resulting in the destruction of the Fc bound cell (42, 138). ADCC is frequently associated with anti-CD20 antibodies. Corroborative studies have shown the failure of anti-CD20 therapy in FcδR knock out mice (139-141). In human studies, allelic variation in the genes encoding FcδR can impact the outcome of treatment in patients with certain types of cancer. For example, Non-Hodgkin's lymphoma patients with high affinity variants of FcδRIIIA exhibit better response rates with anti-CD20 therapy (142). This correlation however could not be extended to patients with CLL (143). The appreciation of the importance of ADCC is evident in the design of GA101, one of the newest anti-CD20 antibodies. Its Fc domain was glyco-engineered to improve binding to

FcδRIII receptors, a modification that resulted in a 100-fold enhancement of ADCC activity (144). Further studies will help to better define what role modifications like these have with treatment.

#### *5.2.2.3 ADCP: Antibody Dependent Cell mediated Phagocytosis*

FcδR interactions may alternatively result in phagocytosis if the effector cell is a monocyte or macrophage. Detailed information regarding ADCP is lacking due to the fact that it is often highly variable in in-vitro studies and notoriously difficult to assess in-vivo (145); neither of which is reason to discount its influence. One interesting implication of ADCP, and a potential rationale for observed long-lived remission in cancer patients, is cross-presentation (146). Phagocytes can acquire and present antigens through phagocytosis. These antigens can in turn used to stimulate and activate subsets of T-cells, including highly potent CTL (cytotoxic T lymphocytes) (147). Antibodies like anti-CD20 may act as signals for phagocytes, and if the antigens they acquire are cancer specific may help to give rise to tumour specific subsets of CTLs, thereby establishing long lived anti-tumour immunity.

#### *5.2.2.4 CDC: Complement Dependent Cytotoxicity*

Complement dependent cytotoxicity also relies on the input of additional components from the immune system, in this case not cells but complement proteins. The complement system was discovered more than 100 years ago (148) and predates antibody elucidation. CDC is initiated by the antibodies Fc domain and requires the stepwise cleavage of an additional 30 proteins—both blood borne and membrane bound. These free factors are synthesised in the liver in an inactive “pro-enzyme state” (148) and are found circulating in the blood, lymph and interstitial fluid. Some of these

complement proteins like C1a, C3 and C3b are indicated in Figure 5.1. Their ordered deposition on the afflicted cell surface results in the formation of a membrane attack complex (MAC), a transmembrane pore that disrupts membrane integrity, resulting in the loss of homoeostasis and eventual cell death (149).

CDC is well established effect of anti-CD20 antibodies. Rituximab has been shown to bind C1Q and induce potent CDC in both lymphoma cell lines and primary tumours (150). Studies have shown that the up-regulation of cellular factors known to provide resistance to complement —notably the expression of CD55 and CD59—are also associated with a resistance to anti-CD20 treatment (151). Neutralization of these factors is enough to re-sensitive cells to treatment (152). In-vivo studies in mice and humans have shown that complement is rapidly depleted after rituximab infusion (153). And, that the injection of fresh complement proteins can rescue this effect (154, 155). Other studies, though, have questioned the impact and extent of CDC. For example mice devoid of critical complement factors C1q, C3 or C4 were still susceptible to B-cell induced depletion using anti-CD20 antibodies (140). And in humans with follicular lymphoma and CLL no correlation was found between the expression of complement resistant factors and clinical outcome (156).

These, at times conflicting results, are perhaps not surprising. Elucidating the collective impact of antibody effector mechanisms is complicated. And while antibodies may initiate one or many of these effector mechanisms, the overall outcome may not be synergistic. Studies have shown that the addition of viable serum complement protein inhibited rituximab initiated ADCC; while heat inactivated human serum, whose proteins are denatured, had no such effect (157). Another study showed that the cellular

deposition of complement protein C3B promoted trogocytosis, the removal of antibody bound complexes from the cellular surface by other immune cells (158, 159) the result of which would all but curtail any FcδR mechanisms. The effector mechanism of most clinical antibodies, including anti-CD20s, remains an active area of research.

### 5.2.3 Epitope Specificity

One potential explanation for the variability in effector mechanisms is epitope specificity. Figure 5.2 is a list of all anti-CD20 antibodies approved or in clinical development, their epitope (binding site) and their effector actions (comments). Rituximab is the prototypical anti-CD20 antibody, it is for this reason that mapped epitopes are broadly categorized as type 1 (rituximab based) or type 2 (non-rituximab). Ofatumumab is another, more recent, anti-CD20 antibody. Its epitope is distinct from that of rituximab (29) and in biological assays it has been shown to be a more substantial inducer of CDC than rituximab (55, 56). Teeling et al (55) have suggested that ofatumumabs epitope, which was mapped to the smaller extracellular loop, places it in closer proximity to the cell membrane, and therefore in a location better suited to recruit the membrane factors requires for MAC formation than rituximab. Significantly, and perhaps partly due to the limited nature of epitope analysis or the inherent variability in biological assays, these generalization can't be applied to other antibodies. For example ocrelizumab, veltuzumab, and zevalin are all antibodies that possess the same epitope as rituximab and yet all favour different effector mechanisms.

| mAb | Format | Indication | Manufacturer | Binding site | Comments | Phase Dev |
|---|---|---|---|---|---|---|
| Rituximab Rituxan® MabThera® | cIgG1 | NHL, RA | Genentech, Biogen | Type I | PCD, ADCC, CDC, ADCP | Approved in US 1997 |
| Reditux | cIgG1 | NHL | Dr. Reddy Laboratories | Same as Rituximab | Biosimilar | Approved in India 2007 |
| Y90-Ibritumomab tiuxetan Zevalin® | mIgG1 | NHL | Biogen IDEC | Same as Rituximab | Low ADCC | Approved in US 2002 |
| I131tositumomab Bexxar® | mIgG2a | NHL | GlaxoSmithKline | Different than Rituximab Type II | Low CDC | Approved in US 2003 |
| Ofatumumab Arzerra® | hIgG1 | CLL, NHL, RA | Genmab, GlaxoSmithKline | Different than Rituximab | Low $K_{off}$ High CDC | Approved in US 2009 |
| Ocrelizumab | hIgG1 | NHL, RA | Genentech, Roche, Biogen | Same as Rituximab | High ADCC Low CDC | Phase 3 |
| Veltuzumab | hIgG1 | NHL, ITP | Immunomedics | Same as Rituximab | Low $K_{off}$ High CDC | Phase 2 |
| Obinutuzumab GA101 | hIgG1 | CLL, NHL | Glycart Roche | Type II | High PCD High ADCC Low CDC | Phase 2 |
| AME-133v | hIgG1 | NHL | Applied Molecular Evolution, Eli Lilly | N/A | High ADCC | Phase 2 |
| TRU-015 | SMIP | RA | Trubion Pharma, Wyeth | N/A | High ADCC Low CDC | Phase 2 |
| PRO131921 (Version 114) | hIgG1 | CLL, NHL | Genentech | N/A | High CDC High ADCC | Phase 1/2 |
| LFB-R603/EMAB-6 | cIgG1 | CLL | GTC Biotherapeutics, LFB Biotechnologies | N/A | High ADCC | Phase 1 |

**Figure 5.2. Clinical status of anti-CD20 antibodies.** Depicted for each anti-CD20 antibody is its structural class under format, clinical indication, manufacturer, epitope binding site, the most commonly associated biological effector actions under comments, and its developmental phase. In comments, PCD= programmed cell death, ADCC= antibody dependent cell mediated cytotoxicity, ADCP= antibody dependent cellular phagocytosis and CDC=complement dependent cytotoxicity**.** Reproduced under the Creative Commons Attribution-Noncommercial Liscence: Oflazoglu, E., Audoly L.P. Evolution of anti-CD20 monoclonal antibody therapeutics in oncology. *Mabs*. **2** (1): 14-19 (2010).

Their remains still much to uncover regarding anti-CD20 antibodies and their effector actions. This understanding is complicated significantly by the staggering complexity of the immune system; where neither the cancer, nor the antibody, nor its clearance mechanism can be wholly relied upon to be a predicative indicator of efficacy.

### 5.2.4 Aptamer to Better Elucidate Target-Antibody Dynamics

A more comprehensive understanding of these dynamics is required. Aptamers have proven to be an incredibly useful probative tool to help elucidate, report on, and in some cases even modify, the interaction of antibodies and receptors. Aptamers selected against the immunogenic region of the acetylcholine receptor acts as decoys inhibiting the damaging effect of autoantibodies implicated in Myasthenia Gravis Disease (160). High affinity and highly stable aptamers selected against prostate specific antigen (PSA) inhibit 60% of its activity, while avoiding the immunogenic nature of anti-PSA antibodies (14). Aptamers selected against ErbB-2/HER2, a growth factor receptor and a well-established cancer biomarker, exhibited two fold greater anti-tumour effects when compared to Erb-2/HER2 specific antibodies (58). Therefore, aptamers occupy an important innovative niche and can significantly aid in the elucidation and manipulation of complex antibody-based effector mechanisms.

## 5.3 RESULTS

### 5.3.1 CDC is potently induced by anti-CD20 antibody in naturally CD20 expressing CCL-86 Cells but not in the transfected CD20+HEK cells.

We evaluated CDC induction in CD20+HEK cells and compared it to the naturally CD20 expressing CCL-86 cells. CDC can only be induced by anti-CD20 antibodies in the

presence of viable human serum (HS). As relevant controls, we incubated cells in heat inactivated human serum (HiHS), whose proteins are denatured and therefore are incapable of activting CDC.

Figure 5.3 provides the results of the initial CDC assessment. Naturally CD20 expressing CCL-86 cells incubated with anti-CD20 antibody in either PBS or with heat inactivated human serum will maintain high levels of cellular viability at over 80%. This shows that anti-CD20 antibodies cannot, on their own or when deprived of viable complement proteins, induce CDC. Only when CCL-86 cells are incubated with both anti-CD20 antibodies and viable human serum does the viability drop significantly to 33%. Note the disruption in the shape of the cell population. Unexpectedly, CD20+HEK transfected cells failed to undergo CDC. Here, cellular viability remained constant at over 90% regardless of reaction conditions, in PBS, with viable serum, or with heat-inactivated serum. CD20+HEK cells are therefore not susceptible to CDC.

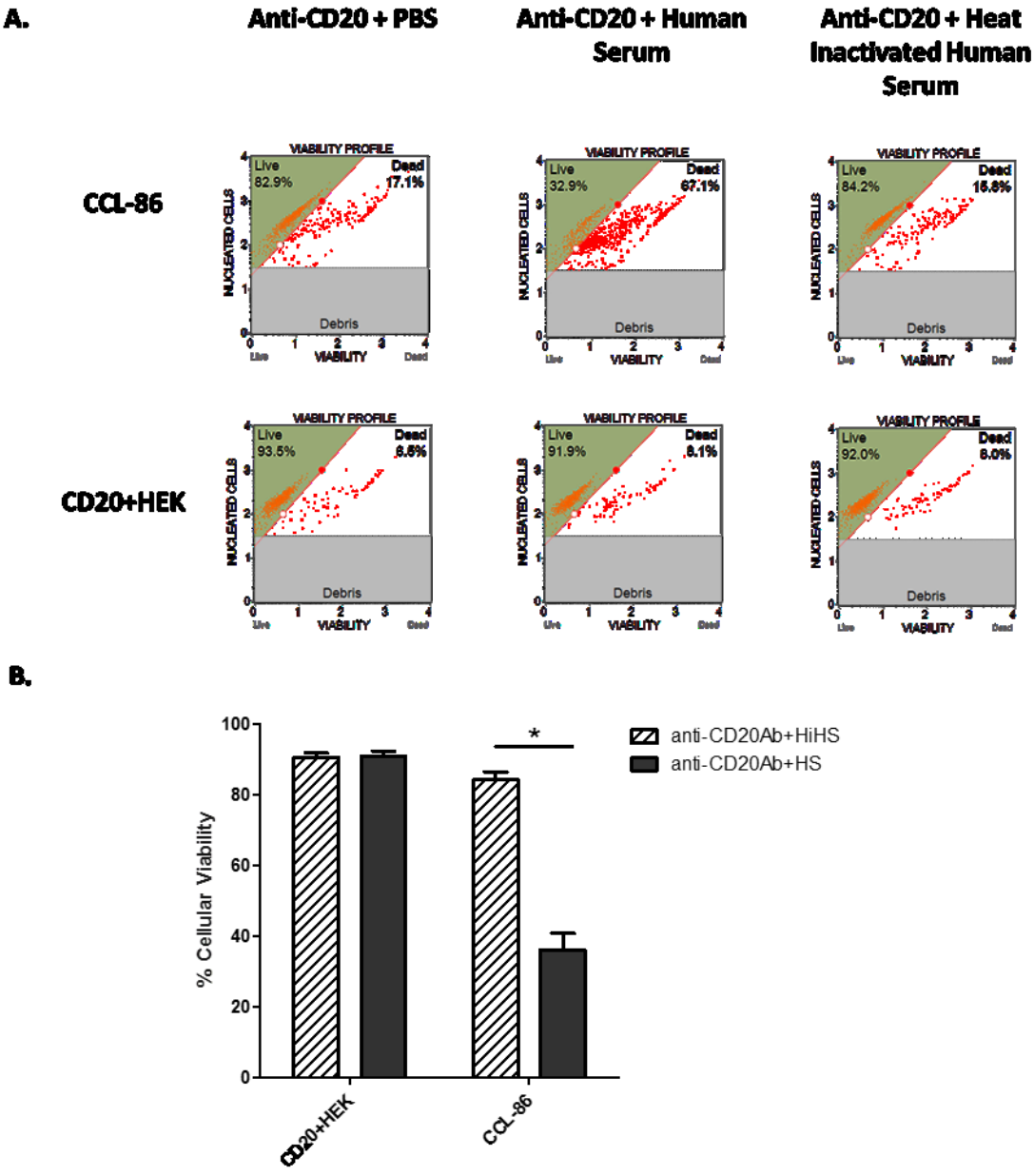


**Figure 5.3. Comparison of CDC induction in naturally CD20 expressing CCL-86 and transfected CD20+HEK cell lines.** CDC was induced using anti-CD20 antibody (10ng/µL) and viable human serum (HS). Heat inactivated human serum (HiHS) was used as a control. **A)** CCL-86 cells incubated with anti-CD20 antibody and provided viable HS undergo CDC, evidenced by the dramatic decrease in cellular viability from 82.9% to 32.9%. CD20+HEK cells, however, were refractive to CDC induction and persisted with high cellular viability regardless of reaction conditions. **B)** Results of triplicate data show the only CCL-86 cells undergo CDC, *$p<0.05$.

### 5.3.2 NLA aptamers can limit extent of CDC in CCL-86 Cells.

The antagonistic action of aptamers selected to receptors is widely known. We were curious to assess the impact our NLA aptamers could exert with CCL-86 cells.

#### *5.3.2.1 NLA aptamer exhibit modest binding affinity to CCL-86 Cells*

We assessed the binding affinity of our CD20+HEK aptamers with both the naturally CD20 expressing cells CCL-86 and the naturally CD20 negative TIB-152. As Figure 5.4 illustrates when pooled, NLA aptamers exhibit significantly greater binding affinity, compared to the library, when incubated with the CD20 positive CCL-86 cells, and not the CD20 negative TIB-152 cells. CCL-86 cells incubated with the library possess an MFI of 5, and when incubated with the pooled clones it is nearly 3 times greater with MFI of 15. With TIB-152 cells, the binding affinity of both the randomized DNA library and the NLA aptamers is comparable and not significant. As NLA aptamer were selected using CD20+HEK cells and, as shown here, exhibit specific binding to the naturally CD20 expressing cells CCL-86 and not the CD20 negative cells lines TIB-152, this proves that NLA aptamers are CD20 specific.

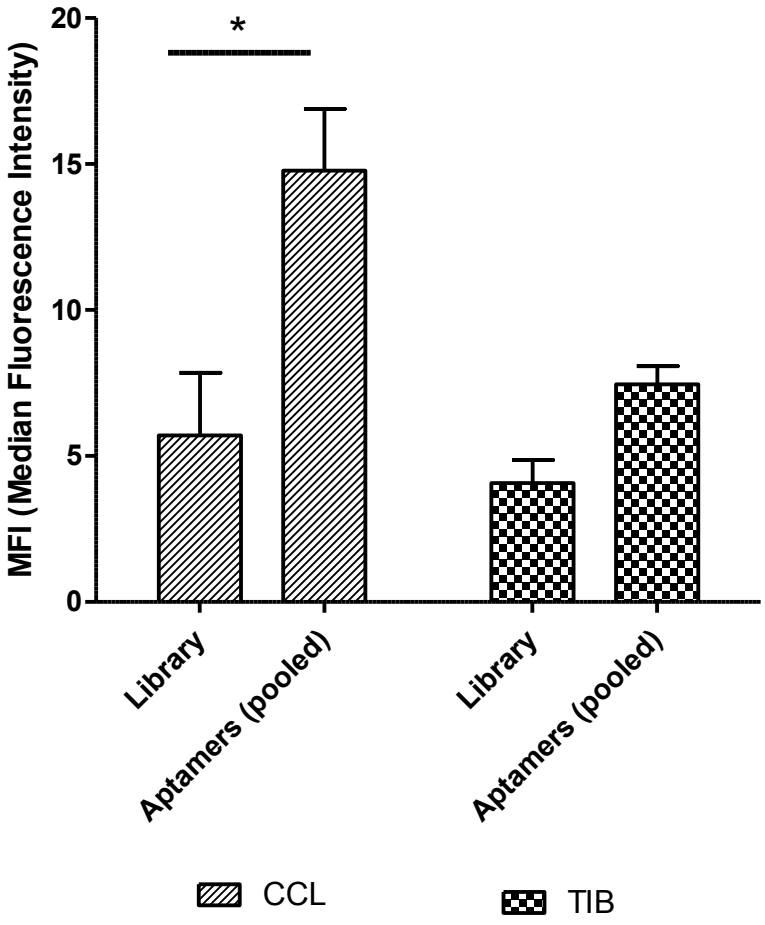


**Figure 5.4 NLA aptamers show specific affinity with the CD20 positive CCL-86 and not the CD20 negative TIB-152.** CCL-86 and TIB-152 cells were stained with 2μM of either the DNA library or pooled NLA aptamers sequences, in triplicate. Naturally CD20 positive CCL-86 cells exhibit significantly greater binding affinity with the pooled aptamers, relative to the unselected DNA library, than the naturally CD20 negative TIB-152 cells, *$p<0.05$. This suggests that NLA aptamers positively label and associate with the CD20 molecule on CCL-86 cells.

#### *5.3.2.2 CDC in CCL-86 cells is associated with significant increases in 7-AAD and Annexin-V Staining*

Due to the inherent variability of biological assays it was important prior to attempting to evaluate the biological impact of NLA aptamers, to evaluate CDC in the form of relevant cell-death markers. To do this we measured total cell death in the form of the vital stain 7-AAD and the pro-apoptosis marker annexin-V. 7-AAD is a DNA intercalating dye; its permeability into cellular nuclei is barred by the presence of intact cellular membranes. Dead cells, whose membranes offer no such protection, will be positively stained by 7-AAD and exhibit high 7-AAD fluorescence. Annexin-V binds phosphatidylserine (PS) a phospholipid whose expression is restricted by flippases to the inner leaflet of the cellular membrane. In apoptotic cells ATP dependent flippases are no longer maintained leading to extracellular PS expression. It is the extracellular PS which is the target of annexin-V antibodies. Together 7-AAD and annexin-V are dual dyes that can be used to differentiate not only between live and dead cells but also live cells committed to undergoing apoptosis.

Figures 5.5 (control) and Figure 5.6 (experimental samples) are representative flow cytometry plots measuring both 7-AAD (captured by FL4) and annexin-V (captured by FL2) fluorescence. Figure 5.7 are the tabulated results of triplicate data. Both dot plots and histograms are provided in Figures 5.5 and 5.6. Dot plot depict total events captured by the flow cytometer, here both SS (internal complexity) and FL4 for 7-AAD were detected. High 7-AAD fluorescence indicates cell death; therefore in the dot plots, the value given for the $I^{++}$ quadrant, represents the total percentage of dead cells in the sample. This is technically also depicted in the 7-AAD histogram.

Figure 5.5 represents the controls samples respectively these are CCL-86 cells that have been incubated in serumless media, with the anti-CD20 antibody diluted in PBS, incubated singly with either HiHS or HS or alternatively the DNA library or pooled NLA aptamer in PBS. Note the relative similarity in both cellular distribution and in the MFI across all samples. This proves that neither the media, nor the antibody alone, neither the DNA library or pooled aptamers or some agent inherent in HS or HiHS can significantly impact cellular viability. There was, admittedly a minor and insignificant increase in 7-AAD and annexin-V in control samples entirely deprived of serum. For example, serum fortified control cells, namely CCL-86+HiHS and CCL-86+HS, did exhibit lower total dead cell percentages in the $I^{++}$ quadrant. In CCL-86 with HiHS or HS, the $I^{++}$ population was limited to 4.51-4.66% compared to 5.18-6.98% in the other samples. Serum fortified cells also had lower MFIs for both 7-AAD and annexin-V. CCL-86 cells in HS or HiHS had MFIs for 7-AAD is in the range of 1.46-1.78 this was lower than the 2.41-2.86 of the other controls. The values for annexin-V were similar. Control cells with serum had MFIs for annexin-V in the range of 1.95-2.19 which is lower than the 5.59-6.78 seen with the others. This suggest that incubating cells wholly without serum for the duration of this experiment is associated with slightly elevated levels of cell death and PS expression. These increases however were insignificant when evaluating CDC.

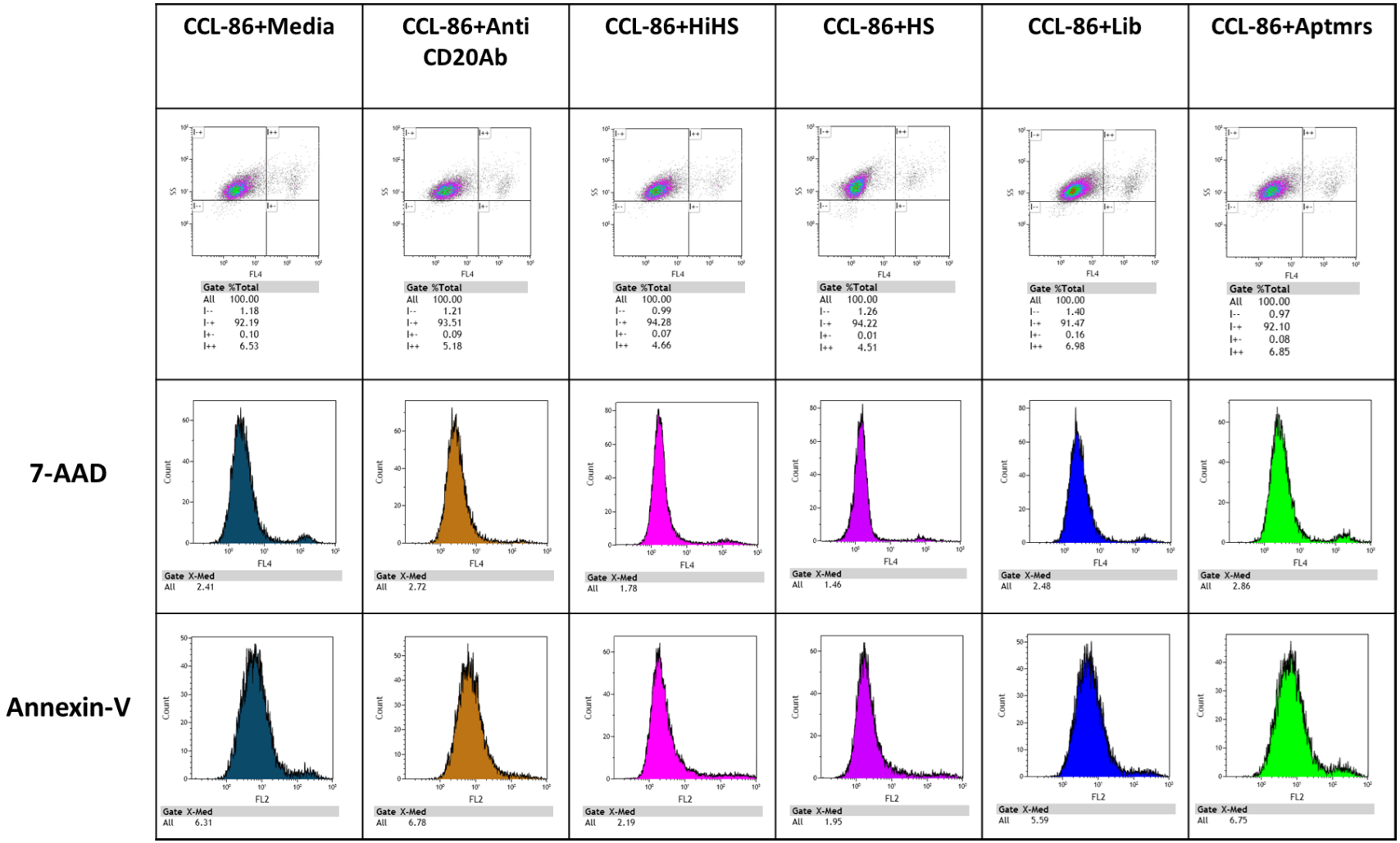


**Figure 5.5. Complement dependent cytotoxicity in CCL-86: control samples.** Represented above are the dot plot and histogram for 7-AAD staining and the histogram depicted annexin-V staining for the following control samples: the CCL-86 cells incubated in unsupplemented media, the CCL-86 cells with 10ng/μL of anti-CD20 antibody, CCL-86 cells with 50% heat inactivated human serum (HiHS), with 50% normal human serum (HS), in 2μM of DNA library or in 2μM of pooled NLA aptamers. This shows that no agent inherent to HiHS, HS, anti-CD20 antibody, unselected DNA library nor pooled NLA aptamers will significantly alter cellular viability.

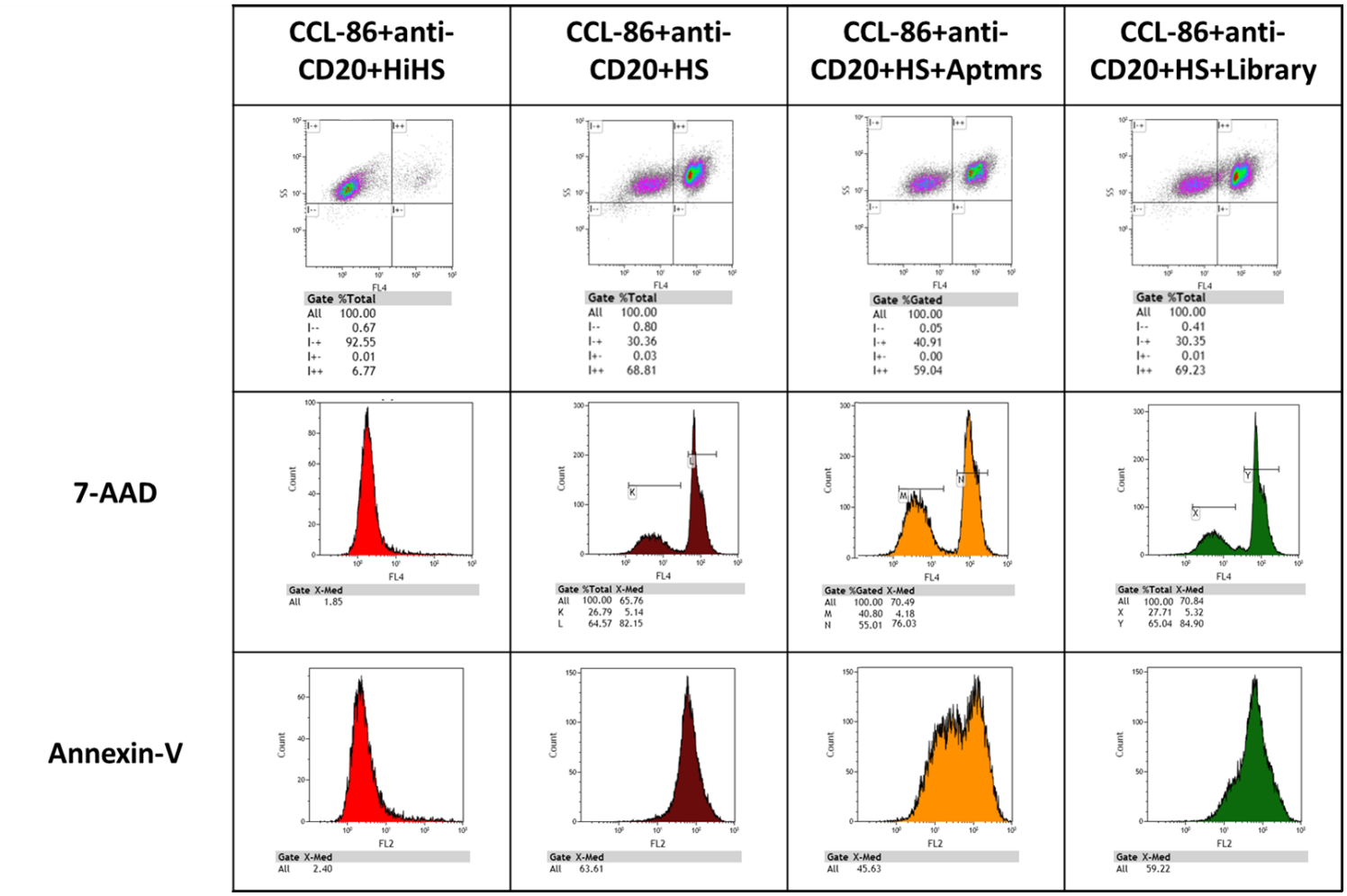


**Figure 5.6. NLA aptamers limit the extent of complement dependent cytotoxicity in CCL-86 cells.** CDC was initiated by incubating cells with 10ng/µL of anti-CD20 in the presence of viable human serum, and was compared against the CCL-86+anti-CD20+HiHS control. The induction of CDC in CCL-86+anti-CD20+HS was associated with increases in total cell death, evidenced by the elevated % of events in the $I^{++}$ quadrant of the dot plot (from 6.77% to 68.81%) and by the significant increases in total 7-AAD and annexin-V staining. Incubating cells with pooled NLA aptamers protected them from CDC and decreased total cell death (68.81% to 59.04%), elevated the % of cells with low 7-AAD staining (26.79% to 40.0%) and decreased total annexin-V staining from an MFI=63.61 to MFI=45.63. The DNA library was not associated with any significant changes. Therefore NLA aptamers, selected against CD20+HEK, protect CCL-86 cells from CDC.

CDC induction results in dramatic alterations in cellular viability, refer to the first two columns of Figure 5.6; compare the 7-AAD and annexin-V measurements between the CCL-86 cells incubated with anti-CD20 antibody and viable HS (CDC positive control) and CCL-86 cells incubated with anti-CD20 antibody and the HiHS (CDC negative control). CDC induces morphological changes in cellular distribution, it dramatically and significantly increases the percentage of cells in the $I^{++}$ quadrant from 6.77% to 68.81%, and it is associated with significant increases in the MFI for both 7-AAD and annexin-V. Note that in the CDC positive control there are two population for 7-AAD, indicated as K and L. By gating each peak one can individually analyze their characteristics. Population K has an MFI of 5, which is only slightly higher than the measures of the viable control samples depicted in Figure 5.5. Population L however is distinctly associated with CDC induction, its MFI of 82 (and roughly 65% of all gated cells) depicts the total amount of dead cells.

CDC also resulted in substantially increased annexin-V staining from an MFI of 2.40 in the CDC negative control to MFI signal of 63.61 with the CDC positive control. This increase is significantly higher than that observed with the serum deprived controls of Figure 5.5 (maximum of 6.78). Note that only staining with 7-AAD, and not annexin-V, can resolve the cell into two discrete populations. This shows that even technically viable cells, exhibiting low 7-AAD fluorescence, are nonetheless committed to apoptosis. Therefore in this assay, the induction of CDC results in significant increases in cell death, up to 70% of total population, and in the elevation of pro-apoptosis markers 7-AAD and annexin-V.

#### *5.3.2.3 NLA aptamers protect CCL-86 cells from CDC*

To evaluate the effect of CD20+HEK aptamers on CDC we incubated CCL-86 cells with 2μM of either DNA library or the pooled NLA aptamers for one hour, and then initiated CDC using viable human serum and anti-CD20 antibodies. Representative flow diagrams are depicted in the last two columns of Figure 5.6, with the relevant tabulated MFIs of triplicate data in Figure 5.7. We found that incubating CCL-86 cells with the NLA aptamers, and not the DNA library, resulted in greater cellular viability. In the CDC positive control the $I^{++}$ population dead cell population is maximal at 68.81%. In CCL-86 cells pre-incubated with NLA aptamers this value is 59.04%, a reduction of nearly 10%. The protective effect of the aptamers is also reflected in the lower MFI reading for both 7-AAD and annexin-V. There are still two peaks in the NLA treated 7-AAD histogram but the peak associated with a lower MFI is markedly greater. Population M contains 40.80% of all events, this is contrasted to the low 7-AAD population of the CDC control which contains 26.79%, and the DNA library treated sample with 27.71%. These results are also shown in Figure 5.7. NLA incubated CCL-86 cells also exhibited lower annexin-V staining. The aptamer pre-incubated sample has a slightly bimodal distribution whose MFI of 45.63 is notably lower than the MFI for annexin-V from either the CDC control (MFI=63.61) or the DNA library treated sample (MFI=59.22).

Figure 5.7 is the tabulated MFI results from triplicate data. Cumulatively, it shows that CDC induced CCL-86 cells or CCL-86 cells incubated with DNA library resulted in similar effects, the amounts of total cell death was 71-76% of all cells, the percentage of cells with low 7-AAD staining is 20-25%, and level of annexin-V staining is MFI=60-67. The NLA aptamers treated cells differ; they exhibit a lower total percentages of dead cells with 61%, leaving the percentage of cells with low 7-AAD markedly higher at 38%,

and with significantly reduced annexin-V staining down to an MFI of 48. The NLA treated cells exhibited lower 7-AAD and extracellular PS staining, characteristics which are consistent with greater viability. Therefore NLA aptamers, and not the DNA library, appear to protect CCL-86 cells from the cytotoxic effects of anti-CD20 induced CDC.

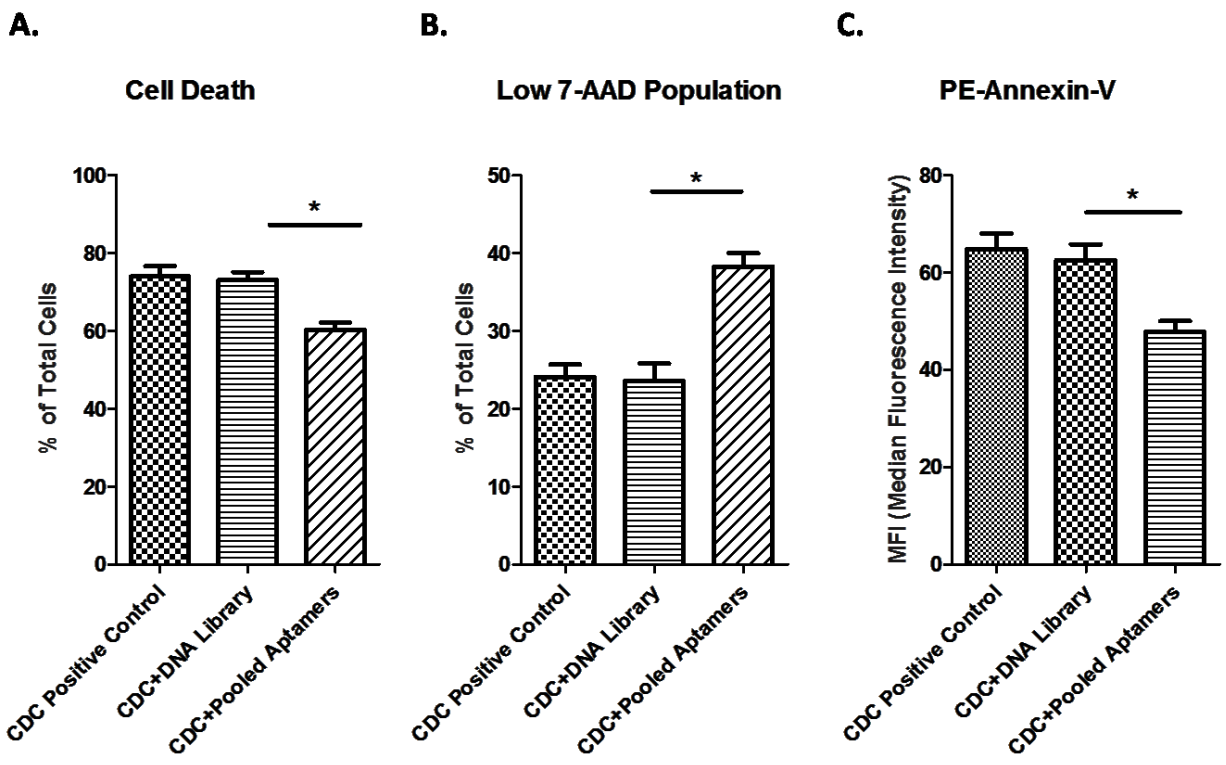


**Figure 5.7. NLA protected CCL-86 cells exhibit greater viability and have decreased staining of the pro-apoptotic marker annexin-V.** CDC was induced in CCL-86 cells using 10ng/µl of anti-CD20 antibody and viable human serum. To evaluate the effect of aptamers, CCL-86 cells were incubated with 2µM of either the DNA library or the pooled NLA aptamers before the induction of CDC. After 4 hours the cell death markers 7-AAD and annexin-V were measured. All samples were performed in triplicate. The DNA-library incubated cells exhibited comparable cytotoxicity levels as the CDC positive control with equitable values for total cell death, the % of cells with low 7-AAD staining, and MFIs for annexin-V labelling. Therefore the DNA library exerts no effect against CDC. However, CCL-86 cells incubated with the NLA aptamers exhibited decreased total cell death, with proportional increases in number of cells with low-7-AAD staining, and also significantly decreased the staining of annexin-V, *$p<0.05$. Therefore incubating CCL-86 cells with aptamers derived from CD20+HEK selection protects and limits the extent of cellular damage induced by CDC.

The results from the biological analysis validate that NLA aptamers, selected to CD20 on transfected HEK cells, exhibit both specific binding and a biologically protective effect against anti-CD20 antibody induced CDC. NLA aptamers significantly decreased the total number of dead cells by almost 10%, and lowered the MFI values of the apoptotic markers 7-AAD and annexin-V. Importantly, this effect was restricted to the usage of the NLA aptamers. The unselected DNA library, which did not exhibit specific binding with CCL-86 cells, provided no protective effects and led to 7-AAD and annexin-V levels consistent with the CDC positive control.

## 5.4 Discussion

Transfection permits the expression of a target gene in a cell line that would ordinarily lack it. Expression does not necessarily guarantee, however, that the gene or its protein product will function in a manner consistent with its original state. Protein function depends on a series factors, whose interactions can be obscure and complex, and which transfection alone may not satisfy.

CD20+HEK cells failed to undergo CDC. This is in spite of the fact that CDC is a well-established anti-CD20 mediated mechanism. Their resistance to CDC is shown in Figure 5.3. It is possible that CD20 expression on HEK293 cells was not at the threshold levels required to appreciably induce CDC. Some papers have shown that low expression levels of CD20 abrogates the action of anti-CD20 antibodies, while increases in total expression can reverse this (161). In a clinical setting, susceptibility to anti-CD20 therapy closely mirrors its expression level. For example rituximab is a much more potent CDC inducer in follicular lymphoma cells which are high CD20 expressing, than small lymphocytic lymphoma which express low levels of CD20 (162). In one study, 29%

of patients with diffuse large B cell lymphoma relapsed due to a CD20-negative transformation (163). As our data from Chapter 2 transfection shows (pg=44), CD20+HEK cells do possess a significantly weaker anti-CD20 MFI signal when compared to CCL-86 cells. The low expression level of CD20 in the transfected cells represent one plausible explanation for the failure of CDC.

We cannot eliminate the possibility that the inherent cellular composition of HEK293 cells may have had some influence. The expression of complement resistant factors like CD55 and CD59 will inhibit CDC (156). It stands to reason that molecules likes these, or others yet undiscovered, may also have had some role in inhibiting CDC induction in the CD20+HEK cells. Unfortunately, the expression of complement resistant factors CD55 and CD59 were not assessed with HEK293 cells nor was any relevant information found in published literature.

Another important consideration comes from papers that have evaluated biological actions of CD20 transfected cells. In these papers positive effector actions were noted only when the transfected cell line was of immune origin. For example, Teeling et al (55) transfected CD20 into both HEK 293T and CEM cells (a T-cell line) to elucidate epitope specificity. While binding assays were performed on the CD20 transfected HEK293 cells, the biological analysis—including CDC— was only positively evaluated with the CEM T-cells. No data concerning CDC in the CD20 transfected HEK cells was available. Similar results were uncovered by Introna et al (164) where CD20 was successfully transfected and CDC positively induced in human derived and blood borne T cells. The work of Griffioen et al (165) suggests that the transfection of CD20 into T-cells could be an important regulatory element for adoptive T cell therapy.

CD20 is a receptor whose natural distribution among cells is remarkably narrow; naturally its expression is restricted to B-cells. The work of Teeling, Introna and Griffioen—all of whom transfected CD20 into T-cells— strongly suggest that the cellular constitution of T-cells, which share a common hematopoietic origin with B-cells, may possess a uniquely primed microenvironment for the expression and elicitation of CDC. Perhaps in ways that the composition of HEK293 cells, which originate from a different precursor entirely, fail to reproduce.

CD20+HEK invulnerability to CDC abrogated their use in the biological analysis and so we focused on CCL-86, which are naturally CD20 expressing. In Figure 5.4, we show that when pooled NLA aptamer possess significantly greater binding affinity with CCL-86 cells than the unselected library. TIB-152 cells, which are CD20 negative, fail to as officiously labelled with either the DNA library or the NLA aptamers. This demonstrates that the NLA aptamers, selected against CD20+HEK, appear to be target specific to the CD20 molecule.

It is worth mentioning that this binding is noticeably lower than what was observed initially with pool 10 (pg=48). Indeed binding with the NLA aptamers required significantly greater amounts until appreciable detection, after washing, became obvious. Aptamer pool 10 positively labelled CCL-86 cells at a 200nM concentration; nearly 10 times that amount was necessary to see binding with the clones. Whether this is as a result of the inherent selection strategy or the NGS selection is not known. It is possible that refining the NLA aptamers structure and shape, as well as a more thorough evaluation of its binding dynamics could help to improve its binding characteristics.

We were curious to evaluate the impact that CD20 specific aptamers had on antibody mediated CDC in CCL-86 cells. CDC requires both anti-CD20 antibody and viable human serum. In our assay, CDC was associated with increases in total cell death, evidenced by greater 7-AAD staining but also significantly elevated levels of annexin-V, a well-established pro-apoptosis marker. Incubating CCL-86 cells with the aptamers, and not the DNA library, was able to protect the cells from the total extent of CDC, reducing the total burden of cell death by nearly 10% and lowering both 7-AAD and annexin-V staining. Importantly, since this was not observed when cells were incubated with the unselected DNA library, it shows that these effects are inherent to the NLA aptamers themselves and are not the by-product of the DNA itself. Cumulatively, this data shows that aptamers selected to CD20+HEK cells appear to be specific to the CD20 molecule, even when expressed on CCL-86 cells, and can modestly limit the total extent of anti-CD20 antibody induced CDC.

# 5. CONCLUSION

Aptamers are important tools to elucidate, probe and evaluate complex chemical and biological interactions. Here NLA aptamers, produced using transfected CD20+HEK cells, showed appreciable and specific binding with the CD20 expressing cells CCL-86, and not the CD20 negative TIB-152. Incubating CCL-86 cells with the NLA aptamers also protected them from the total extent of CDC induced cell death, increasing total cell viability and lowering the amount of death cell markers 7-AAD and annexin-V. Cumulatively, this demonstrates the validity of using target positive cell-SELEX to generate aptamers with both specific binding affinity and biological efficacy.

# 6 GENERAL CONCLUSION

Conventional selection strategies are intrinsically imperfect. Solid state SELEX is ideal for the direct selection of ligands to known targets. However, it fails to adequately appreciate how these targets may be expressed in live cellular systems. Cell-SELEX can isolate for aptamers in their functionally active state but the identification of the intended target remains a complex and exhaustive task.

Viral transfection incorporates the best attributes of both methods. By transfecting a gene and establishing target positive and target negative cell lines we were able to select aptamers in a target specific and a biologically conscious context. We transfected CD20 cDNA into HEK293 cells and successfully evolved CD20+HEK cells. We used CD20+HEK and their untransfected HEK counterparts in a novel SELEX method and generated pools of aptamers with increased affinity to the CD20+HEK. Pool 10 was the greatest binder of CD20+HEK and proved capable of validated CD20 expression in 2 different cell lines. Pool 10 positively associated with the CD20 expressing CCL-86 cells and not the CD20-negative TIB-152. Pool 10 was a discriminative pool and contained aptamers specific to the CD20 molecule.

We employed NGS analyses to analyze the sequences in pool 10 with a greater depth and sensitivity than what would be afforded with general bacterial cloning and Sanger sequencing. We showed that pool 10 exhibited dramatic sequence consolidation, as evidenced by the phylogenetic assessment, HCN sequences and the MEME motifs. The most abundantly expressed sequences, the HCNs, possessed a copy number bias even

when compared to highly similar aptamers. This demonstrates that the evolution of sequences was target directed and not random.

The top HCNs, the NLA aptamers, exhibited potent and specific binding to the CD20+HEK cells, with $K_d$s less than 100nM. In co-staining experiments incubating CD20+HEK cells with NLA aptamers decreased the binding of the anti-CD20 antibody by more than half. The unselected DNA library had no effect. This suggests that NLA aptamers may bind mutually recognizable sites on the CD20 molecule as the anti-CD20 antibody itself.

Anti-CD20 antibodies are clinically established immunotherapeutics, capable of eliciting rapid cell death. One method by which they do this is through complement dependent cytotoxicity, a process that is initiated by a proteolytic cascade of serum complement factors, and which results in the formation of a cytolytic, pore forming, membrane attack complex. We showed that CD20+HEK cells, though positive for CD20 expression, were refractive to CDC induction. However, NLA aptamers not only positively and specifically recognized CCL-86 cells, but in the CDC assay they exerted a protective effect decreasing total cell death by 10% and also significantly reducing the cell death markers 7-AAD and annexin-V. This shows that aptamers selected using target positive SELEX possess not only physical and specific binding capacities but, due to the biologically conscious selection strategy, also have in-vitro applicability.

In summary, the selection of aptamers using a lentiviral mediated cell-SELEX method was successful in evolving sequences that are both strong and specific binders for the target CD20 molecule, as expressed in both transfected CD20+HEK and on native cells like CCL-86. NLA aptamers were also biologically effective limiting the

cytotoxic effects of anti-CD20 antibody induced CDC. This demonstrates the utilitarian value of lentiviral specific cell-SELEX; a strategy that is simultaneously specific and universal with the capacity to generate targeted aptamers that physically associate and actively augment the biological mechanism of their intended molecule.

# 7 REFERENCES


1. Dominy BN. Molecular recognition and binding free energy calculations in drug development. Curr Pharm Biotechnol. 2008 Apr;9(2):87-95.

2. Vanneman M, Dranoff G. Combining immunotherapy and targeted therapies in cancer treatment. Nat Rev Cancer. 2012 Mar 22;12(4):237-51.

3. Allen TM. Ligand-targeted therapeutics in anticancer therapy. Nat Rev Cancer. 2002 Oct;2(10):750-63.

4. Srinivasarao M, Galliford CV, Low PS. Principles in the design of ligand-targeted cancer therapeutics and imaging agents. Nat Rev Drug Discov. 2015 Mar;14(3):203-19.

5. Lequin RM. Enzyme immunoassay (EIA)/enzyme-linked immunosorbent assay (ELISA). Clin Chem. 2005 Dec;51(12):2415-8.

6. Green MR. Targeting targeted therapy. N Engl J Med. 2004 May 20;350(21):2191-3.

7. Ross JS, Schenkein DP, Pietrusko R, Rolfe M, Linette GP, Stec J, et al. Targeted therapies for cancer 2004. Am J Clin Pathol. 2004 Oct;122(4):598-609.

8. Morse DL, Gillies RJ. Molecular Imaging and Targeted Therapies. Biochem Pharmacol. 2010 Sep 1;80(5):731-8.

9. Haber DA, Gray NS, Baselga J. The evolving war on cancer. Cell. 2011 Apr 1;145(1):19-24.

10. Voller A, Bidwell DE, Bartlett A. Enzyme immunoassays in diagnostic medicine: Theory and practice. Bull World Health Organ. 1976;53(1):55-65.

11. van Weemen BK. The rise of EIA/ELISA. Clin Chem. 2005 Dec;51(12):2226.

12. Dotan E, Aggarwal C, Smith MR. Impact of Rituximab (Rituxan) on the Treatment of B-Cell Non-Hodgkin's Lymphoma. P T. 2010 Mar;35(3):148-57.

13. Scott AM, Wolchok JD, Old LJ. Antibody therapy of cancer. Nat Rev Cancer. 2012 Mar 22;12(4):278-87.

14. Svobodova M, Bunka DH, Nadal P, Stockley PG, O'Sullivan CK. Selection of 2'F-modified RNA aptamers against prostate-specific antigen and their evaluation for diagnostic and therapeutic applications. Anal Bioanal Chem. 2013 Nov;405(28):9149-57.

15. Hicke BJ, Marion C, Chang YF, Gould T, Lynott CK, Parma D, et al. Tenascin-C aptamers are generated using tumor cells and purified protein. J Biol Chem. 2001 Dec 28;276(52):48644-54.

16. Jimenez E, Sefah K, Lopez-Colon D, Van Simaeys D, Chen HW, Tockman MS, et al. Generation of lung adenocarcinoma DNA aptamers for cancer studies. PLoS One. 2012;7(10):e46222.

17. Stoltenburg R, Reinemann C, Strehlitz B. SELEX--a (r)evolutionary method to generate high-affinity nucleic acid ligands. Biomol Eng. 2007 Oct;24(4):381-403.

18. Ellington AD, Szostak JW. In vitro selection of RNA molecules that bind specific ligands. Nature. 1990 Aug 30;346(6287):818-22.

19. Sefah K, Shangguan D, Xiong X, O'Donoghue MB, Tan W. Development of DNA aptamers using Cell-SELEX. Nat Protoc. 2010 Jun;5(6):1169-85.

20. Famulok M, Hartig JS, Mayer G. Functional aptamers and aptazymes in biotechnology, diagnostics, and therapy. Chem Rev. 2007 Sep;107(9):3715-43.

21. Rajendran M, Ellington AD. Selection of fluorescent aptamer beacons that light up in the presence of zinc. Anal Bioanal Chem. 2008 Feb;390(4):1067-75.

22. Ashrafuzzaman M, Tseng CY, Kapty J, Mercer JR, Tuszynski JA. A computationally designed DNA aptamer template with specific binding to phosphatidylserine. Nucleic Acid Ther. 2013 Dec;23(6):418-26.

23. Kupakuwana GV, Crill JE,2nd, McPike MP, Borer PN. Acyclic identification of aptamers for human alpha-thrombin using over-represented libraries and deep sequencing. PLoS One. 2011;6(5):e19395.

24. Karapetis CS, Khambata-Ford S, Jonker DJ, O'Callaghan CJ, Tu D, Tebbutt NC, et al. K-ras mutations and benefit from cetuximab in advanced colorectal cancer. N Engl J Med. 2008 Oct 23;359(17):1757-65.

25. Friedman HS, Prados MD, Wen PY, Mikkelsen T, Schiff D, Abrey LE, et al. Bevacizumab alone and in combination with irinotecan in recurrent glioblastoma. J Clin Oncol. 2009 Oct 1;27(28):4733-40.

26. Van Cutsem E, Kohne CH, Hitre E, Zaluski J, Chang Chien CR, Makhson A, et al. Cetuximab and chemotherapy as initial treatment for metastatic colorectal cancer. N Engl J Med. 2009 Apr 2;360(14):1408-17.

27. Shan D, Ledbetter JA, Press OW. Apoptosis of malignant human B cells by ligation of CD20 with monoclonal antibodies. Blood. 1998 Mar 1;91(5):1644-52.

28. Smith MR. Rituximab (monoclonal anti-CD20 antibody): mechanisms of action and resistance. Oncogene. 2003 Oct 20;22(47):7359-68.

29. Teeling JL, French RR, Cragg MS, van den Brakel J, Pluyter M, Huang H, et al. Characterization of new human CD20 monoclonal antibodies with potent cytolytic activity against non-Hodgkin lymphomas. Blood. 2004 Sep 15;104(6):1793-800.

30. Aggarwal S. Targeted cancer therapies. Nat Rev Drug Discov. 2010 Jun;9(6):427-8.

31. IMS Health Study: Cancer Drug Innovation Surges As Cost Growth Moderates [Internet].; 2015 []. Available from: http://www.imshealth.com/portal/site/imshealth/menuitem.

32. Strome SE, Sausville EA, Mann D. A mechanistic perspective of monoclonal antibodies in cancer therapy beyond target-related effects. Oncologist. 2007 Sep;12(9):1084-95.

33. Zhang C. Hybridoma technology for the generation of monoclonal antibodies. Methods Mol Biol. 2012;901:117-35.

34. Liu JK. The history of monoclonal antibody development - Progress, remaining challenges and future innovations. Ann Med Surg (Lond). 2014 Sep 11;3(4):113-6.

35. Kelley B. Industrialization of mAb production technology: the bioprocessing industry at a crossroads. MAbs. 2009 Sep-Oct;1(5):443-52.

36. Shaughnessy AF. Monoclonal antibodies: magic bullets with a hefty price tag. BMJ. 2012 Dec 12;345:e8346.

37. Coyle D, Cheung MC, Evans GA. Opportunity cost of funding drugs for rare diseases: the cost-effectiveness of eculizumab in paroxysmal nocturnal hemoglobinuria. Med Decis Making. 2014 Nov;34(8):1016-29.

38. Klijn JG, Berns PM, Schmitz PI, Foekens JA. The clinical significance of epidermal growth factor receptor (EGF-R) in human breast cancer: a review on 5232 patients. Endocr Rev. 1992 Feb;13(1):3-17.

39. Martinelli E, De Palma R, Orditura M, De Vita F, Ciardiello F. Anti-epidermal growth factor receptor monoclonal antibodies in cancer therapy. Clin Exp Immunol. 2009 Oct;158(1):1-9.

40. Wolchok JD, Saenger Y. The mechanism of anti-CTLA-4 activity and the negative regulation of T-cell activation. Oncologist. 2008;13 Suppl 4:2-9.

41. Philips GK, Atkins M. Therapeutic uses of anti-PD-1 and anti-PD-L1 antibodies. Int Immunol. 2015 Jan;27(1):39-46.

42. Oflazoglu E, Audoly LP. Evolution of anti-CD20 monoclonal antibody therapeutics in oncology. MAbs. 2010 Jan-Feb;2(1):14-9.

43. Kuijpers TW, Bende RJ, Baars PA, Grummels A, Derks IA, Dolman KM, et al. CD20 deficiency in humans results in impaired T cell-independent antibody responses. J Clin Invest. 2010 Jan;120(1):214-22.

44. Dalakas MC. B cells as therapeutic targets in autoimmune neurological disorders. Nat Clin Pract Neurol. 2008 Oct;4(10):557-67.

45. Einfeld DA, Brown JP, Valentine MA, Clark EA, Ledbetter JA. Molecular cloning of the human B cell CD20 receptor predicts a hydrophobic protein with multiple transmembrane domains. EMBO J. 1988 Mar;7(3):711-7.

46. Ruuls SR, van Bueren JJL, van de Winkel JGJ, Parren PWHI. Novel human antibody therapeutics: The age of the Umabs. Biotechnol J. 2008 Oct;3(9-10):1157-71.

47. Bubien JK, Zhou LJ, Bell PD, Frizzell RA, Tedder TF. Transfection of the CD20 cell surface molecule into ectopic cell types generates a Ca2+ conductance found constitutively in B lymphocytes. J Cell Biol. 1993 Jun;121(5):1121-32.

48. Golay J, Cusmano G, Introna M. Independent regulation of c-myc, B-myb, and c-myb gene expression by inducers and inhibitors of proliferation in human B lymphocytes. J Immunol. 1992 Jul 1;149(1):300-8.

49. Uchida J, Lee Y, Hasegawa M, Liang Y, Bradney A, Oliver JA, et al. Mouse CD20 expression and function. Int Immunol. 2004 Jan;16(1):119-29.

50. McLaughlin P, Grillo-Lopez AJ, Link BK, Levy R, Czuczman MS, Williams ME, et al. Rituximab chimeric anti-CD20 monoclonal antibody therapy for relapsed indolent lymphoma: half of patients respond to a four-dose treatment program. J Clin Oncol. 1998 Aug;16(8):2825-33.

51. Cheung MC, Haynes AE, Meyer RM, Stevens A, Imrie KR, Members of the Hematology, Disease Site Group of the Cancer Care Ontario Program in Evidence-Based Care. Rituximab in lymphoma: a systematic review and consensus practice guideline from Cancer Care Ontario. Cancer Treat Rev. 2007 Apr;33(2):161-76.

52. Summers KM, Kockler DR. Rituximab treatment of refractory rheumatoid arthritis. Ann Pharmacother. 2005 Dec;39(12):2091-5.

53. Forstpointner R, Unterhalt M, Dreyling M, Bock HP, Repp R, Wandt H, et al. Maintenance therapy with rituximab leads to a significant prolongation of response duration after salvage therapy with a combination of rituximab, fludarabine, cyclophosphamide, and mitoxantrone (R-FCM) in patients with recurring and refractory follicular and mantle cell lymphomas: Results of a prospective randomized study of the German Low Grade Lymphoma Study Group (GLSG). Blood. 2006 Dec 15;108(13):4003-8.

54. Wierda WG, Kipps TJ, Mayer J, Stilgenbauer S, Williams CD, Hellmann A, et al. Ofatumumab as single-agent CD20 immunotherapy in fludarabine-refractory chronic lymphocytic leukemia. J Clin Oncol. 2010 Apr 1;28(10):1749-55.

55. Teeling JL, Mackus WJ, Wiegman LJ, van den Brakel JH, Beers SA, French RR, et al. The biological activity of human CD20 monoclonal antibodies is linked to unique epitopes on CD20. J Immunol. 2006 Jul 1;177(1):362-71.

56. Pawluczkowycz AW, Beurskens FJ, Beum PV, Lindorfer MA, van de Winkel JG, Parren PW, et al. Binding of submaximal C1q promotes complement-dependent cytotoxicity (CDC) of B cells opsonized with anti-CD20 mAbs ofatumumab (OFA) or rituximab (RTX): considerably higher levels of CDC are induced by OFA than by RTX. J Immunol. 2009 Jul 1;183(1):749-58.

57. Tuerk C, Gold L. Systematic evolution of ligands by exponential enrichment: RNA ligands to bacteriophage T4 DNA polymerase. Science. 1990 Aug 3;249(4968):505-10.

58. Mahlknecht G, Maron R, Mancini M, Schechter B, Sela M, Yarden Y. Aptamer to ErbB-2/HER2 enhances degradation of the target and inhibits tumorigenic growth. Proc Natl Acad Sci U S A. 2013 May 14;110(20):8170-5.

59. Kubik MF, Stephens AW, Schneider D, Marlar RA, Tasset D. High-affinity RNA ligands to human alpha-thrombin. Nucleic Acids Res. 1994 Jul 11;22(13):2619-26.

60. Tang Z, Shangguan D, Wang K, Shi H, Sefah K, Mallikratchy P, et al. Selection of aptamers for molecular recognition and characterization of cancer cells. Anal Chem. 2007 Jul 1;79(13):4900-7.

61. Jayasena SD. Aptamers: an emerging class of molecules that rival antibodies in diagnostics. Clin Chem. 1999 Sep;45(9):1628-50.

62. Song KM, Lee S, Ban C. Aptamers and their biological applications. Sensors (Basel). 2012;12(1):612-31.

63. Liu J, You M, Pu Y, Liu H, Ye M, Tan W. Recent developments in protein and cell-targeted aptamer selection and applications. Curr Med Chem. 2011;18(27):4117-25.

64. Wang RE, Wu H, Niu Y, Cai J. Improving the stability of aptamers by chemical modification. Curr Med Chem. 2011;18(27):4126-38.

65. Hanly WC, Artwohl JE, Bennett BT. Review of Polyclonal Antibody Production Procedures in Mammals and Poultry. ILAR J. 1995;37(3):93-118.

66. Leenaars M, Hendriksen CF. Critical steps in the production of polyclonal and monoclonal antibodies: evaluation and recommendations. ILAR J. 2005;46(3):269-79.

67. Bruno JG, Kiel JL. In vitro selection of DNA aptamers to anthrax spores with electrochemiluminescence detection. Biosens Bioelectron. 1999 May 31;14(5):457-64.

68. Gopinath SC, Misono TS, Kawasaki K, Mizuno T, Imai M, Odagiri T, et al. An RNA aptamer that distinguishes between closely related human influenza viruses and inhibits haemagglutinin-mediated membrane fusion. J Gen Virol. 2006 Mar;87(Pt 3):479-87.

69. Sefah K, Tang ZW, Shangguan DH, Chen H, Lopez-Colon D, Li Y, et al. Molecular recognition of acute myeloid leukemia using aptamers. Leukemia. 2009 Feb;23(2):235-44.

70. Shangguan D, Meng L, Cao ZC, Xiao Z, Fang X, Li Y, et al. Identification of liver cancer-specific aptamers using whole live cells. Anal Chem. 2008 Feb 1;80(3):721-8.

71. Wang C, Zhang M, Yang G, Zhang D, Ding H, Wang H, et al. Single-stranded DNA aptamers that bind differentiated but not parental cells: subtractive systematic evolution of ligands by exponential enrichment. J Biotechnol. 2003 Apr 10;102(1):15-22.

72. Ng EW, Shima DT, Calias P, Cunningham ET,Jr, Guyer DR, Adamis AP. Pegaptanib, a targeted anti-VEGF aptamer for ocular vascular disease. Nat Rev Drug Discov. 2006 Feb;5(2):123-32.

73. Sundaram P, Kurniawan H, Byrne ME, Wower J. Therapeutic RNA aptamers in clinical trials. Eur J Pharm Sci. 2013 Jan 23;48(1-2):259-71.

74. Bruno JG, Kiel JL. Use of magnetic beads in selection and detection of biotoxin aptamers by electrochemiluminescence and enzymatic methods. BioTechniques. 2002 Jan;32(1):178,80, 182-3.

75. Stoltenburg R, Reinemann C, Strehlitz B. FluMag-SELEX as an advantageous method for DNA aptamer selection. Anal Bioanal Chem. 2005 Sep;383(1):83-91.

76. Challa S, Tzipori S, Sheoran A. Selective Evolution of Ligands by Exponential Enrichment to Identify RNA Aptamers against Shiga Toxins. J Nucleic Acids. 2014;2014:10.1155/2014/214929.

77. Rotherham LS, Maserumule C, Dheda K, Theron J, Khati M. Selection and Application of ssDNA Aptamers to Detect Active TB from Sputum Samples. PLoS One. 2012;7(10):e46862. doi:10.1371/journal.pone.0046862.

78. Mosing RK, Mendonsa SD, Bowser MT. Capillary electrophoresis-SELEX selection of aptamers with affinity for HIV-1 reverse transcriptase. Anal Chem. 2005 Oct 1;77(19):6107-12.

79. Cho M, Xiao Y, Nie J, Stewart R, Csordas AT, Oh SS, et al. Quantitative selection of DNA aptamers through microfluidic selection and high-throughput sequencing. Proc Natl Acad Sci U S A. 2010 Aug 31;107(35):15373-8.

80. Meyer S, Maufort JP, Nie J, Stewart R, McIntosh BE, Conti LR, et al. Development of an efficient targeted cell-SELEX procedure for DNA aptamer reagents. PLoS One. 2013 Aug 13;8(8):e71798.

81. Cheng C, Chen YH, Lennox KA, Behlke MA, Davidson BL. In vivo SELEX for Identification of Brain-penetrating Aptamers. Mol Ther Nucleic Acids. 2013 Jan 8;2:e67.

82. Ohuchi S. Cell-SELEX Technology. Biores Open Access. 2012 Dec;1(6):265-72.

83. Cao HY, Yuan AH, Shi XS, Chen W, Miao Y. Evolution of a gastric carcinoma cell-specific DNA aptamer by live cell-SELEX. Oncol Rep. 2014 Nov;32(5):2054-60.

84. Ding F, Guo S, Xie M, Luo W, Yuan C, Huang W, et al. Diagnostic applications of gastric carcinoma cell aptamers in vitro and in vivo. Talanta. 2015 Mar;134:30-6.

85. Dickinson H, Lukasser M, Mayer G, Huttenhofer A. Cell-SELEX: in vitro selection of synthetic small specific ligands. Methods Mol Biol. 2015;1296:213-24.

86. Ozer A, Pagano JM, Lis JT. New Technologies Provide Quantum Changes in the Scale, Speed, and Success of SELEX Methods and Aptamer Characterization. Mol Ther Nucleic Acids. 2014 Aug 5;3:e183.

87. Pestourie C, Cerchia L, Gombert K, Aissouni Y, Boulay J, De Franciscis V, et al. Comparison of different strategies to select aptamers against a transmembrane protein target. Oligonucleotides. 2006 Winter;16(4):323-35.

88. Boltz A, Piater B, Toleikis L, Guenther R, Kolmar H, Hock B. Bi-specific aptamers mediating tumor cell lysis. J Biol Chem. 2011 Jun 17;286(24):21896-905.

89. Kim TK, Eberwine JH. Mammalian cell transfection: the present and the future. Anal Bioanal Chem. 2010 Aug;397(8):3173-8.

90. Levine AJ. The common mechanisms of transformation by the small DNA tumor viruses: The inactivation of tumor suppressor gene products: p53. Virology. 2009 Feb 20;384(2):285-93.

91. Cockrell AS, Kafri T. Gene delivery by lentivirus vectors. Mol Biotechnol. 2007 Jul;36(3):184-204.

92. Hendrie PC, Russell DW. Gene targeting with viral vectors. Mol Ther. 2005 Jul;12(1):9-17.

93. Goecks J, Nekrutenko A, Taylor J, Galaxy Team. Galaxy: a comprehensive approach for supporting accessible, reproducible, and transparent computational research in the life sciences. Genome Biol. 2010;11(8):R86,2010-11-8-r86. Epub 2010 Aug 25.

94. Blankenberg D, Von Kuster G, Coraor N, Ananda G, Lazarus R, Mangan M, et al. Galaxy: a web-based genome analysis tool for experimentalists. Curr Protoc Mol Biol. 2010 Jan;Chapter 19:Unit 19.10.1-21.

95. Giardine B, Riemer C, Hardison RC, Burhans R, Elnitski L, Shah P, et al. Galaxy: a platform for interactive large-scale genome analysis. Genome Res. 2005 Oct;15(10):1451-5.

96. Li W, Cowley A, Uludag M, Gur T, McWilliam H, Squizzato S, et al. The EMBL-EBI bioinformatics web and programmatic tools framework. Nucleic Acids Res. 2015 Apr 6.

97. Bailey TL, Johnson J, Grant CE, Noble WS. The MEME Suite. Nucleic Acids Res. 2015 May 7.

98. Bellaousov S, Reuter JS, Seetin MG, Mathews DH. RNAstructure: Web servers for RNA secondary structure prediction and analysis. Nucleic Acids Res. 2013 Jul;41(Web Server issue):W471-4.

99. Moore MA, Hakki ZW, Gregory RL, Gfell LE, Kim-Park WK, Kowolik MJ. Influence of heat inactivation of human serum on the opsonization of Streptococcus mutans. Ann N Y Acad Sci. 1997 Dec 15;832:383-93.

100. Iida S, Misaka H, Inoue M, Shibata M, Nakano R, Yamane-Ohnuki N, et al. Nonfucosylated therapeutic IgG1 antibody can evade the inhibitory effect of serum immunoglobulin G on antibody-dependent cellular cytotoxicity through its high binding to FcgammaRIIIa. Clin Cancer Res. 2006 May 1;12(9):2879-87.

101. Tiscornia G, Singer O, Verma IM. Production and purification of lentiviral vectors. Nat Protoc. 2006;1(1):241-5.

102. Aiken C. Pseudotyping human immunodeficiency virus type 1 (HIV-1) by the glycoprotein of vesicular stomatitis virus targets HIV-1 entry to an endocytic pathway and suppresses both the requirement for Nef and the sensitivity to cyclosporin A. J Virol. 1997 Aug;71(8):5871-7.

103. Naldini L, Blomer U, Gallay P, Ory D, Mulligan R, Gage FH, et al. In vivo gene delivery and stable transduction of nondividing cells by a lentiviral vector. Science. 1996 Apr 12;272(5259):263-7.

104. Kafri T, van Praag H, Gage FH, Verma IM. Lentiviral vectors: regulated gene expression. Mol Ther. 2000 Jun;1(6):516-21.

105. Gossen M, Bujard H. Tight control of gene expression in mammalian cells by tetracycline-responsive promoters. Proc Natl Acad Sci U S A. 1992 Jun 15;89(12):5547-51.

106. Pluta K, Luce MJ, Bao L, Agha-Mohammadi S, Reiser J. Tight control of transgene expression by lentivirus vectors containing second-generation tetracycline-responsive promoters. J Gene Med. 2005 Jun;7(6):803-17.

107. Gossen M, Freundlieb S, Bender G, Muller G, Hillen W, Bujard H. Transcriptional activation by tetracyclines in mammalian cells. Science. 1995 Jun 23;268(5218):1766-9.

108. Thomas P, Smart TG. HEK293 cell line: a vehicle for the expression of recombinant proteins. J Pharmacol Toxicol Methods. 2005 May-Jun;51(3):187-200.

109. Gopinath SC. Methods developed for SELEX. Anal Bioanal Chem. 2007 Jan;387(1):171-82.

110. Schutze T, Wilhelm B, Greiner N, Braun H, Peter F, Morl M, et al. Probing the SELEX process with next-generation sequencing. PLoS One. 2011;6(12):e29604.

111. Jellinek D, Green LS, Bell C, Janjic N. Inhibition of receptor binding by high-affinity RNA ligands to vascular endothelial growth factor. Biochemistry. 1994 Aug 30;33(34):10450-6.

112. Vavalle JP, Cohen MG. The REG1 anticoagulation system: a novel actively controlled factor IX inhibitor using RNA aptamer technology for treatment of acute coronary syndrome. Future Cardiol. 2012 May;8(3):371-82.

113. Paige JS, Nguyen-Duc T, Song W, Jaffrey SR. Fluorescence imaging of cellular metabolites with RNA. Science. 2012 Mar 9;335(6073):1194.

114. Pasternak A, Hernandez FJ, Rasmussen LM, Vester B, Wengel J. Improved thrombin binding aptamer by incorporation of a single unlocked nucleic acid monomer. Nucleic Acids Res. 2011 Feb;39(3):1155-64.

115. Tatarinova O, Tsvetkov V, Basmanov D, Barinov N, Smirnov I, Timofeev E, et al. Comparison of the â€˜Chemicalâ€™ and â€˜Structuralâ€™ Approaches to the Optimization of the Thrombin-Binding Aptamer. PLoS One. 2014;9(2):e89383. doi:10.1371/journal.pone.0089383.

116. Hoon S, Zhou B, Janda KD, Brenner S, Scolnick J. Aptamer selection by high-throughput sequencing and informatic analysis. BioTechniques. 2011 Dec;51(6):413-6.

117. Metzker ML. Sequencing technologies - the next generation. Nat Rev Genet. 2010 Jan;11(1):31-46.

118. Kircher M, Kelso J. High-throughput DNA sequencing--concepts and limitations. Bioessays. 2010 Jun;32(6):524-36.

119. Grada A, Weinbrecht K. Next-generation sequencing: methodology and application. J Invest Dermatol. 2013 Aug;133(8):e11.

120. Cho M, Soo Oh S, Nie J, Stewart R, Eisenstein M, Chambers J, et al. Quantitative selection and parallel characterization of aptamers. Proc Natl Acad Sci U S A. 2013 Nov 12;110(46):18460-5.

121. Zimmermann B, Gesell T, Chen D, Lorenz C, Schroeder R. Monitoring genomic sequences during SELEX using high-throughput sequencing: neutral SELEX. PLoS One. 2010 Feb 11;5(2):e9169.

122. Wiegand TW, Williams PB, Dreskin SC, Jouvin MH, Kinet JP, Tasset D. High-affinity oligonucleotide ligands to human IgE inhibit binding to Fc epsilon receptor I. J Immunol. 1996 Jul 1;157(1):221-30.

123. Cohen SN, Chang ACY, Hsu L. Nonchromosomal Antibiotic Resistance in Bacteria: Genetic Transformation of Escherichia coli by R-Factor DNA. Proc Natl Acad Sci U S A. 1972 Aug;69(8):2110-4.

124. Yanisch-Perron C, Vieira J, Messing J. Improved M13 phage cloning vectors and host strains: nucleotide sequences of the M13mp18 and pUC19 vectors. Gene. 1985;33(1):103-19.

125. Keohavong P, Thilly WG. Fidelity of DNA polymerases in DNA amplification. Proc Natl Acad Sci U S A. 1989 Dec;86(23):9253-7.

126. Vanhercke T, Ampe C, Tirry L, Denolf P. Reducing mutational bias in random protein libraries. Anal Biochem. 2005 Apr 1;339(1):9-14.

127. Tindall KR, Kunkel TA. Fidelity of DNA synthesis by the Thermus aquaticus DNA polymerase. Biochemistry. 1988 Aug 9;27(16):6008-13.

128. Shendure J, Ji H. Next-generation DNA sequencing. Nat Biotechnol. 2008 Oct;26(10):1135-45.

129. Mardis ER. Next-generation DNA sequencing methods. Annu Rev Genomics Hum Genet. 2008;9:387-402.

130. Beck A, Wurch T, Bailly C, Corvaia N. Strategies and challenges for the next generation of therapeutic antibodies. Nat Rev Immunol. 2010 May;10(5):345-52.

131. States DJ, Gish W. Combined use of sequence similarity and codon bias for coding region identification. J Comput Biol. 1994 Spring;1(1):39-50.

132. Altschul SF, Gish W, Miller W, Myers EW, Lipman DJ. Basic local alignment search tool. J Mol Biol. 1990 Oct 5;215(3):403-10.

133. Sievers F, Wilm A, Dineen D, Gibson TJ, Karplus K, Li W, et al. Fast, scalable generation of high-quality protein multiple sequence alignments using Clustal Omega. Mol Syst Biol. 2011;7:539.

134. Thompson WA, Newberg LA, Conlan S, McCue LA, Lawrence CE. The Gibbs Centroid Sampler. Nucleic Acids Res. 2007 Jul;35(Web Server issue):W232-7.

135. Zuker M. Mfold web server for nucleic acid folding and hybridization prediction. Nucleic Acids Res. 2003 Jul 1;31(13):3406-15.

136. Henke W, Herdel K, Jung K, Schnorr D, Loening SA. Betaine improves the PCR amplification of GC-rich DNA sequences. Nucleic Acids Res. 1997 Oct 1;25(19):3957-8.

137. Dabney J, Meyer M. Length and GC-biases during sequencing library amplification: a comparison of various polymerase-buffer systems with ancient and modern DNA sequencing libraries. BioTechniques. 2012 Feb;52(2):87-94.

138. Okroj M, Osterborg A, Blom AM. Effector mechanisms of anti-CD20 monoclonal antibodies in B cell malignancies. Cancer Treat Rev. 2013 Oct;39(6):632-9.

139. Hamaguchi Y, Xiu Y, Komura K, Nimmerjahn F, Tedder TF. Antibody isotype-specific engagement of Fcgamma receptors regulates B lymphocyte depletion during CD20 immunotherapy. J Exp Med. 2006 Mar 20;203(3):743-53.

140. Minard-Colin V, Xiu Y, Poe JC, Horikawa M, Magro CM, Hamaguchi Y, et al. Lymphoma depletion during CD20 immunotherapy in mice is mediated by macrophage FcgammaRI, FcgammaRIII, and FcgammaRIV. Blood. 2008 Aug 15;112(4):1205-13.

141. Uchida J, Hamaguchi Y, Oliver JA, Ravetch JV, Poe JC, Haas KM, et al. The innate mononuclear phagocyte network depletes B lymphocytes through Fc receptor-dependent mechanisms during anti-CD20 antibody immunotherapy. J Exp Med. 2004 Jun 21;199(12):1659-69.

142. Wu J, Edberg JC, Redecha PB, Bansal V, Guyre PM, Coleman K, et al. A novel polymorphism of FcgammaRIIIa (CD16) alters receptor function and predisposes to autoimmune disease. J Clin Invest. 1997 Sep 1;100(5):1059-70.

143. Farag SS, Flinn IW, Modali R, Lehman TA, Young D, Byrd JC. Fc gamma RIIIa and Fc gamma RIIa polymorphisms do not predict response to rituximab in B-cell chronic lymphocytic leukemia. Blood. 2004 Feb 15;103(4):1472-4.

144. Robak T. GA-101, a third-generation, humanized and glyco-engineered anti-CD20 mAb for the treatment of B-cell lymphoid malignancies. Curr Opin Investig Drugs. 2009 Jun;10(6):588-96.

145. Jiang XR, Song A, Bergelson S, Arroll T, Parekh B, May K, et al. Advances in the assessment and control of the effector functions of therapeutic antibodies. Nat Rev Drug Discov. 2011 Feb;10(2):101-11.

146. Weiner LM, Surana R, Wang S. Monoclonal antibodies: versatile platforms for cancer immunotherapy. Nat Rev Immunol. 2010 May;10(5):317-27.

147. Durrant LG, Pudney VA, Spendlove I. Using monoclonal antibodies to stimulate antitumor cellular immunity. Expert Rev Vaccines. 2011 Jul;10(7):1093-106.

148. Kolev M, Le Friec G, Kemper C. Complement--tapping into new sites and effector systems. Nat Rev Immunol. 2014 Dec;14(12):811-20.

149. Kondos SC, Hatfaludi T, Voskoboinik I, Trapani JA, Law RH, Whisstock JC, et al. The structure and function of mammalian membrane-attack complex/perforin-like proteins. Tissue Antigens. 2010 Nov;76(5):341-51.

150. Di Gaetano N, Cittera E, Nota R, Vecchi A, Grieco V, Scanziani E, et al. Complement activation determines the therapeutic activity of rituximab in vivo. J Immunol. 2003 Aug 1;171(3):1581-7.

151. Golay J, Zaffaroni L, Vaccari T, Lazzari M, Borleri GM, Bernasconi S, et al. Biologic response of B lymphoma cells to anti-CD20 monoclonal antibody rituximab in vitro: CD55 and CD59 regulate complement-mediated cell lysis. Blood. 2000 Jun 15;95(12):3900-8.

152. Macor P, Tripodo C, Zorzet S, Piovan E, Bossi F, Marzari R, et al. In vivo targeting of human neutralizing antibodies against CD55 and CD59 to lymphoma cells increases the antitumor activity of rituximab. Cancer Res. 2007 Nov 1;67(21):10556-63.

153. Kennedy AD, Beum PV, Solga MD, DiLillo DJ, Lindorfer MA, Hess CE, et al. Rituximab infusion promotes rapid complement depletion and acute CD20 loss in chronic lymphocytic leukemia. J Immunol. 2004 Mar 1;172(5):3280-8.

154. Klepfish A, Rachmilewitz EA, Kotsianidis I, Patchenko P, Schattner A. Adding fresh frozen plasma to rituximab for the treatment of patients with refractory advanced CLL. QJM. 2008 Sep;101(9):737-40.

155. Klepfish A, Gilles L, Ioannis K, Rachmilewitz EA, Schattner A. Enhancing the action of rituximab in chronic lymphocytic leukemia by adding fresh frozen plasma: complement/rituximab interactions & clinical results in refractory CLL. Ann N Y Acad Sci. 2009 Sep;1173:865-73.

156. Weng WK, Levy R. Expression of complement inhibitors CD46, CD55, and CD59 on tumor cells does not predict clinical outcome after rituximab treatment in follicular non-Hodgkin lymphoma. Blood. 2001 Sep 1;98(5):1352-7.

157. Wang SY, Racila E, Taylor RP, Weiner GJ. NK-cell activation and antibody-dependent cellular cytotoxicity induced by rituximab-coated target cells is inhibited by the C3b component of complement. Blood. 2008 Feb 1;111(3):1456-63.

158. Beum PV, Kennedy AD, Williams ME, Lindorfer MA, Taylor RP. The shaving reaction: rituximab/CD20 complexes are removed from mantle cell lymphoma and chronic lymphocytic leukemia cells by THP-1 monocytes. J Immunol. 2006 Feb 15;176(4):2600-9.

159. Williams ME, Densmore JJ, Pawluczkowycz AW, Beum PV, Kennedy AD, Lindorfer MA, et al. Thrice-weekly low-dose rituximab decreases CD20 loss via shaving and promotes enhanced targeting in chronic lymphocytic leukemia. J Immunol. 2006 Nov 15;177(10):7435-43.

160. Hwang B, Lee SW. Improvement of RNA aptamer activity against myasthenic autoantibodies by extended sequence selection. Biochem Biophys Res Commun. 2002 Jan 18;290(2):656-62.

161. van Meerten T, van Rijn RS, Hol S, Hagenbeek A, Ebeling SB. Complement-induced cell death by rituximab depends on CD20 expression level and acts complementary to antibody-dependent cellular cytotoxicity. Clin Cancer Res. 2006 Jul 1;12(13):4027-35.

162. Manches O, Lui G, Chaperot L, Gressin R, Molens JP, Jacob MC, et al. In vitro mechanisms of action of rituximab on primary non-Hodgkin lymphomas. Blood. 2003 Feb 1;101(3):949-54.

163. Hiraga J, Tomita A, Sugimoto T, Shimada K, Ito M, Nakamura S, et al. Down-regulation of CD20 expression in B-cell lymphoma cells after treatment with rituximab-containing combination chemotherapies: its prevalence and clinical significance. Blood. 2009 May 14;113(20):4885-93.

164. Introna M, Barbui AM, Bambacioni F, Casati C, Gaipa G, Borleri G, et al. Genetic modification of human T cells with CD20: a strategy to purify and lyse transduced cells with anti-CD20 antibodies. Hum Gene Ther. 2000 Mar 1;11(4):611-20.

165. Griffioen M, van Egmond EHM, Kester MGD, Willemze R, Falkenburg JHF, Heemskerk MHM. Retroviral transfer of human CD20 as a suicide gene for adoptive T-cell therapy. Haematologica. 2009 Sep;94(9):1316-20.

# 8 APPENDIX

The author wishes to credit the following for the permission to reproduce copyrighted material.

For the permission to reproduce Figure 1.2:

NATURE PUBLISHING GROUP LICENSE
TERMS AND CONDITIONS

May 28, 2015

This is a License Agreement between Nadia Al youssef ("You") and Nature Publishing Group ("Nature Publishing Group") provided by Copyright Clearance Center ("CCC"). The license consists of your order details, the terms and conditions provided by Nature Publishing Group, and the payment terms and conditions.

| | |
|---|---|
| License Number | 3636051089075 |
| License date | May 25, 2015 |
| Licensed content publisher | Nature Publishing Group |
| Licensed content publication | Nature Reviews Cancer |
| Licensed content title | Antibody therapy of cancer |
| Licensed content author | Andrew M. Scott, Jedd D. Wolchok and Lloyd J. Old |
| Licensed content date | Apr 1, 2012 |
| Volume number | 12 |
| Issue number | 4 |
| Type of Use | reuse in a dissertation / thesis |
| Requestor type | academic/educational |
| Format | electronic |
| Portion | figures/tables/illustrations |
| Number of figures/tables/illustrations | 1 |
| High-res required | no |
| Figures | Figure 1 |
| Author of this NPG article | no |
| Your reference number | None |
| Title of your thesis / dissertation | The selection of aptamers to CD20 and their application as inhibitors of complement dependent cytotoxicity |
| Expected completion date | Jun 2015 |

Permissions to reproduce Figures 1.3 and 1.4:

JOHN WILEY AND SONS LICENSE
TERMS AND CONDITIONS

May 28, 2015

---

---

This Agreement between Nadia Al youssef ("You") and John Wiley and Sons ("John Wiley and Sons") consists of your li
and the terms and conditions provided by John Wiley and Sons and Copyright Clearance Center.

| | |
|---|---|
| License Number | 3636041308077 |
| License date | May 25, 2015 |
| Licensed Content Publisher | John Wiley and Sons |
| Licensed Content Publication | Biotechnology Journal |
| Licensed Content Title | Novel human antibody therapeutics: The age of the Umabs |
| Licensed Content Author | Sigrid R. Ruuls,Jeroen J. Lammerts van Bueren,Jan G. J. van de Winkel,Paul W. H. I. Parren |
| Licensed Content Date | Aug 13, 2008 |
| Pages | 15 |
| Type of use | Dissertation/Thesis |
| Requestor type | University/Academic |
| Format | Electronic |
| Portion | Figure/table |
| Number of figures/tables | 2 |
| Original Wiley figure/table number(s) | Figure 4 Figure 5 |
| Will you be translating? | No |
| Title of your thesis / dissertation | The selection of aptamers to CD20 and their application as inhibitors of complement dependent cytotoxicity |
| Expected completion date | Jun 2015 |

Permission to reproduce Figure 1.5:

NATURE PUBLISHING GROUP LICENSE
TERMS AND CONDITIONS
May 28, 2015

This is a License Agreement between Nadia Al youssef ("You") and Nature Publishing Group ("Nature Publishing Group") provided by Copyright Clearance Center ("CCC"). The license consists of your order details, the terms and conditions provided by Nature Publishing Group, and the payment terms and conditions.

| | |
|---|---|
| License Number | 3636050964526 |
| License date | May 25, 2015 |
| Licensed content publisher | Nature Publishing Group |
| Licensed content publication | Nature Protocols |
| Licensed content title | Development of DNA aptamers using Cell-SELEX |
| Licensed content author | Kwame Sefah, Dihua Shangguan, Xiangling Xiong, Meghan B O'Donoghue and Weihong Tan |
| Licensed content date | Jun 3, 2010 |
| Volume number | 5 |
| Issue number | 6 |
| Type of Use | reuse in a dissertation / thesis |
| Requestor type | academic/educational |
| Format | print and electronic |
| Portion | figures/tables/illustrations |
| Number of figures/tables/illustrations | 1 |
| High-res required | no |
| Figures | Figure 1 |
| Author of this NPG article | no |
| Your reference number | None |
| Title of your thesis / dissertation | The selection of aptamers to CD20 and their application as inhibitors of complement dependent cytotoxicity |
| Expected completion date | Jun 2015 |

Permission to reproduce Figure 3.1:

SPRINGER LICENSE
TERMS AND CONDITIONS
May 28, 2015

This is a License Agreement between Nadia Al youssef ("You") and Springer ("Springer") provided by Copyright Clearance Center ("CCC"). The license consists of your order details, the terms and conditions provided by Springer, and the payment terms and conditions.

| | |
|---|---|
| License Number | 3636050099054 |
| License date | May 25, 2015 |
| Licensed content publisher | Springer |
| Licensed content publication | Molecular Biotechnology |
| Licensed content title | Gene delivery by lentivirus vectors |
| Licensed content author | Adam S. Cockrell |
| Licensed content date | Jan 1, 2007 |
| Volume number | 36 |
| Issue number | 3 |
| Type of Use | Thesis/Dissertation |
| Portion | Figures |
| Author of this Springer article | No |
| Order reference number | None |
| Original figure numbers | Figure 1 |
| Title of your thesis / dissertation | The selection of aptamers to CD20 and their application as inhibitors of complement dependent cytotoxicity |
| Expected completion date | Jun 2015 |

Permission to reproduce Figure 4.2:

NATURE PUBLISHING GROUP LICENSE
TERMS AND CONDITIONS
May 28, 2015

This is a License Agreement between Nadia Al youssef ("You") and Nature Publishing Group ("Nature Publishing Group") provided by Copyright Clearance Center ("CCC"). The license consists of your order details, the terms and conditions provided by Nature Publishing Group, and the payment terms and conditions.

| | |
|---|---|
| License Number | 3636050803230 |
| License date | May 25, 2015 |
| Licensed content publisher | Nature Publishing Group |
| Licensed content publication | Nature Reviews Genetics |
| Licensed content title | Sequencing technologies [mdash] the next generation |
| Licensed content author | Michael L. Metzker |
| Licensed content date | Jan 1, 2010 |
| Volume number | 11 |
| Issue number | 1 |
| Type of Use | reuse in a dissertation / thesis |
| Requestor type | academic/educational |
| Format | print and electronic |
| Portion | figures/tables/illustrations |
| Number of figures/tables/illustrations | 1 |
| High-res required | no |
| Figures | Figure 1 Figure 2 |
| Author of this NPG article | no |
| Your reference number | None |
| Title of your thesis / dissertation | The selection of aptamers to CD20 and their application as inhibitors of complement dependent cytotoxicity |
| Expected completion date | Jun 2015 |